

**MECHANISTIC ANALYSIS OF *IN VITRO* AND *IN VIVO* DRUG
RELEASE FROM PLGA MICROSPHERES**

by

Amy Christine Doty

A dissertation submitted in partial fulfillment
of the requirements for the degree of
Doctor of Philosophy
(Pharmaceutical Sciences)
in the University of Michigan
2015

Doctoral Committee:

Professor Steven P. Schwendeman, Chair
Professor Gordon L. Amidon
Research Professor Gregory E. Amidon
Professor Joerg Lahann

© Amy Christine Doty

2015

Dedication

To my parents with my love and gratitude.

Acknowledgements

I would like to thank my graduate research advisor Dr. Steven Schwendeman for his guidance and support since I joined his lab 4 years ago. He has encouraged me to think critically and to become a strong and independent scientist, for which I will always be thankful. While in his lab, Dr. Schwendeman offered me many wonderful opportunities to present and discuss my research with other scientists, and that has enabled me to develop a confidence that will continue to help me throughout the rest of my career. I am also very thankful to Dr. Anna Schwendeman for all of her invaluable advice and encouragement. I would also like to thank the rest of my committee; Dr. Gregory Amidon, Dr. Gordon Amidon, and Dr. Joerg Lahann for their time and helpful insights and comments they offered during the course of my research.

I cannot thank my parents, Mark and Linda Doty, enough for their constant love and encouragement. I always know that no matter where I am, your comforting words of assurance are only a phone call away. I truly cannot thank you enough for everything you've done for me. I must also thank my sister Casey. I cannot imagine going through anything without your support, especially not the long journey of graduate school. Having the love of my entire family has only made this accomplishment easier and I feel lucky to have such amazing people in my life.

Next, I would like to thank the FDA for the support of the research for the last 2+ years. The insight of the team there, especially Yan Wang and Stephanie Choi, has helped this project and my own scientific growth tremendously. The questions and comments posed during monthly discussions made this research stronger, and made me a stronger scientist. Working closely with the FDA was a unique experience and one that I am very grateful to have had.

Working in such a great lab with such wonderful labmates, past and present, has really made my time in graduate school enjoyable. There have been many people in the lab over the last several years but I would like to specifically thank Karl Olsen for his help with my animal studies, Rose Ackermann for her technical help and expertise, and Dr. Keiji Hirota for his collaboration and help with this project. My fellow graduate students in the Schwendeman group always made the lab a place I wanted to be, making even the most challenging days seem like fun: J. Maxwell Mazzara, Brittany Bailey, Kellisa Hansen, Rae Sung Chang, Karthik Pisupati, Morgan Giles, Jia Zhou, Dan Li, Kari Nieto, and Dan Li. Thank you all for creating a wonderful work environment that I will miss very much.

I would now like to thank everyone who has been by my side over the past 5 years and has made my time in Ann Arbor truly special and memorable. I am grateful to my wonderful boyfriend Ricky who has supported me and encouraged me since the day I met him. Thank you for believing in me and pushing me to reach and even surpass my own goals; your love and support has made the last year so much easier. Finally, I don't know how it would be possible to go through graduate school without the amazing friends I have been lucky enough to make in Michigan. There are too many to name individually, but I would like to especially thank Dr. Maya Lipert, Dr. Maria Posada, Dr. Jamie Connarn, Kellisa Hansen, Morgan Giles, Max Mazzara, and Karthik Pisupati. Thank you all for making this experience so enjoyable and memorable. I am blessed to have met you all and I'm looking forward to staying connected with you all as we progress in our careers.

GO BLUE!

Table of Contents

Dedication	ii
Acknowledgements	iii
List of Figures	viii
List of Tables	xiii
List of Appendices	xiv
Abstract	xvi
Chapter 1 : Introduction	1
1.1 Controlled Release Drug Products	1
1.2 PLGA Controlled Release Formulations	1
1.3 Mechanisms of Controlled Release	3
<i>1.3.1 Osmosis and osmotic-induced drug release mechanisms</i>	<i>4</i>
<i>1.3.2 Diffusion through Polymer Phase</i>	<i>5</i>
<i>1.3.3 Diffusion through Pores</i>	<i>5</i>
<i>1.3.4 Water Uptake</i>	<i>6</i>
<i>1.3.5 Hydrolysis and Erosion</i>	<i>7</i>
1.4 In vitro and In vivo Controlled Release from PLGA	7
<i>1.4.1 Accepted In vitro Release Conditions</i>	<i>7</i>
<i>1.4.1.1 Release Methods</i>	<i>8</i>
<i>1.4.1.2 Release Media</i>	<i>8</i>
<i>1.4.1.3 Drug Release from PLGA Microparticles in vitro</i>	<i>9</i>
<i>1.4.2 Drug Release from PLGA Microparticles in vivo</i>	<i>9</i>
<i>1.4.3 Factors Affecting in vivo Drug Release</i>	<i>11</i>
<i>1.4.3.1 Biological factors</i>	<i>12</i>
<i>1.4.3.2 Physical-chemical factors</i>	<i>15</i>
1.5 Research Scope and Impact	17
1.6 Thesis Overview	18
1.7 References	21

Chapter 2 : Mechanistic Analysis of Triamcinolone Acetonide Release from PLGA Microspheres as a Function of Varying <i>in vitro</i> Release Conditions.....	26
2.1 Abstract	26
2.2 Introduction	27
2.3 Materials	29
2.4 Methods.....	29
2.4.1 <i>Microsphere Preparation.....</i>	29
2.4.2 <i>Scanning Electron Microscopy.....</i>	30
2.4.3 <i>Determination of Tr-A Loading and Encapsulation Efficiency.....</i>	30
2.4.4 <i>Tr-A Quantification by UPLC.....</i>	30
2.4.5 <i>Assessment of Drug Release in vitro.....</i>	31
2.4.6 <i>Mass Loss and Water Uptake of Microspheres:.....</i>	31
2.4.7 <i>Molecular Weight of PLGA</i>	32
2.4.8 <i>BODIPY uptake and Laser Scanning Confocal Microscopy (LSCM):.....</i>	32
2.4.9 <i>Modelling Tr-A diffusion-controlled release</i>	33
2.4.10 <i>Statistical and Regression Analysis</i>	33
2.5 Results and Discussion.....	33
2.6 Conclusions	45
2.7 References	46
2.8 Supplementary Information.....	48
2.8.1 <i>Selection of Tr-A/PLGA Microspheres</i>	48
2.8.2 <i>Regression Analysis</i>	50
2.8.3 <i>Additional LCSM images of Tr-A_1 and Tr-A_2 microspheres</i>	53
2.8.4 <i>Development of diffusion-controlled release models.....</i>	55
Chapter 3 : Cage Implant System for Assessing <i>in vivo</i> Controlled Release Performance of Long-acting Release PLGA Microspheres.....	57
3.1 Abstract.....	57
3.2 Introduction	58
3.3 Materials	60
3.4 Methods.....	61
3.4.1 <i>Microsphere Preparation.....</i>	61
3.4.2 <i>Determination of Loading and Encapsulation Efficiency.....</i>	61
3.4.3 <i>Cage Construction and Preparation.....</i>	62

3.4.4	<i>In vitro Release</i>	62
3.4.5	<i>Quantification of Tr-A and Leuprolide in vitro</i>	63
3.4.6	<i>Surgical Procedures</i>	63
3.4.7	<i>Pharmacokinetic Studies</i>	64
3.4.8	<i>Tr-A Quantification in Plasma</i>	64
3.4.9	<i>Leuprolide Quantification in Plasma</i>	65
3.4.10	<i>In vivo release from Microspheres</i>	65
3.4.11	<i>Histology</i>	65
3.5	Results and Discussion	66
3.6	Conclusions	76
3.7	References	77
3.8	Supplementary Information	80
3.8.1	<i>Tr-A release in vivo (Tr-A_1)</i>	80
3.8.2	<i>In vitro release and Pharmacokinetics (Tr-A_1)</i>	81
3.8.3	<i>Bodipy Diffusion in vitro</i>	82
Chapter 4 : Mechanisms of Release of Triamcinolone Acetonide from PLGA Microspheres		
<i>in vivo</i>	84
4.1	Abstract	84
4.2	Introduction	85
4.3	Materials	87
4.4	Methods	87
4.4.1	<i>Surgical Procedures</i>	88
4.4.2	<i>Assessment of Drug Release in vitro from Cage Implant</i>	88
4.4.3	<i>Release and Mechanistic Analyses in vivo</i>	89
4.4.4	<i>Statistical and Regression Analysis</i>	89
4.5	Results and Discussion	89
4.6	Conclusions	96
4.7	References	98
4.8	Supplementary Information	100
4.8.1	<i>Regression Analysis</i>	100
4.8.2	<i>In vitro release under various mixing conditions</i>	102
4.8.3	<i>Subcutaneous pH</i>	103
Chapter 5 : Conclusions, Implications, and Future Directions		
		104

List of Figures

Figure 1.1: Molecular structure of PLGA and its monomers produced during hydrolysis, lactic and glycolic acids.....	2
Figure 1.2: Mechanisms of drug release from PLGA microspheres: (A) diffusion through aqueous pore networks, (B) diffusion through the polymer phase, (C) osmotic pumping and swelling induced pore formation, (D) hydrolysis and erosion. (Figure from [6])	4
Figure 1.3: <i>in vitro</i> vs. <i>in vivo</i> drug release from PLGA microspheres. Release of dexamethasone from PLGA microspheres of two molecular weights <i>in vitro</i> (A) and <i>in vivo</i> (B) Dexamethasone release was measured by extraction of drug from on a small sample of microspheres recovered from the administration site [18]. Release of VEGF and hydrolysis of PLGA <i>in vitro</i> and <i>in vivo</i> (C). VEGF concentration was determined by separating microspheres from subcutaneous tissue and measuring total remaining drug at each time point [33].	11
Figure 1.4: The temporal variation in the three phases of inflammatory response resulting from administration of biodegradable microspheres. (Figure from [37]).....	13
Figure 1.5: The complex nature of how different factors may affect drug release from PLGA matrices. (Figure from [6])	17
Figure 2.1 SEM micrographs of Tr-A micronized by mortar and pestle (A) and after by Retsch [®] cryo-mill (B). Micronized Tr-A powder was then encapsulated in Tr-A_1 (C) and Tr-A_2 (D) microspheres.....	34
Figure 2.2: <i>In vitro</i> release from Tr-A_1 (A) and Tr-A_2 (B) microspheres in various media. Data represent mean \pm SEM, n=3. Note: in some cases, release average release was slightly greater than 100% due to slight error in measurement.	36
Figure 2.3: Decline of molecular weight of PLGA in Tr-A_1 (A) and Tr-A_2 (B) microspheres in various <i>in vitro</i> release media. Data represent mean \pm SEM, n=3.....	38
Figure 2.4: Mass loss of Tr-A_1 (A) and Tr-A_2 (B) microspheres in various <i>in vitro</i> release media. Data represent mean \pm SEM, n=3.	38
Figure 2.5: Release vs. mass loss of Tr-A_1 (A) and Tr-A_2 (B) microspheres. Dashed line represents release = mass loss, indicating pure erosion controlled release. X and Y data represent mean \pm SEM, n=3.....	40
Figure 2.6: Water uptake Tr-A_1 (A) and Tr-A_2 (B) microspheres in various <i>in vitro</i> release media. Data represent mean \pm SEM, n=3.	41
Figure 2.7: Representative images of Tr-A_1 (A) and Tr-A_2 (B) microspheres following 3 days release in PBST pH 7.4 and 3 hours in 5 μ g/mL bodipy in PBST pH 7.4 and resulting bodipy concentration gradient plots shown at right.....	42

Figure 2.8: BODIPY diffusion coefficients in degrading Tr-A_1 (A) and Tr-A_2 (B) microspheres in varying release media. Data represent mean \pm SEM, n=6. X indicates no diffusion coefficient could be determined due to agglomeration and/or saturation of microspheres.	43
Figure 2.9: Theoretical Tr-A release profiles from Tr-A_1 (A) and Tr-A_2 (B) microspheres for diffusion-controlled release. Profiles were generated using representative diffusion coefficients with and without the plasticizer triethyl citrate that were determined at early (1-3 days) and late times (7+ days) during the release incubation.	44
Figure S 2.1: <i>In vitro</i> release of initial Tr-A/PLGA microsphere formulations using PLGA 502H (A) and ester end-capped, moderate molecular weight PLGA (B). Data represent mean \pm SEM, n=3.	49
Figure S 2.2: Linear regression fits of Tr-A_1 hydrolysis data. Rate constants shown in Table 2.2 were determined from these regressions.	50
Figure S 2.3: Linear regression fits of Tr-A_2 hydrolysis data. Rate constants shown in Table 2.2 were determined from these regressions.	50
Figure S 2.4: Four parameter logistic nonlinear fits of Tr-A_1 release data. $T_{50,release}$ values and associated errors were determined from the associated equations.	51
Figure S 2.5: Four parameter logistic nonlinear fits of Tr-A_2 release data. $T_{50,release}$ values and associated errors were determined from the associated equations.	51
Figure S 2.6: Four parameter logistic nonlinear fits of Tr-A_1 mass loss data. $T_{50,erosion}$ values and associated errors were determined from the associated equations.	52
Figure S 2.7: Four parameter logistic nonlinear fits of Tr-A_2 mass loss data. $T_{50,erosion}$ values and associated errors were determined from the associated equations.	52
Figure S 2.8: Confocal images of Tr-A_1 microspheres following 1, 3, and 7 days incubation in various release media. Microspheres incubated in PBST pH 6.5, PBS + 1.0% TC and HBST pH 7.4 are not pictured at 7 days due to complete dye saturation and/or agglomeration at this and future time points.	53
Figure S 2.9: Confocal images of Tr-A_2 microspheres following 1, 3, 7, 14, and 21 days incubation in various release media. Microspheres incubated in PBS + 1.0% TC are not pictured at 21 days due to complete dye saturation and/or agglomeration at this and future time points.	54
Figure S 2.10: Tr-A uptake in blank PLGA microspheres and resulting fits to Crank's solution (shown). Estimated diffusion coefficients resulting from these fits are shown in the legend.	55
Figure S 2.11: Representative confocal images of Blank_1 (A) and Blank_2 (B) microspheres following 1 day incubation in PBST pH 7.4 and 3 hours in bodipy solution.	55
Figure 3.1: Cage implant design and use in rats. (A) Schematic of cage design and dimensions. (B) Top view (left) and side view (right) of a cage implant. Cages are implanted in the subcutaneous space in rats (C and D). Following euthanasia, cages are retrieved and the microspheres are retrieved and rinsed on a sieve prior to analysis (E).	67

Figure 3.2: Release of Tr-A (A) and leuprolide (B) <i>in vitro</i> in PBST pH 7.4. Solid symbols represent release from suspended microspheres, open symbols represent release from microspheres restrained in cages. Data represent mean \pm SEM, n=3.	69
Figure 3.3: Pharmacokinetics of of Tr-A (A) and leuprolide (B) following administration in rats as a suspension (open symbols) or in a cage implant (solid symbols). Inset in panel B shows leuprolide concentrations in plasma for the first 24 hours after administration, units are the same as the parent graph. Data represent mean \pm SEM, n=2-4.....	69
Figure 3.4: Release of Tr-A (A) and leuprolide (B) <i>in vitro</i> in PBST pH 7.4 and <i>in vivo</i> . Data represent mean \pm SEM, n=3.....	71
Figure 3.5: H&E stained images of tissue samples taken from the site of cage implantation or SC injection. Tissue was removed at the time of euthanasia. Scale bar represents 50 μ m.	73
Figure S 3.1: Release of Tr-A from Tr-A_1 microspheres <i>in vitro</i> in PBST pH 7.4 and <i>in vivo</i> . Data represent mean \pm SEM, n=3.....	80
Figure S 3.2: Pharmacokinetics of of Tr-A_1 following Tr-A_1 administration in rats as a suspension (open symbols) or in a cage implant (solid symbols). Data represent mean \pm SEM, n=2-4.....	81
Figure S 3.3: Release of Tr-A from Tr-A_1 microspheres restrained in cages or suspended in PBST pH 7.4. Data represent mean \pm SEM, n=3.....	81
Figure S 3.4: LCSM images of microspheres following one week incubation in PBST.	83
Figure S 3.5: Diffusion coefficients of BODIPY in degrading microspheres either freely suspended or caged in PBST pH 7.4. There is no significant difference between the two conditions at any time point. Data represent mean + SEM, n=6.	83
Figure 4.1: <i>in vitro</i> and <i>in vivo</i> release from Tr-A_1 (A) and Tr-A_2 (B) microspheres. Release was measured using cage model. Data represent mean \pm SEM, n=3-4.	90
Figure 4.2: <i>in vitro</i> and <i>in vivo</i> PLGA hydrolysis kinetics in Tr-A_1 (A) and Tr-A_2 (B) microspheres. Data represent mean \pm SEM, n=3-5.	91
Figure 4.3: <i>in vitro</i> and <i>in vivo</i> mass loss of Tr-A_1 (A) and Tr-A_2 (B) microspheres. Data represent mean \pm SEM, n=3-5.	92
Figure 4.4: <i>in vitro</i> and <i>in vivo</i> water uptake in Tr-A_1 (A) and Tr-A_2 (B) microspheres. Data represent mean \pm SEM, n=3-5.	93
Figure 4.5: Representative confocal images of Tr-A_1 and Tr-A_2 microspheres during <i>in vitro</i> and <i>in vivo</i> release. Images were taken following incubation in aqueous solution of BODIPY FL for 10 min or 3 h.....	94
Figure 4.6: BODIPY diffusion coefficients in degrading Tr-A_1 (A) and Tr-A_2 (B) microspheres <i>in vitro</i> and <i>in vivo</i> . Data represent mean \pm SEM, n=6. *p < 0.05.	94
Figure 4.7: Theoretical Tr-A release profiles from Tr-A_1 (A) and Tr-A_2 (B) microspheres for diffusion-controlled release. <i>In vitro</i> profiles (in grey) were generated using representative diffusion coefficients with and without the plasticizer triethyl citrate that were determined at early (1-3 days) and late times (7+ days) during the release incubation.....	96

Figure S 4.1: Four parameter logistic nonlinear fits of Tr-A_1 release (A) and mass loss data (B); linear regression fits of Tr-A_1 hydrolysis data (C). Fits were used to estimate relevant t_{50} values and first order rate constant of PLGA hydrolysis.	100
Figure S 4.2: Four parameter logistic nonlinear fits of Tr-A_2 release (A) and mass loss data (B); linear regression fits of Tr-A_2 hydrolysis data (C). Fits were used to estimate relevant t_{50} values and first order rate constant of PLGA hydrolysis.	101
Figure S 4.3: <i>In vitro</i> release from Tr-A_1 microspheres caged (A) or suspended freely (B) in PBST pH 7.4 under varying mixing conditions. Data represent mean \pm SEM, n=3.	102
Figure S 4.4: <i>In vitro</i> release from Tr-A_2 microspheres caged (A) or suspended freely (B) in PBST pH 7.4 under varying mixing conditions. Data represent mean \pm SEM, n=3.	103
Figure A. 1: Primary structure of liraglutide. Modifications from GLP-1(7-37) are highlighted: K34R and C16 fatty acid conjugated to K20 via a glutamate linker.	113
Figure A. 2: Schematic showing salt treatment of PLGA-COOH resulting in electrostatic interaction with liraglutide.	114
Figure A. 3: Liraglutide sorption to untreated and salt-treated PLGA 502H following 24 hours incubation with peptide solution. Data represent mean \pm SEM, n=3.	114
Figure A. 4: Liraglutide release from salt-treated PLGA 502H in HBS pH 7.4. Data represent mean \pm SEM, n=3.	115
Figure A. 5: (A) Liraglutide sorption isotherm using MgCl ₂ -treated 502H. Four concentrations of liraglutide were used: 0.2, 0.5, 1.0 and 5.0 mg/mL. Total sorption after 24 hours incubation in each concentration is shown in (B). Data represent mean \pm SEM, n=3. ..	116
Figure A. 6: SEM images of Mg-502H microspheres before (A) and after (B) liraglutide loading for 24 hours at 37°C.	117
Figure A. 7: Liraglutide loading in microspheres. Loading was performed using 10mg microspheres in 1 mL of 5.0 mg/mL liraglutide solution in HEPES buffer pH 7.4 at 37°C for 24 hours. Table at right includes loading values and initial burst (24-hour release) determined in HBS. Data represent mean \pm SEM, n=3.	118
Figure A. 8: SEM images of Mg-503H microspheres before (A) and after (B) liraglutide loading for 24 hours at 37°C.	118
Figure A. 9: Liraglutide loading (A) and encapsulation efficiency (B) in PLGA 503H microspheres. Loading was performed using 10mg microspheres in 1 mL of 1.0 mg/mL liraglutide solution in 3.75mM Na ₂ HPO ₄ pH 8.1 at 37°C for 24 hours. Data represent mean \pm SEM, n=3.	119
Figure A. 10: <i>in vitro</i> release of liraglutide from microspheres in HBS pH 7.4 (A and C), PBST pH 7.4 (B). Release was quantified by UPLC of release media (A and B) or amino acid analysis of microspheres (C). Data represent mean \pm SEM, n=3.	121
Figure A. 11: UPLC chromatograms of release from Mg503H + MgCO ₃ microspheres in HBS and PBST; and a standard prepared in loading solution. Peak shift was observed in release samples in HBS (retention time 1.2 minutes vs. 2.8 minutes).....	122

Figure A. 12: Liraglutide content remaining in solution during incubation at 37°C. Initial concentrations were 100 µg/mL (A) and 50 µg/mL (B).	122
Figure A. 13: Liraglutide concentrations in plasma of SD rats following a single subcutaneous injection of liraglutide-loaded Mg503H + MgCO ₃ microspheres at low (A) or high (B) dose.	123
Figure B. 1: Representative SEM images of four microsphere formulations. A) 800PLA, B) 800PLA-T, C) 1000PLA, D) PLA/PLGA	132
Figure B. 2 Brimonidine release from four polymer microsphere formulations <i>in vitro</i> , PBST pH 7.4. Data are expressed as mean ± SE, n=3.	134

List of Tables

Table 1.1: Endogenous compounds which may affects drug release from PLGA microspheres and their expected concentrations in subcutaneous interstitial fluid (ISF).....	14
Table 2.1: Characterization of microsphere formulations prepared using unmilled and milled Tr-A. All values are reported as mean \pm SEM, n=3.	35
Table 2.2: Initial first order rate constants (day^{-1}) of PLGA hydrolysis in Tr-A_1 and Tr-A_2 microspheres as determined by linear regression analysis of data shown in Figure 2.3. Values were taken from regression over the first 14 days.	38
Table 2.3: Characteristic times (in days) of release and erosion from Tr-A_1 and Tr-A_2 microspheres. Values represent mean \pm SEM, n=3. T_{50} ratios were calculated from mean values of $t_{50, \text{release}}$ and $t_{50, \text{erosion}}$ in each media.	40
Table S 2.1: Initial Tr-A/PLGA microsphere formulation parameters and characterization.	49
Table S 2.2: Estimated diffusion coefficients of Tr-A and bodipy in blank microspheres.	56
Table S 2.3: Estimated partition coefficients and solubilities of Tr-A in PLGA.....	56
Table 2.4: $T_{50, \text{diffusion}}$ estimated using diffusion-controlled release models shown in Figure 2.9..	45
Table 3.1: AUC and F2 similarity factor values for Tr-A and leuprolide following microspheres administration in rats.....	70
Table 4.1: Initial first order rate constants (day^{-1}) of PLGA hydrolysis in Tr-A_1 and Tr-A_2 microspheres as determined by linear regression analysis of data shown in Figure 4.2. Values were taken from regression over the first 14 days.	92
Table 4.2: Characteristic times (in days) of release and erosion from Tr-A_1 and Tr-A_2 microspheres. Values represent mean \pm SEM, n=3. T_{50} ratios were calculated from mean values of $t_{50, \text{release}}$ and $t_{50, \text{erosion}}$	92
Table 4.3: $T_{50, \text{diffusion}}$ values estimated using diffusion-controlled release models shown in Figure 4.7.....	96
Table S 4.1: Subcutaneous pH values measured during release.	103
Table B. 1: Brimonidine Microsphere Formulation Parameters.....	130
Table B. 2: Characterization of Brimonidine Microencapsulation (Data expressed as mean \pm SE, n=3).....	131

List of Appendices

Appendix A: Remote Loading of Liraglutide in PLGA Microspheres for Controlled Release	106
A.1 Introduction	106
A.2 Materials	108
A.3 Methods	108
A.3.1 Salt Treatment of PLGA	108
A.3.2 Liraglutide Sorption to salt-treated PLGA 502H	108
A.3.3 Liraglutide Release from salt-treated PLGA 502H	108
A.3.4 Sorption Isotherm of Liraglutide to salt-treated PLGA 502H	109
A.3.5 Microsphere Formulation	109
A.3.6 Microsphere Imaging	109
A.3.7 Liraglutide Loading in Microspheres	110
A.3.8 Determination of Peptide Loading in Microspheres (mass loss, extraction)	110
A.3.9 Ultra Performance Liquid Chromatography (UPLC)	110
A.3.10 Loading optimization	111
A.3.11 Liraglutide Release from Microspheres	111
A.3.12 Stability of Liraglutide in Release Media—appendix?	111
A.3.13 Amino Acid Analysis	111
A.3.14 Pharmacokinetics	112
A.4 Results and Discussion	113
A.5 Conclusions	123
A.6 References	124
Appendix B: : Poly (lactic acid) and Poly (lactic-co-glycolic acid) Microspheres for Intraocular Controlled Release of the Glaucoma Drug Brimonidine	126
B.1 Abstract	126
B.2 Introduction	127
B.3 Materials	129
B.4 Methods	129
B.4.1 Removal of LMW acids from PLA	129
B.4.2 Microsphere preparation	129
B.4.3 Scanning Electron Microscopy	130

<i>B.4.4</i>	<i>Determination of Brimonidine Loading and Encapsulation Efficiency.....</i>	<i>130</i>
<i>B.4.5</i>	<i>In vitro Release Kinetics of Brimonidine</i>	<i>131</i>
<i>B.4.6</i>	<i>Brimonidine Quantification</i>	<i>131</i>
B.5	Results and Discussion.....	131
B.6	Conclusions	134
B.7	References	135

Abstract

Poly (lactic-co-glycolic) acid (PLGA) microspheres have been extensively studied for controlled drug delivery, and more than a dozen PLGA formulations are currently on the market. However, surprisingly little information is available about how the administration environment affects microsphere properties that result in drug release *in vivo*, and there is a lack of *in vitro-in vivo* correlation data for microsphere formulations. As a result, *in vitro* tests used to predict drug release during development are rarely designed to represent actual formulation behavior *in vivo*.

Two microsphere formulations encapsulating a model drug, triamcinolone acetonide, were prepared from PLGAs of different molecular weights and end-capping (18 kDa acid-capped, 54 kDa ester-capped). *In vitro* release and the corresponding mechanisms (hydrolysis, erosion, water uptake, and diffusion) were studied in four release media: PBST pH 7.4 (standard condition), PBST pH 6.5, PBS + 1.0% triethyl citrate (TC), and HBST pH 7.4. The release mechanism in PBST and HBST without TC was primarily polymer erosion-controlled in both formulations as indicated by the similarity of release and mass loss kinetics. The addition of TC resulted in primarily diffusion-controlled release from the low MW PLGA. By using a novel cage implant to restrain microspheres in the SC space, similar analyses were performed on microspheres administered *in vivo*. Drug release was much faster *in vivo* than in any of the *in vitro* media studied (release over 2-3 weeks vs. 4-7 weeks). Furthermore, PLGA water uptake, hydrolysis and mass loss were greatly augmented in the subcutaneous space. The study of microsphere morphology revealed an osmotically induced pore network in the higher MW formulation, indicating the potential for release controlled by water uptake, a mechanism

previously unseen *in vitro*. Therefore, *in vitro* tests could benefit by incorporating relevant components of interstitial fluid, which more closely mimic those conditions that control key release mechanisms *in vivo*. The novel application of the cage model to uncover significant changes to mechanism-indicating processes of PLGA microspheres *in vivo* is highly significant.

Hence, this thesis demonstrates the importance of understanding *in vivo* release mechanisms in order to design release tests, which accurately predict release upon administration.

Chapter 1 : Introduction

1.1 Controlled Release Drug Products

Controlled release systems have been developed as a drug delivery solution for a number of pharmaceuticals for which common routes of administration, e.g. oral dosage forms, are not possible or desirable. Modified release formulation strategies have become increasingly important recently, as many new drugs are poorly soluble small molecules or therapeutic macromolecules such as proteins and peptides [1, 2]. For these molecules, controlled-release products offer advantages over conventional dosage forms such as: increased half-life of rapidly degraded drugs, local administration and low systemic toxicity, improved efficacy, increased bioavailability, improved administration in under-privileged areas, and increased patient compliance due to comfort and less frequent dosing [3, 4]. Biodegradable polymers such as poly (lactic-*co*-glycolic acid) (PLGA) have been successfully implemented in the sustained delivery of small molecules and proteins [1, 2, 5]. As biodegradable polymers such as PLGA erode, the therapeutic molecule they carry is continuously released from polymer matrix to the body, resulting in sustained therapeutic plasma drug concentrations and prolonged efficacy. By controlling the rate of polymer degradation and erosion, one can tailor the rate of release to result in desired drug concentrations in blood or at the site of action [6, 7].

1.2 PLGA Controlled Release Formulations

PLGA is one of the most widely used biomaterials for controlled drug delivery systems due to its biocompatibility, use in numerous Food and Drug Administration (FDA)-approved commercial products, and tunable mechanical properties. In the presence of water, the ester

bonds of PLGA are hydrolyzed to yield lactic and glycolic acid monomers, which are then further metabolized and eliminated from the body. The rate of PLGA degradation can be controlled by variations in molecular weight and lactic : glycolic acid ratios. Glycolic acid (GA) is more hydrophilic than lactic acid, thus a higher content of glycolic acid from 0-50% enhances water uptake and accelerates the rate of hydrolysis of the polymer. At GA contents above 50%, crystallites begin to form, limiting the polymer solubility and making it less useful for controlled-release dosage forms. PLGA 50:50 with racemic lactic acid is the most commonly studied of the PLGAs and has the fastest degradation time, usually resulting in drug release over 4-6 weeks [2]. Additionally, PLGA containing amorphous D,L-lactic acid degrades faster than PLGA containing only crystallizable L- or D-lactic acids [5]. Because of its biocompatibility and tunable properties, PLGA has been implemented in a variety of controlled release formulations such as microparticles, implants, and *in situ* forming depots [8]. The focus of this thesis is on the design and evaluation of PLGA microparticles for drug delivery.

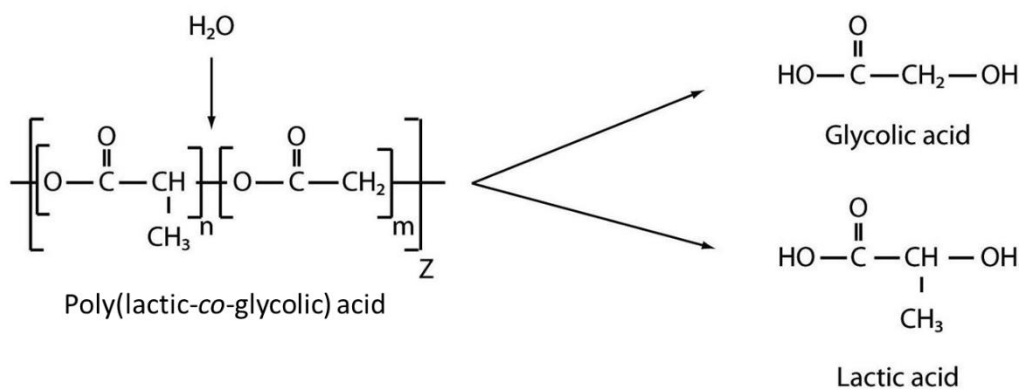


Figure 1.1: Molecular structure of PLGA and its monomers produced during hydrolysis, lactic and glycolic acids.

Among controlled release PLGA formulations, microparticles are the most widely used and the most commercially successful products [9]. Microparticles can be made in a number of ways including emulsion-solvent evaporation, coacervation, and spray drying [2]. To form

microparticles by emulsion-solvent evaporation, an aqueous solution of drug or solid drug powder is added to a solution of PLGA dissolved in an organic solvent such as methylene chloride. This mix is homogenized, forming either a solid/oil (S/O) suspension or water/oil (W/O) emulsion. An aqueous solution of emulsifier is added, then vortexed to form a complex emulsion (either S/O/W or $W_1/O/W_2$, depending on how the drug was added). If the drug is sufficiently soluble in organic solvent, the process would only involve a single O/W emulsion. The final emulsion is stirred in an aqueous bath to allow for organic solvent evaporation. Formed microspheres can be sieved to an appropriate size range and freeze-dried for storage before use.

Microparticles are an attractive delivery strategy for a wide variety of drugs including proteins, peptides, water soluble small molecules and hydrophobic small molecules. Drug release from PLGA microspheres can be designed to suit the needs of the therapeutic molecule they carry by altering polymer molecular weight, polymer hydrophilicity, and particle size. PLGA microsphere formulations currently on the market include Vivitrol® and Lupron Depot®, which release naltrexone and leuprolide acetate, respectively. While Vivitrol® is formulated with PLGA 50:50 and needs to be administered every two weeks, Lupron Depot® is made with PLGA of greater hydrophobicity (i.e. PLGA 75:25) and needs to be administered just every 1-6 months depending on indication, dose and specific polymer formulation used. [2, 8-10]

1.3 Mechanisms of Controlled Release

Controlled release drug products are designed for sustained release of drugs in the human body for enhanced drug therapy. While designing these systems, it is important to know which mechanisms are responsible for causing drug release. A number of mechanisms have been developed to achieve custom drug release profiles desired for a particular drug product. Often, more than one mechanism is operative in a given formulation and different mechanisms may

primarily control drug release at different times. It is also important to note that these mechanisms, specifically in the case of PLGA microspheres, are not independent of one another and drug release is often the result of the interplay of more than one of these processes. The following provides a discussion on mechanisms of controlled release from polymeric controlled release systems and their applications in PLGA microspheres (Figure 1.2 [6]).

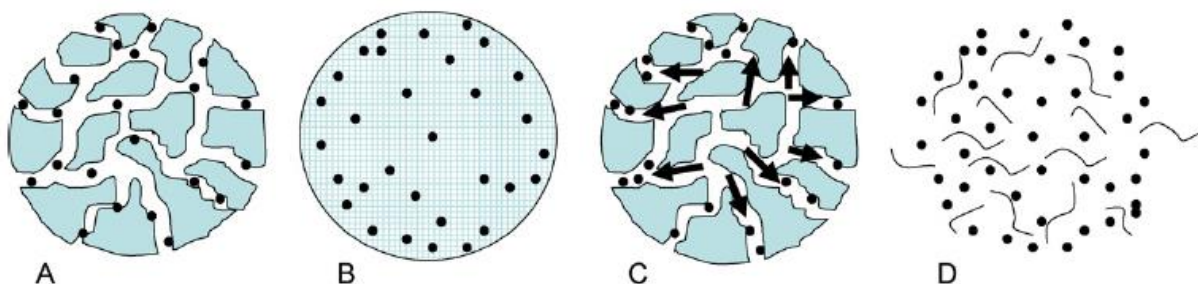


Figure 1.2: Mechanisms of drug release from PLGA microspheres: (A) diffusion through aqueous pore networks, (B) diffusion through the polymer phase, (C) osmotic pumping and swelling induced pore formation, (D) hydrolysis and erosion. (Figure from [6])

1.3.1 Osmosis and osmotic-induced drug release mechanisms

Osmosis is defined as the bulk flow of solvent across a semi-permeable membrane from a region of low solute concentration to a region of high solute concentration. If drug particles are coated with a semi-permeable polymer, water will cross the polymer and dissolve the encapsulated drug. This creates a greater driving force for water to cross the polymer and the continued influx of water eventually causes rupturing of the polymer coating, causing drug release. Another variation of controlled release governed by osmosis is porous polymer microparticles. An osmotic gradient will drive water into the particle pores, dissolving drug and allowing drug diffusion through the pore network, either initially available or created by the force of the flowing pore liquid, into the external environment. [7] Alternatively, when the polymer swells when first in contact with water during release, new pores are created, and the drug may then be released by pore-diffusion as opposed to osmotic flow [11].

1.3.2 *Diffusion through Polymer Phase*

Polymer matrices in controlled release systems present a barrier to drug diffusion from the polymer phase into the surrounding media. When there is no percolating network of pores available for the drug and the drug can partition in the polymer, the release from these particles is often governed by diffusion through the polymer phase. One example of this type of release are reservoir systems, in which drug is surrounded by polymer and diffusion through the polymer is the rate-limiting step in release. In this case, release rates are governed by Fick's first law of diffusion and is dependent its relative affinities for the polymer and aqueous phases, drug solubility and drug loading, implant geometry, and self-diffusion coefficient in the polymer phase [3, 4, 7]. A second example of a diffusion-controlled system are matrix systems, where drug can be molecularly dispersed or dissolved in the polymer matrix. Matrix systems can be generally classified into four categories depending on drug solubility in the polymer and the porosity of the matrix, and the resulting non-zero order initial release rates can predicted using equations [4]. Plasticization of the polymer also results in increased chain mobility, resulting in faster drug diffusion. Uptake of water and subsequent polymer swelling and pore formation can also decrease tortuosity, resulting in controlled drug release governed by diffusion through the polymer [3, 6].

1.3.3 *Diffusion through Pores*

The presence of pores in a controlled-release polymeric system will allow water soluble drugs to diffuse to the external environment, resulting in controlled release. A prime example of this phenomenon is porous PLGA microparticles. Particles formed by a W/O/W double emulsion-solvent evaporation method result in voids in the polymer matrix owing to the removal of the organic solvent and the primary emulsion. These voids can result in an interconnected pore

network within the microparticle, through which drug may diffuse upon introduction to the release environment. This pore network becomes a dynamic system upon polymer hydration. Hydration can cause additional pore opening and lead to faster drug release, but polymer healing can cause these pores to close and slow drug release from the microparticle. Non-porous PLGA microspheres can also exhibit pore-diffusion release, as a pore network will develop upon polymer hydration, hydrolysis and subsequent erosion. These aqueous pores will then serve as channels to transport drug from the polymer matrix to the release environment. [6, 11, 12]

1.3.4 *Water Uptake*

Upon introduction to *in vitro* release media or administration *in vivo*, PLGA microparticles will take up water and the polymer chains will become hydrated. This results in depression of the glass transition temperature, causing the transition of the amorphous polymer into a rubber-like, mobile state. Molecules dispersed within a PLGA matrix will exhibit improved diffusion through a mobile polymer (above its glass transition) than through the same polymer in its glassy state. The resulting swelling of the microparticles causes improved mobility of polymer chains and an increase in volume, resulting in increased effective diffusion coefficient of drug as well as the exposure of more drug molecules to aqueous diffusion pathways. It is important to note that typically by far most of the water molecules that enter the PLGA matrix distribute into the pore liquid as opposed to the polymer phase. For example, a medium end-capped PLGA 50/50 is only expected to take up about 2% w/w water in the polymer phase [13], whereas the protein controlled release systems prepared from the same polymer may take up more than 100% their weight in water owing to the presence of high levels of encapsulated protein and salt [14]. The uptake of water can also induce pore formation due to polymer-chain swelling and a build-up of osmotic pressure; this opening of additional

interconnected pores creates a pathway for drug diffusion out of the polymeric system, as described above. Finally, water uptake in PLGA phase of the microspheres causes hydrolysis of the polymer chains, as described in detail below. [6, 11, 12]

1.3.5 *Hydrolysis and Erosion*

In the presence of water, the ester bonds in PLGA will break to yield lactic acid and glycolic acid monomers which are then eliminated by natural biological processes. This hydrolysis results in the shortening of polymer chains and a decrease in the PLGA MW. As hydrolysis proceeds, acidic oligomeric byproducts are produced and will further catalyze hydrolysis. Once the polymer chains hydrolyze to a critical chain length, overall matrix erosion begins. At this point, byproducts are able to escape from the polymer matrix, resulting in less tortuous pathways by which drug can be released from the microparticle. This also results in an overall erosion, or mass loss, of the polymer matrix and is associated with decreased integrity of the original microparticle. This process is known as bulk erosion which is in contrast to surface erosion, where mass loss is only observed from the surface of the formulation.

1.4 ***In vitro* and *In vivo* Controlled Release from PLGA**

1.4.1 *Accepted In vitro Release Conditions*

Unlike for standard dosage forms such as oral and transdermal products, there are no specific guidelines set by the FDA or United States Pharmacopeia (USP) regarding *in vitro* release testing for modified release drug products [15]. As such, a wide variety of release conditions are used by different researchers and the methods employed often depend on drug and polymer characteristics.

1.4.1.1 *Release Methods*

In vitro methods currently used to assess drug release from PLGA microparticles can be categorized into three groups: flow-through cell, dialysis, and sample-and-separate. USP apparatus 4, originally designed for modified release oral dosage forms, has been adapted to test microparticulate systems using flow-through methods. Release media is continuously circulated through cells packed with glass beads and microparticles, media samples are collected at pre-determined time points and analyzed for drug content. Dialysis release tests are set up with drug-loaded microparticles separated from bulk release media by a semi-permeable membrane. Drug release is assessed by measuring drug content in the bulk. The sample-and-separate method has been the most widely used technique for assessing drug release from microparticles.

Microspheres are suspended in a volume of release media sufficient to ensure sink conditions for the duration of release, and this suspension is agitated continuously to prevent aggregation of microspheres. At appropriate time points, the microparticles are separated from the media by filtration or centrifugation and release media is either partially or completely removed then replenished. [16, 17]

1.4.1.2 *Release Media*

While release methods are fairly consistent among *in vitro* release tests for controlled release microparticles, the media used by researchers is highly dependent on the particular formulation and the lab. Changes in buffering system, pH, temperature, ionic strength, presence of surfactant, and volume are all variables that are altered depending on drug solubility and dose, as well as established methods of the lab [18-20]. Some researchers have attempted to model the *in vivo* environment by altering the *in vitro* release conditions, but these efforts have been limited to single formulations and the conditions used among these groups are not consistent [18, 21-24].

Furthermore, while it is well understood that different media can change the rate of drug release, there is little understanding of how differing release media may change the underlying mechanisms of release.

1.4.1.3 *Drug Release from PLGA Microparticles in vitro*

Typical drug release profiles from PLGA 50:50 microparticles *in vitro* can be described as triphasic, controlled by a combination of erosion and diffusion. Initial drug release (the “initial burst”) is very fast (i.e. within 1-3 days) and is affected by a number of factors such as presence of initial interconnected pores, polymer swelling, polymer pore opening and closing, and surface-associated or poorly encapsulated drug. For water-soluble drugs, pore opening associated with hydration of the polymer can cause significant drug release via pore diffusion as long as the pores remain interconnected. Pores will commonly seal off by polymer healing. The second phase of release, typically referred to as the “lag phase”, is controlled by polymer erosion. Depending on the properties of the PLGA used, the polymer will take some time to degrade to a critical chain length, at which point further hydrolysis causes polymer mass loss. During this lag time, very little drug release is seen if the molecular weight of the polymer is sufficiently high such that no polymer chains are water soluble. As degradation of the polymer proceeds past the critical chain length, erosion causes the third and final phase of drug release, which is often rapid and follows apparent zero-order kinetics. [2, 3, 11, 12, 25, 26]

1.4.2 *Drug Release from PLGA Microparticles in vivo*

During each stage of formulation development, *in vitro* assays are routinely used to monitor drug release from microsphere products in aqueous media. However, there is surprisingly little data available to understand to what extent such a release test is predictive of microsphere drug product performance when injected *in vivo*. Oftentimes, the release from

microspheres *in vivo* is different than the release measured during *in vitro* tests and yet there has been little discussion on the underlying causes for these discrepancies. Whereas there are numerous reports of pharmacokinetics (PK) of microsphere depots, few have attempted to understand the mechanisms of release when *in vitro-in vivo* differences arise [21, 22, 27-32]. In addition to disagreements between *in vitro* and *in vivo* drug release from microspheres of a single formulation, there are also differences between *in vivo* drug release profiles of different classes of therapeutic molecules [18, 28, 33-35]. For example, it has been reported in the literature that the small molecule dexamethasone exhibits faster release *in vivo* than *in vitro*, whereas the protein vascular endothelial growth factor (VEGF) releases slower *in vivo* (Figure 1.3) [18, 33]. In these reports, both dexamethasone and VEGF were extracted from microspheres following administration in rats by removing subcutaneous tissue at the time of animal euthanasia and then scraping a small sample of particles from the tissue and performing extractions.

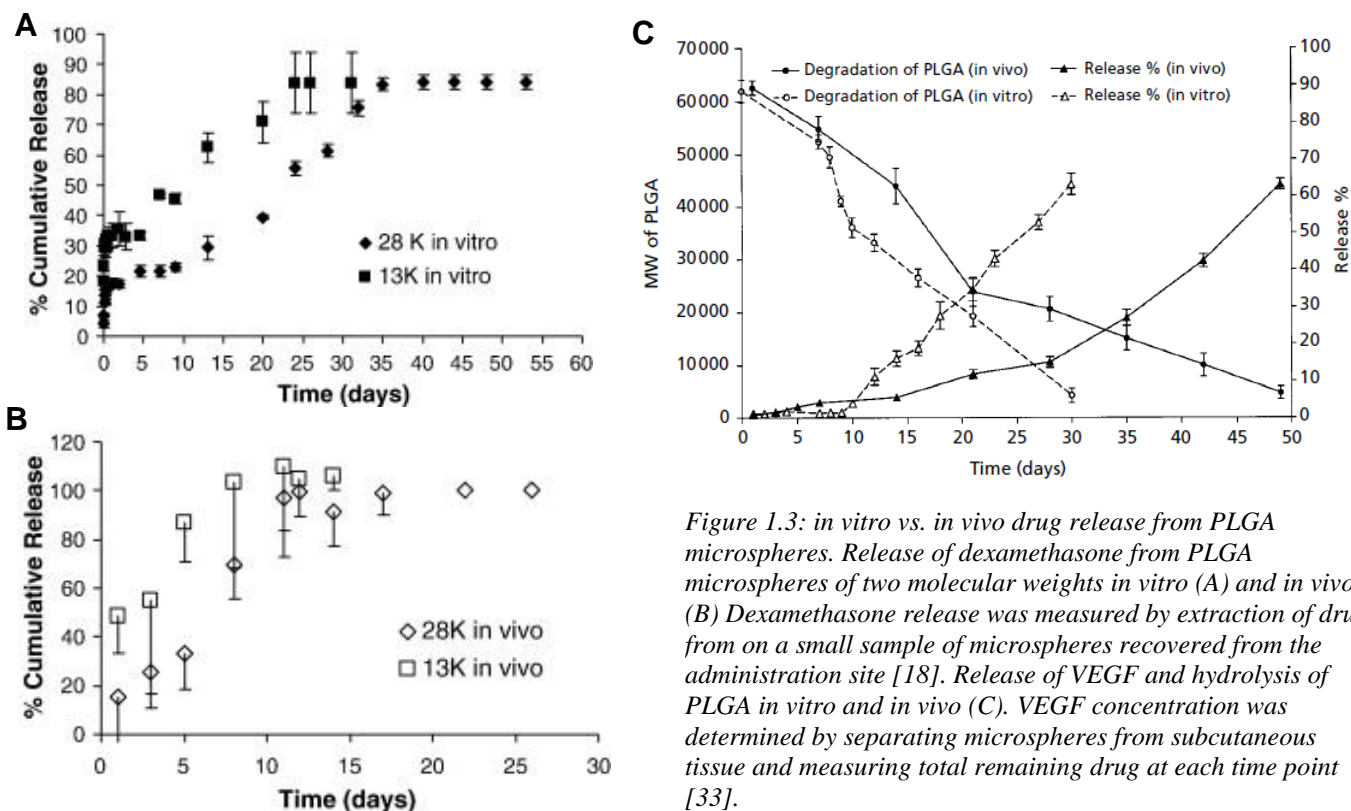


Figure 1.3: *in vitro* vs. *in vivo* drug release from PLGA microspheres. Release of dexamethasone from PLGA microspheres of two molecular weights *in vitro* (A) and *in vivo* (B) Dexamethasone release was measured by extraction of drug from on a small sample of microspheres recovered from the administration site [18]. Release of VEGF and hydrolysis of PLGA *in vitro* and *in vivo* (C). VEGF concentration was determined by separating microspheres from subcutaneous tissue and measuring total remaining drug at each time point [33].

1.4.3 Factors Affecting *in vivo* Drug Release

In order to fully understand why there are differences in drug release profiles from PLGA microparticles *in vitro* and *in vivo*, we must understand the mechanisms of drug release from PLGA *in vivo*. Factors present in the subcutaneous administration environment that are not accurately represented by current *in vitro* release environments have been discussed by some authors, but little work to date has been done in attempt to validate their hypotheses regarding how these factors influence drug release [34, 36-40]. Factors present *in vivo* that may alter the mechanism and/or rate of drug release from microparticles can be divided into two major categories: biological and physical-chemical.

1.4.3.1 *Biological factors*

It is clear that the subcutaneous administration of PLGA microparticles drastically changes the environment for drug release as compared to *in vitro* release conditions. Biological factors that may influence the way drugs are released from PLGA matrices include the inflammatory response and the presence of enzymes, lipids, organic amines, and other endogenous compounds present in the administration environment. It is well known that administration of any foreign material to the body will induce an inflammatory response; what is unknown is how this affects PLGA degradation and drug release from microparticles [34, 36, 41]. The tissue response to PLGA microsphere administration can be divided into three phases (Figure 1.4 [37]). The first phase, or the acute phase of the inflammatory response, occurs within one week following administration and is characterized by the presence of neutrophils in the area of the injection or implant. The second phase, or the onset of the chronic phase of inflammation, is characterized by the appearance of monocytes and macrophages. The duration of this phase depends on the rate of biodegradation of the microspheres; PLGA 50:50 microspheres have been shown to result in a phase II response of 40-50 days [42]. At later stages of the inflammatory response, fibroblasts infiltrate the site and collagen deposition is initiated to form a fibrous capsule. Neo-angiogenesis is also observed during this period [37]. Neutrophils, macrophages and foreign body giant cells which migrate to subcutaneous sites following microparticle injection may release enzymes, radicals, lipids, and acids which could influence both the rate and the mechanism of PLGA erosion [37, 39, 40]. Chronic phases of inflammation may lead to the formation of a fibrous capsule which surrounds the microspheres. This “walling off” could entrap PLGA acidic by-products and drug molecules, increasing auto-catalyzed PLGA hydrolysis and also preventing drug diffusion away from the microparticles [37]. Previous work

has shown that release of anti-inflammatory drugs from PLGA microparticles is faster *in vivo* than *in vitro*, whereas release of protein is slower *in vitro* [18, 33, 34]. It has also been reported that PLGA degradation is slower in muscle than in subcutaneous tissue, where the inflammatory response is more robust [43]. From this information, we can hypothesize that the inflammatory response may be an important modulator of drug release from PLGA microparticles *in vivo*.

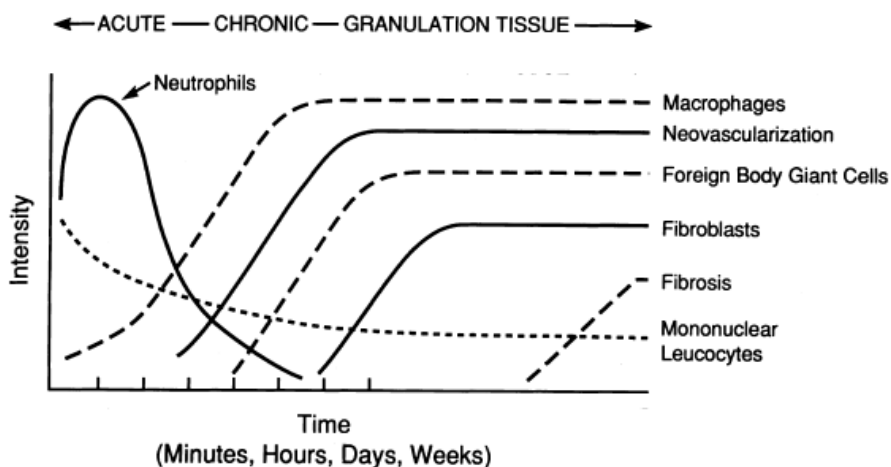


Figure 1.4: The temporal variation in the three phases of inflammatory response resulting from administration of biodegradable microspheres. (Figure from [37])

The presence of enzymes *in vivo* may influence the degradation of the polymer, as hydrolysis of the ester linkages in PLGA may be catalyzed by enzymes such as acid phosphatase, a hydrolase released from neutrophils and macrophages [36, 44]. If PLGA degradation is catalyzed by enzymes, microparticles undergo surface hydrolysis and erosion as well as bulk erosion which occurs due to autocatalysis [18]. It should be noted that the role of enzymes in PLGA hydrolysis is contested in the literature but has not yet been proved or disproved [45]. Another important factor to consider when studying drug release from PLGA *in vivo* is the presence of biological lipids which may act as plasticizers. Lipid chains may interact with the polymer and increase PLGA chain fluidity, decreasing the tortuosity of the drug diffusion pathway [34, 46]. It has previously been shown that plasticizers such as triethyl citrate increase

water uptake in PLGA and accelerate its hydrolysis and mass loss; all of which can contribute to accelerated drug release [47]. Finally, it is known that organic amines can strongly partition into PLGA and catalyze hydrolysis [48, 49]. Given the presence of amines such as monomethylamine and dimethylamine in the interstitial fluid (Table 1.1), it is reasonable to expect that these molecules may contribute to accelerated hydrolysis, erosion and subsequent release from PLGA microspheres *in vivo*.

Table 1.1: Endogenous compounds which may affects drug release from PLGA microspheres and their expected concentrations in subcutaneous interstitial fluid (ISF)

	Ion/Molecule	Concentration (mM)
Major Components of ISF [50-53]	Na ⁺	142
	K ⁺	5
	Mg ²⁺	1
	Ca ²⁺	2.5
	Cl ⁻	103
	HCO ₃ ⁻	27
	HPO ₄ ²⁻	1.0
	SO ₄ ²⁻	0.5
	Lactate	1.2
	Glucose	5.6
	Urea	5.0
	Albumin (protein)	0.375
	Creatinine	62
Urate	0.470	
Organic Amines	Monomethylamine[54]	0.10
	Dimethylamine[54]	0.333
	Ethylamine[55]	0.013
	Trimethylamine[56]	0.0004
	Ethanolamine[57]	0.06
Enzymes [58, 59]	Acid phosphatase	~5 U/L
	Alkaline phosphatase	~10 U/L
	Paraoxanase (PON1)[60]	0.021 g/L
Lipids [57, 61, 62]	Phosphatidylcholine	1.4
	Phosphatidylethanolamine	0.15
	Phosphatidylinositol	0.2
	Phosphatidylserine	0.1
	Lysophosphatidylcholine	0.6
Other Molecules of Interest	Ammonia[63]	0.29
	Fructosamine[64]	2.3
	Dopamine[65]	0.02
	Melanin[66]	5.4

1.4.3.2 *Physical-chemical factors*

Among the physical-chemical factors that may alter mechanisms of release from PLGA microspheres *in vivo* as compared to *in vitro* are the pH and buffering systems, fluid volume, and convection. While physiological pH is near 7, the interfacial pH between inflammatory cells (i.e. macrophages) and polymer surfaces can be as low as 3 [37, 41]. Lysosomes within inflammatory cells also have pH values around 3, suggesting that an inflammatory response to PLGA microspheres could drop the local pH lower than 7, the pH at which most drug products are tested for *in vitro* release [37]. In addition to the pH fluctuations due to the biological environment, the pH in the environment of the microspheres may become more acidic as PLGA erodes into lactic and glycolic acid. This is especially true if fibrous encapsulation occurs, which could potentially inhibit the diffusion of the acidic degradation products away from the polymer [18, 67]. The buildup of acidity in the environment surrounding microspheres may also be governed by physiological buffer systems and their buffering capacities. If the subcutaneous bicarbonate buffer system is capable of resisting changes in pH caused by the factors discussed here, perhaps pH changes caused by biological factors are negligible. It is also conceivable that components of the physiologic buffering system, i.e. carbonate-bicarbonate, may influence mechanisms of release differently than buffer systems used during *in vitro* release testing, such as phosphate buffers. A crucial part of any *in vitro* release test is the volume of media used. In most cases, sink conditions are maintained throughout the release test to prevent dissolution-controlled release and thus release volumes are determined by drug solubility [2]. Subcutaneous tissue, however, does not contain an excess of fluid and so it is likely that sink conditions do not actually apply *in vivo*. This is especially a concern for poorly soluble molecules, as a drug-concentrated external environment would inhibit further release from particles. Aggregation of

microspheres caused by fibrous encapsulation and low fluid volume convection will also decrease the volume available for drug diffusion, increase the thickness of unstirred boundary layers surrounding particles, and serve as a physical barrier for diffusion of drugs as well as acidic degradation products [36]. It has been shown that microspheres when aggregated in a gel to simulate *in vivo* aggregation will degrade faster than non-aggregated microspheres, presumably due to the autocatalytic effect of acidic byproducts trapped near the particles [68].

It is clear that the body's reaction to the administration of PLGA microparticles is a complex process made up of a number of factors which could potentially affect drug release in a variety of ways. It is generally believed that not any one factor is solely responsible, rather the interplay between these processes results in *in vivo* drug release kinetics different from those observed *in vitro*. What is important to understand is not just how these factors may change drug release rates, but the underlying causes for these changes. That is, what mechanisms of release (i.e. water uptake, hydrolysis, erosion, diffusion) are affected by the *in vivo* environment and what the resulting contributions are to drug release rates. The complicated nature of drug release and the multitude of factors, which affect this process is illustrated in Figure 1.5 [6].

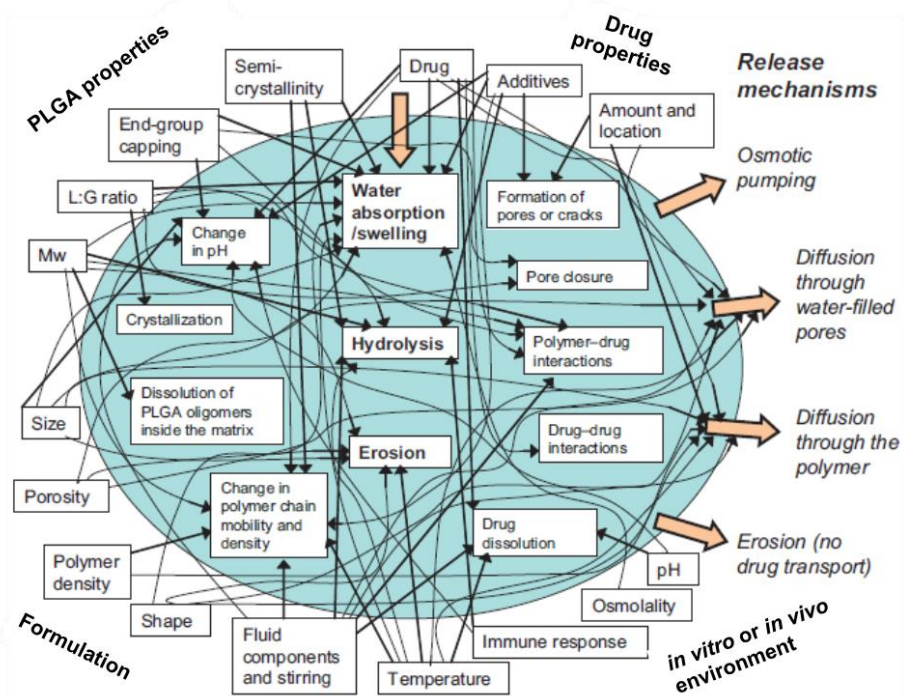


Figure 1.5: The complex nature of how different factors may affect drug release from PLGA matrices. (Figure from [6])

1.5 Research Scope and Impact

Drug release from PLGA microparticles can range from weeks to months, making *in vivo* drug release studies during formulation development not only time consuming but also very expensive. For these reasons, correlation between *in vitro* and *in vivo* drug release kinetics is crucial for controlled release product development. Using proper *in vitro* tests, we can model drug release from controlled release products and thus predict drug pharmacokinetics based on a comprehensive understanding of formulation behavior *in vivo*, resulting in *in vitro-in vivo* correlations (IVIVCs). Generally, IVIVCs are used as surrogates for *in vivo* dissolution and release tests, to validate *in vitro* release methods, and for quality control during product development and manufacturing. IVIVC development for controlled release systems is crucial for the continued development of these important drug delivery products. With reliable *in vitro* release methods, *in vivo* drug levels will be accurately predicted and expensive *in vivo* tests may

not be required during development [15, 69, 70]. IVIVCs also offer the ability to modify the product to perform in a desired way without having to gather *in vivo* data upon each modification. Not only would this drastically reduce development costs, but it would also decrease the time needed for final product development. Thus, it is vital to develop *in vitro* tests that can be used as reliable surrogates for extraneous *in vivo* studies to predict product performance [15, 71-73]. The research presented here will contribute to the development of mechanism-based *in vitro-in vivo* correlations (IVIVCs) for PLGA microspheres.

1.6 Thesis Overview

The preceding discussion highlights that one major difficulty in the development of controlled release injectable PLGA microparticles is that drug release *in vivo* is often different than what is predicted from *in vitro* release tests. This gap in knowledge can be linked to a lack of a mechanistic understanding of drug release from these dosage forms *in vivo*. *In vitro* release tests currently used and described in the literature are not designed to simulate the administration environment, resulting in poor prediction of performance. Design of *in vitro* test conditions should be performed only after the *in vivo* environment has been studied and *in vivo* drug release kinetics have been characterized [73].

The overall goal of this thesis is to investigate the major mechanisms of release from PLGA microspheres *in vivo* and in a variety of *in vitro* conditions, with the overall intent of determining how these processes differ. This will provide insight as to why *in vitro* release tests are sometimes poor predictors of *in vivo* performance of PLGA controlled release products. Ultimately, the research described here will help to design better *in vitro* release tests for these products based on a mechanistic understanding of *in vivo* drug release.

Chapter 2 of this thesis describes the development of PLGA microspheres encapsulating a model drug, triamcinolone acetonide (Tr-A), and determination of release mechanisms in a variety of *in vitro* release media. This section highlights the effects varying release conditions can have on drug release rate and mechanisms of release, including water uptake, hydrolysis, mass loss and diffusion. This work shows how *in vitro* release tests can be designed to incorporate different buffers and additives to alter release rates and mechanisms of release.

Chapter 3 describes the development of a system allowing the study of PLGA microspheres following administration *in vivo*. The major challenge faced during development of these formulations is a poor understanding of mechanisms of release *in vivo*. In this section, an implant was designed to constrain PLGA microparticles in the subcutaneous space so that the formulation itself can be studied following exposure to the *in vivo* release environment. Two drugs, Tr-A and leuprolide, were used to prove the utility of the cage model in a series of *in vitro* and *in vivo* experiments. The work discussed here shows that the cage does not strongly influence drug release after the initial burst and thus is a good tool to study *in vivo* microsphere performance. This cage implant is a novel system and can be used to study a number of injectable controlled release formulations with the ultimate goal being the development of a mechanistic understanding of *in vivo* behavior in order to better design *in vitro* tests.

Chapter 4 discusses the experiments utilizing the previously developed cage implant to determine kinetics of release and the relevant mechanisms *in vivo*. Tr-A release is shown to be much faster *in vivo* than *in vitro*, a result that is in good agreement with the previously discussed literature. Although release *in vivo* has been studied by a number of authors before, a comprehensive mechanistic analysis of PLGA microspheres during *in vivo* release has never

been published. Using two formulations of Tr-A, we were able to determine how mechanisms of release differ from those studied in Chapter 2.

The conclusions of this work and implications for future studies are discussed in Chapter 5. There are two appendices highlighting formulation work done outside the scope of the main content of this dissertation work. Much of this thesis is in preparation for publication. Chapter 2 is under review for publication in *Molecular Pharmaceutics*. Chapter 3 will be submitted for publication once additional *in vivo* experiments with leuprolide are completed. Chapter 4 will be published upon publication of Chapter 3, as it uses the cage model developed in that work. Finally, Appendix B, including additional *in vivo* data produced by collaborators, has been submitted to *Journal of Controlled Release* for review.

1.7 References

1. Schwendeman, S.P., et al., *Progress and challenges for peptide, protein, and vaccine delivery from implantable polymeric systems*, in *Controlled Drug Delivery: Challenges and Strategies*, K. Park, Editor. 1997, The American Chemical Society: Washington, D.C. p. 229-267.
2. Wischke, C. and S.P. Schwendeman, *Principles of encapsulating hydrophobic drugs in PLA/PLGA microparticles*. *International Journal of Pharmaceutics*, 2008. **364**(2): p. 298-327.
3. Urich, K.E., et al., *Polymeric Systems for Controlled Drug Release*. *Chemical Reviews*, 1999. **99**(11): p. 3181-3198.
4. Langer, R.S. and N.A. Peppas, *Present and future applications of biomaterials in controlled drug delivery systems*. *Biomaterials*, 1981. **2**(4): p. 201-214.
5. Makadia, H.K. and S.J. Siegel, *Poly Lactic-co-Glycolic Acid (PLGA) as Biodegradable Controlled Drug Delivery Carrier*. *Polymers*, 2011. **3**(3): p. 1377-1397.
6. Fredenberg, S., et al., *The mechanisms of drug release in poly(lactic-co-glycolic acid)-based drug delivery systems—A review*. *International Journal of Pharmaceutics*, 2011. **415**(1–2): p. 34-52.
7. Siegel, R.A. and M.J. Rathbone, *Overview of Controlled Release Mechanisms: Fundamentals and Applications of Controlled Release Drug Delivery*, J. Siepmann, R.A. Siegel, and M.J. Rathbone, Editors. 2012, Springer US. p. 19-43.
8. Jain, R.A., *The manufacturing techniques of various drug loaded biodegradable poly(lactide-co-glycolide) (PLGA) devices*. *Biomaterials*, 2000. **21**(23): p. 2475-2490.
9. Rhee, Y.-S., et al., *Sustained-Release Injectable Drug Delivery*. *Pharmaceutical Technology*, Nov 1 2010: p. s6-s13.
10. *Abbott Lupron Depot Prescribing Information*. 2012.
11. Wang, J., B.M. Wang, and S.P. Schwendeman, *Characterization of the initial burst release of a model peptide from poly(d,l-lactide-co-glycolide) microspheres*. *Journal of Controlled Release*, 2002. **82**(2–3): p. 289-307.
12. Allison, S.D., *Analysis of initial burst in PLGA microparticles*. *Expert Opin Drug Deliv*, 2008. **5**(6): p. 615-28.
13. Ding, A.G., A. Shenderova, and S.P. Schwendeman, *Prediction of Microclimate pH in Poly(lactic-co-glycolic Acid) Films*. *Journal of the American Chemical Society*, 2006. **128**(16): p. 5384-5390.
14. Zhu, G. and S.P. Schwendeman, *Stabilization of Proteins Encapsulated in Cylindrical Poly(lactide-co-glycolide) Implants: Mechanism of Stabilization by Basic Additives*. *Pharmaceutical Research*, 2000. **17**(3): p. 351-357.
15. Young, D., C. Farrell, and T. Shepard, *In Vitro/In Vivo Correlation for Modified Release Injectable Drug Delivery Systems*, in *Injectable Dispersed Systems: Formulation, Processing and Performance*, D. Burgess, Editor. 2005, Taylor & Francis Group: Boca Raton. p. 159-176.
16. Zolnik, B.S., *In Vitro and In Vivo Release Testing of Controlled Release Parenteral Microspheres*, in *Pharmaceutics*. 2005, University of Connecticut: Storrs.
17. D'Souza, S. and P. DeLuca, *Methods to Assess In Vitro Drug Release from Injectable Polymeric Particulate Systems*. *Pharmaceutical Research*, 2006. **23**(3): p. 460-474.

18. Zolnik, B.S. and D.J. Burgess, *Evaluation of in vivo-in vitro release of dexamethasone from PLGA microspheres*. Journal of Controlled Release, 2008. **127**(2): p. 137-145.
19. Zolnik, B.S. and D.J. Burgess, *In Vitro–In Vivo Correlation on Parenteral Dosage Forms*, in *Biopharmaceutics Applications in Drug Development*, R. Krishna and L. Yu, Editors. 2008, Springer US. p. 336-358.
20. Martinez, M., et al., *In vitro and in vivo considerations associated with parenteral sustained release products: A review based upon information presented and points expressed at the 2007 Controlled Release Society Annual Meeting*. Journal of Controlled Release, 2008. **129**(2): p. 79-87.
21. Blanco-Prieto, M.a.J., et al., *In vitro and in vivo evaluation of a somatostatin analogue released from PLGA microspheres*. Journal of Controlled Release, 2000. **67**(1): p. 19-28.
22. Liu, W.H., et al., *Preparation and in vitro and in vivo release studies of Huperzine A loaded microspheres for the treatment of Alzheimer's disease*. Journal of Controlled Release, 2005. **107**(3): p. 417-427.
23. Mundargi, R.C., et al., *Development and evaluation of novel biodegradable microspheres based on poly(d,l-lactide-co-glycolide) and poly(ε-caprolactone) for controlled delivery of doxycycline in the treatment of human periodontal pocket: In vitro and in vivo studies*. Journal of Controlled Release, 2007. **119**(1): p. 59-68.
24. Schliecker, G., et al., *In vitro and in vivo correlation of buserelin release from biodegradable implants using statistical moment analysis*. Journal of Controlled Release, 2004. **94**(1): p. 25-37.
25. Makino, K., et al., *Pulsatile drug release from poly (lactide-co-glycolide) microspheres: how does the composition of the polymer matrices affect the time interval between the initial burst and the pulsatile release of drugs?* Colloids and Surfaces B: Biointerfaces, 2000. **19**(2): p. 173-179.
26. Huang, X. and C.S. Brazel, *On the importance and mechanisms of burst release in matrix-controlled drug delivery systems*. Journal of Controlled Release, 2001. **73**(2–3): p. 121-136.
27. Heya, T., et al., *Controlled release of thyrotropin releasing hormone from microspheres: evaluation of release profiles and pharmacokinetics after subcutaneous administration*. J Pharm Sci, 1994. **83**(6): p. 798-801.
28. Heya, T., et al., *In vitro and in vivo evaluation of thyrotrophin releasing hormone release from copoly (dl-lactic/glycolic acid) microspheres*. Journal of Pharmaceutical Sciences, 1994. **83**(5): p. 636-640.
29. Kostanski, J.W., et al., *Evaluation of Orntide microspheres in a rat animal model and correlation to in vitro release profiles*. AAPS PharmSciTech, 2000. **1**(4): p. E27.
30. Negrin, C.M., et al., *In vivo-in vitro study of biodegradable methadone delivery systems*. Biomaterials, 2001. **22**(6): p. 563-70.
31. Rawat, A., U. Bhardwaj, and D.J. Burgess, *Comparison of in vitro-in vivo release of Risperdal((R)) Consta((R)) microspheres*. Int J Pharm, 2012. **434**(1-2): p. 115-21.
32. Morita, T., et al., *Evaluation of in vivo release characteristics of protein-loaded biodegradable microspheres in rats and severe combined immunodeficiency disease mice*. J Control Release, 2001. **73**(2-3): p. 213-21.
33. Kim, T.-K. and D.J. Burgess, *Pharmacokinetic characterization of 14C-vascular endothelial growth factor controlled release microspheres using a rat model*. Journal of Pharmacy and Pharmacology, 2002. **54**(7): p. 897-905.

34. Tracy, M.A., et al., *Factors affecting the degradation rate of poly(lactide-co-glycolide) microspheres in vivo and in vitro*. *Biomaterials*, 1999. **20**(11): p. 1057-62.
35. Diaz, R.V., M. Llabrés, and C. Évora, *One-month sustained release microspheres of 125I-bovine calcitonin: In vitro—in vivo studies*. *Journal of Controlled Release*, 1999. **59**(1): p. 55-62.
36. Anderson, J.M., A. Rodriguez, and D.T. Chang, *Foreign body reaction to biomaterials*. *Seminars in Immunology*, 2008. **20**(2): p. 86-100.
37. Anderson, J.M. and M.S. Shive, *Biodegradation and biocompatibility of PLA and PLGA microspheres*. *Advanced Drug Delivery Reviews*, 1997. **28**(1): p. 5-24.
38. Williams, D.F., *Some Observations on the Role of Cellular Enzymes in the In-Vivo Degradation of Polymers*, in *Corrosion and Degradation of Implant Materials*, ASTM STP 684, B.C. Syrett and A. Acharya, Editors. 1979, American Society for Testing and Materials. p. 61-75.
39. Xia, Z. and J.T. Triffitt, *A review on macrophage responses to biomaterials*. *Biomed Mater*, 2006. **1**(1): p. R1-9.
40. Ali, S.A.M., P.J. Doherty, and D.F. Williams, *Molecular biointeractions of biomedical polymers with extracellular exudate and inflammatory cells and their effects on the biocompatibility, in vivo*. *Biomaterials*, 1994. **15**(10): p. 779-785.
41. Anderson, J.M., *In Vitro and In Vivo Monocyte, Macrophage, Foreign Body Giant Cell, and Lymphocyte Interactions with Biomaterials*, in *Biological Interactions on Materials Surfaces*, D.A. Puleo and R. Bizios, Editors. 2009, Springer New York. p. 225-244.
42. Visscher, G.E., et al., *Biodegradation of and tissue reaction to 50:50 poly(DL-lactide-co-glycolide) microcapsules*. *J Biomed Mater Res*, 1985. **19**(3): p. 349-65.
43. Chu, D.-F., et al., *Pharmacokinetics and in vitro and in vivo correlation of huperzine A loaded poly(lactic-co-glycolic acid) microspheres in dogs*. *International Journal of Pharmaceutics*, 2006. **325**(1-2): p. 116-123.
44. Schakenraad, J.M., et al., *Enzymatic activity toward poly(L-lactic acid) implants*. *Journal of Biomedical Materials Research*, 1990. **24**(5): p. 529-545.
45. Alexis, F., *Factors affecting the degradation and drug-release mechanism of poly(lactic acid) and poly[(lactic acid)-co-(glycolic acid)]*. *Polymer International*, 2005. **54**(1): p. 36-46.
46. Menei, P., et al., *Biodegradation and brain tissue reaction to poly(D,L-lactide-co-glycolide) microspheres*. *Biomaterials*, 1993. **14**(6): p. 470-478.
47. Kranz, H., et al., *Physicomechanical properties of biodegradable poly(D,L-lactide) and poly(D,L-lactide-co-glycolide) films in the dry and wet states*. *Journal of Pharmaceutical Sciences*, 2000. **89**(12): p. 1558-1566.
48. Maulding, H.V., et al., *Biodegradable microcapsules: Acceleration of polymeric excipient hydrolytic rate by incorporation of a basic medicament*. *Journal of Controlled Release*, 1986. **3**(1-4): p. 103-117.
49. Pitt, C.G., et al., *Sustained drug delivery systems. I. The permeability of poly(epsilon-caprolactone), poly(DL-lactic acid), and their copolymers*. *J Biomed Mater Res*, 1979. **13**(3): p. 497-507.
50. Sirieix, D., et al., *Tris-hydroxymethyl aminomethane and sodium bicarbonate to buffer metabolic acidosis in an isolated heart model*. *American Journal of Respiratory and Critical Care Medicine*, 1997. **155**(3): p. 957-963.

51. Marques, M.R.C., R. Loebenberg, and M. Almukainzi, *Simulated Biological Fluids with Possible Application in Dissolution Testing*. Dissolution Technologies, 2011. **18**(3): p. 15-28.
52. Fogh-Andersen, N., et al., *Composition of interstitial fluid*. Clinical Chemistry, 1995. **41**(10): p. 1522-5.
53. Oyane, A., et al., *Preparation and assessment of revised simulated body fluids*. Journal of Biomedical Materials Research Part A, 2003. **65A**(2): p. 188-195.
54. Aronov, P.A., et al., *Colonic Contribution to Uremic Solutes*. Journal of the American Society of Nephrology, 2011. **22**(9): p. 1769-1776.
55. Raff, A.C., et al., *Relationship of impaired olfactory function in ESRD to malnutrition and retained uremic molecules*. Am J Kidney Dis, 2008. **52**(1): p. 102-10.
56. Bain, M.A., et al., *Accumulation of trimethylamine and trimethylamine-N-oxide in end-stage renal disease patients undergoing haemodialysis*. Nephrology Dialysis Transplantation, 2006. **21**(5): p. 1300-1304.
57. Sugiyama, K., et al., *Amino acid composition of dietary proteins affects plasma cholesterol concentration through alteration of hepatic phospholipid metabolism in rats fed a cholesterol-free diet*. The Journal of Nutritional Biochemistry, 1996. **7**(1): p. 40-48.
58. Bergsma, J.E., et al., *Biocompatibility study of as-polymerized poly(L-lactide) in rats using a cage implant system*. Journal of Biomedical Materials Research, 1995. **29**(2): p. 173-179.
59. Hassan, S.S.M., H.E.M. Sayour, and A.H. Kamel, *A simple-potentiometric method for determination of acid and alkaline phosphatase enzymes in biological fluids and dairy products using a nitrophenylphosphate plastic membrane sensor*. Analytica Chimica Acta, 2009. **640**(1-2): p. 75-81.
60. Mackness, M.I., et al., *Presence of paraoxonase in human interstitial fluid*. FEBS Letters, 1997. **416**(3): p. 377-380.
61. Deckelbaum, R.J., et al., *Plasma triglyceride determines structure-composition in low and high density lipoproteins*. Arteriosclerosis, Thrombosis, and Vascular Biology, 1984. **4**(3): p. 225-31.
62. Walkey, C.J., et al., *Biochemical and Evolutionary Significance of Phospholipid Methylation*. Journal of Biological Chemistry, 1998. **273**(42): p. 27043-27046.
63. *The Merck Manual, 17th edition*. 1999: Merck Research Labs.
64. Jury, D.R. and P.J. Dunn, *Laboratory assessment of a commercial kit for measuring fructosamine in serum*. Clin Chem, 1987. **33**(1): p. 158-61.
65. Fonteh, A.N., et al., *Free amino acid and dipeptide changes in the body fluids from Alzheimer's disease subjects*. Amino Acids, 2007. **32**(2): p. 213-24.
66. Hegedus, Z.L., *The probable involvement of soluble and deposited melanins, their intermediates and the reactive oxygen side-products in human diseases and aging*. Toxicology, 2000. **145**(2-3): p. 85-101.
67. Zolnik, B.S. and D.J. Burgess, *Effect of acidic pH on PLGA microsphere degradation and release*. Journal of Controlled Release, 2007. **122**(3): p. 338-344.
68. Sansdrap, P. and A.J. Moës, *In vitro evaluation of the hydrolytic degradation of dispersed and aggregated poly(-lactide-co-glycolide) microspheres*. Journal of Controlled Release, 1997. **43**(1): p. 47-58.
69. Burgess, D., et al., *Assuring quality and performance of sustained and controlled release parenterals: EUFEPS workshop report*. The AAPS Journal, 2004. **6**(1): p. 100-111.

70. Lu, Y., S. Kim, and K. Park, *In vitro–in vivo correlation: Perspectives on model development*. International Journal of Pharmaceutics, 2011. **418**(1): p. 142-148.
71. Clark, B. and P. Dickinson, *Case Study: In Vitro/In Vivo Release from Injectable Microspheres*, in *Injectable Dispersed Systems: Formulation, Processing and Performance* D. Burgess, Editor. 2005, Taylor & Francis Group: Boca Raton, FL. p. 543-570.
72. Uppoor, V.R.S., *Regulatory perspectives on in vitro (dissolution)/in vivo (bioavailability) correlations*. Journal of Controlled Release, 2001. **72**(1–3): p. 127-132.
73. Mitra, A. and Y. Wu, *Use of In Vitro-In Vivo Correlation (IVIVC) to Facilitate the Development of Polymer-Based Controlled Release Injectable Formulations*. Recent Patents on Drug Delivery and Formulation, 2010. **4**(2): p. 94-104.

Chapter 2 : Mechanistic Analysis of Triamcinolone Acetonide Release from PLGA Microspheres as a Function of Varying *in vitro* Release Conditions

2.1 Abstract

In vitro tests for controlled release PLGA microspheres in their current state often do not accurately predict *in vivo* performance of these products during formulation development. In order to develop more predictive release tests, mechanisms of drug release from PLGA microparticles *in vivo* and *in vitro* must be understood. Two microsphere formulations encapsulating a model drug, triamcinolone acetonide, were prepared from PLGAs of different molecular weights and end-capping (18 kDa acid-capped and 54 kDa ester-capped). *In vitro* release kinetics and the corresponding mechanisms (hydrolysis, erosion, water uptake, and diffusion) were studied in four release media: PBST pH 7.4 (standard condition), PBST pH 6.5, PBS + 1.0% triethyl citrate (TC), and HBST pH 7.4. The release mechanism in PBST was primarily polymer erosion-controlled as indicated by the similarity of release and mass loss kinetics. Release from the low MW PLGA was accelerated at low pH due to increased rate of hydrolysis and in the presence of the plasticizer TC due to slightly increased hydrolysis and much higher diffusion in the polymer matrix. TC also increased release from the high MW PLGA due to increased hydrolysis, erosion, and diffusion. This work demonstrates how *in vitro* conditions can be manipulated to change not only rates of drug release from PLGA microspheres but also the mechanism(s) by which release occurs. This approach can in principle be applied to design better, more predictive *in vitro* release tests for these formulations and potentially lead to mechanism-based *in vitro-in vivo* correlations.

2.2 Introduction

Poly(lactic-*co*-glycolic) acid (PLGA) is the most commonly used biodegradable polymer used to achieve long-term controlled drug release over weeks to months [1]. A wide range of therapeutic molecules, such as peptides, proteins, and poorly soluble small molecules, have been encapsulated in PLGA formulations [2, 3]. During the development of these formulations, *in vitro* experiments are performed to measure drug release kinetics, which are used to predict *in vivo* release and pharmacokinetics of the encapsulated drug. Although these tests are routine, no formal FDA guidelines currently exist for assessing *in vitro* release from injectable controlled release (CR) formulations to establish *in vitro-in vivo* correlations (IVIVCs) for accurately predicting *in vivo* performance. This has resulted in inconsistencies in the methods used for *in vitro* release tests reported in the literature and in many cases, poor prediction of *in vivo* release. [4, 5]

Drug release rates measured during *in vitro* tests can change depending on the experimental setup and/or the media used [6-11]. Ideally *in vitro* release tests can be designed to accurately predict *in vivo* release by selecting both the proper setup and media, ultimately resulting in IVIVCs. This need has been thoroughly discussed in recent years in the literature and during regulatory-scientific meetings [4, 12-18]. Discussion of IVIVC development for CR products has focused on the need to design *in vitro* tests to mimic not only the rate of drug release *in vivo*, but the underlying mechanistic factors responsible for drug release *in vivo*.

To begin developing IVIVCs for PLGA microspheres, a mechanistic understanding of drug release *in vitro* and *in vivo* must be achieved. The purpose of this work was to study mechanisms of *in vitro* drug release from two PLGA microsphere formulations in varying bio-

relevant media with the overall objective of understanding how to design *in vitro* release conditions to mimic mechanisms of drug release *in vivo*.

To develop our mechanistic analysis, we selected the poorly soluble corticosteroid triamcinolone acetonide (Tr-A) as a model drug. Tr-A was chosen for this mechanistic study for several reasons, including 1) its low susceptibility to polymorphism, 2) good stability, and 3) ease of quantitation using standard analytical techniques. It also represents poorly soluble small molecules in BCS classes II and IV for which traditional formulations (e.g. oral tablets or capsules) may be difficult to develop but represent a growing number of new chemical entities. Various drugs in this class have been developed in commercial PLGA controlled release products. These drugs also often 1) have a wide therapeutic index, 2) require a low daily dose, and 3) are for long-term treatment of chronic disease, all conditions favorable for a PLGA controlled release strategy.

Drug release from PLGA microspheres can be controlled principally by at least three rate-limiting release mechanisms or combinations thereof; 1) diffusion through the polymer matrix, 2) water-mediated transport processes, and 3) polymer hydrolysis and subsequent erosion. It is important to note that drug release is often the result of more than one of these mechanisms and that these mechanisms are not independent of each other. For example, water uptake in the polymer matrix will cause hydrolysis of the PLGA chains. The resulting monomers and oligomers will then diffuse out of the polymer through aqueous pores, resulting in overall erosion.

It is possible to determine the major mechanisms contributing to drug release from PLGA microspheres at certain times by determining time scales of each mechanism and comparing to the kinetics of overall release. For example, if erosion dominates drug release it is expected that

these two processes would occur roughly on the same time scale, meaning that if 50% of the polymer matrix has eroded we would expect roughly 50% of drug to be released at that time. Similarly, drug release from a purely diffusion controlled system can be modeled using the appropriate matrix diffusion model [19]. These strategies, among others, were applied herein to determine the contributions of each mechanism to overall drug release in several types of *in vitro* release media. This discussion will highlight the need to design *in vitro* release tests that will predict not only drug release rates *in vivo*, but the mechanisms by which release occurs following administration.

2.3 Materials

Triamcinolone acetonide (Tr-A) and PLGA RESOMER® 502H (i.v. = 0.19 dL/g, free acid terminated) were purchased from Sigma-Aldrich. Poly vinyl alcohol (PVA, 88% hydrolyzed, MW ~ 25,000) was purchased from Polysciences, Inc. (Warrington, PA). PLGA (i.v. = 0.61 dL/g, ester terminated) was purchased from Lactel (Birmingham, AL). BODIPY® FL (4,4-Difluoro-5,7-Dimethyl-4-Bora-3a,4a-Diaza-s-Indacene-3-Propionic Acid) was purchased from Life Technologies. All solvents used were HPLC grade and were purchased from Fisher Scientific and unless otherwise noted, all other chemicals were purchased from Sigma-Aldrich.

2.4 Methods

2.4.1 *Microsphere Preparation*

Microspheres were prepared by using solid-in-oil-in-water (s/o/w) double-emulsion solvent evaporation methods. Two polymers were used to encapsulate Tr-A to result in two formulations. The first (Tr-A_1) used a low molecular weight, free acid terminated PLGA 502H (18 kDa); Tr-A_2 used a moderate molecular weight, ester terminated (e.t.) PLGA (54 kDa). Control studies from a wide number of formulations were used to select these two formulations

for further evaluations (see supplementary information). Tr-A was first micronized in a cryo-mill (Retsch®, PA, USA) prior to formulation to obtain drug particle sizes < 10 µm. Micronized or unmicronized drug (5% w/w theoretical Tr-A loading) was mixed with PLGA dissolved in methylene chloride (Tr-A_1: 1000 mg/mL; Tr-A_2: 400 mg/mL) and homogenized at 10,000 rpm for 1 minute to form a s/o suspension. Next, 4 mL of a 5% PVA solution was added and vortexed at high speed for 1 minute. This s/o/w emulsion was rapidly transferred to 100 mL 0.5% PVA stirring bath. The methylene chloride was allowed to evaporate for 3 h and the hardened microspheres were collected by sieve (63-90µm) and washed thoroughly with ddH₂O. Microspheres were then lyophilized and stored at -20°C before use.

2.4.2 *Scanning Electron Microscopy*

Prior to imaging, lyophilized microspheres were mounted by using double sided carbon tape and coated with a thin layer of gold under vacuum. Scanning electron microscopy (SEM) was performed on a Hitachi S3200N scanning electron microscope (Hitachi, Japan). Images were captured by EDAX® software.

2.4.3 *Determination of Tr-A Loading and Encapsulation Efficiency*

Prepared microspheres (~5 mg) were dissolved in 20 mL acetonitrile. The resulting solution was filtered and analyzed for Tr-A content by ultra-performance liquid chromatography (UPLC), as described below. Drug loading was calculated from the ratio of the mass of drug in the microspheres to the mass of the microspheres. Encapsulation efficiency was calculated by the measured drug loading divided by the theoretical loading.

2.4.4 *Tr-A Quantification by UPLC*

Tr-A content in loading solutions and release media was determined using UPLC (Acquity UPLC, Waters, USA). The mobile phase was composed of either 40 : 60 v/v (acetonitrile :

ddH₂O) or 70 : 30 v/v (methanol : water) and the flow rate was set to 0.5 mL/minute. Samples and standards prepared in either acetonitrile or PBST were injected onto a C18 (Acquity BEH C18, 1.7µm, 2.1 x 100mm) column maintained at 30°C. Tr-A was detected at 254 nm.

2.4.5 *Assessment of Drug Release in vitro*

Drug release and mechanistic analyses of microspheres was carried out in four types of release media: PBS (137mM NaCl, 3mM KCl, 7.74 mM Na₂HPO₄, 2.26 mM NaH₂PO₄) at pH 7.4 and 6.5; 10 mM HBS (HEPES-buffered saline) at pH 7.4; and PBS with 1.0% triethyl citrate (TC) at pH 7.4. PBS pH 7.4, PBS pH 6.5, and HBS all contained 0.02% Tween 80 and all media contained 0.05% NaN₃. These media were chosen to determine the effects of various pH, buffering species, and presence of plasticizer expected to represent plasticizing biological species (e.g. lipids). Microspheres (3-5 mg) were placed in 30 ml of media and shaken mildly at 37°C for the duration of the experiment. At each time point (1, 3, 7 days and weekly thereafter), the microspheres were separated from media by centrifugation at 4,000 rpm (3200 g) for 5 min (Eppendorf 5810 R; Eppendorf, Hamburg, Germany)) and the media was completely removed and replaced. Drug content was measured by UPLC, as previously described.

2.4.6 *Mass Loss and Water Uptake of Microspheres:*

During *in vitro* release, mass loss and water content of the PLGA microspheres was determined weekly. Microspheres were separated from release media by filtration and washed with ddH₂O to remove salts. The wet weight of microspheres was recorded and then the microspheres were dried under vacuum to constant weight. Mass loss and water uptake were estimated as previously described [20].

2.4.7 *Molecular Weight of PLGA*

During *in vitro* release, weight-averaged molecular weight (Mw) of degrading PLGA was measured by gel permeation chromatography (GPC) weekly. The Waters 1525 GPC system (Waters, USA) consisted of two styragel columns (HR 1 and HR 5-E columns), a binary HPLC pump, waters 717 plus autosampler, waters 2414 refractive index detector and Breeze software to obtain the molecular weight. Samples were dissolved in tetrahydrofuran (THF) at a concentration of ~1 mg/ml, filtered through a 0.2 μm hydrophobic filter and eluted with THF at 0.35 ml/min. The molecular weight of each sample was calculated using monodisperse polystyrene standards, Mw 820-450000 Da.

2.4.8 *BODIPY uptake and Laser Scanning Confocal Microscopy (LSCM):*

At certain time points during *in vitro* release, a small aliquot of microspheres was removed from release media and incubated in a solution of BODIPY FL (5 $\mu\text{g/mL}$) in the same media at 37°C for 10 min or 3 h under mild agitation. This dye was used due to its preferential partitioning into the polymer phase, making it a suitable marker for solid-state diffusion, as previously described by our lab [20, 21]. BODIPY distribution in degrading microspheres and subsequent image analysis was determined as previously described [21]. Briefly, microspheres were imaged using a Nikon A1 spectral confocal microscope (Nikon, Tokyo, Japan) to observe dye distribution and microsphere morphology. The images were then analyzed using ImageJ software (National Institutes of Health, USA). Normalized dye intensity (I/I_0) – position (r/a) pairs were then fit to the solution of Fick's second law of diffusion using DataFit software (Oakdale Engineering, USA) to determine the effective solid-state diffusion coefficient of bodipy (D_{bodipy}), as described previously [21].

2.4.9 *Modelling Tr-A diffusion-controlled release*

Blank_1 (free acid terminated PLGA, 18 kDa) and Blank_2 (ester terminated PLGA, 54 kDa) microspheres were prepared using the same methods as described above, omitting the addition of the Tr-A during formation of the first emulsion. These microspheres were suspended in PBST pH 7.4 for one day, at which time the release media was replaced with a supersaturated Tr-A suspension in PBST pH 7.4. Microspheres were then separated and washed thoroughly on a 45 μm sieve with cold ddH₂O at 2, 4, 6, 8, 12, 24 and 48h. Tr-A content in microspheres following uptake was determined by extraction with acetonitrile followed by analysis by UPLC. The uptake of Tr-A was fit using DataFit software to Crank's solution using for uptake into or release from particles of spherical morphology to determine an effective solid state diffusion coefficient [22]. This diffusion coefficient ($D_{\text{Tr-A}}$) was then compared to D_{bodipy} in blank microspheres at the same time point to determine $D_{\text{Tr-A}}/D_{\text{bodipy}}$ so that drug diffusion coefficients at each time point could be estimated from the bodipy uptake experiments described above. The resulting $D_{\text{Tr-A}}$ values were then used to develop corresponding theoretical release profiles using the Higuchi equation for spherical systems [23]. See supplementary information for more details.

2.4.10 *Statistical and Regression Analysis*

Statistical analyses and regressions were performed using Prism (Graphpad, San Diego, CA). Rate constants, t_{50} values, and diffusion coefficients in various media were compared to standard conditions (PBST pH 7.4) using unpaired student t-tests to determine two-tailed P-values. The level of significance was established at the 95% confidence interval ($\alpha < 0.05$).

2.5 Results and Discussion

PLGA microspheres encapsulating Tr-A were successfully prepared using micronized API powder in two types of PLGAs: a low molecular weight free-acid terminated PLGA and a

moderate molecular weight ester-end capped PLGA. As Tr-A is poorly soluble in methylene chloride, the drug was encapsulated as a solid during formulation. In an effort to optimize encapsulation and release, the drug powder was micronized to obtain a small particle size which can be efficiently encapsulated by the polymer during formation of the first emulsion. Initially, Tr-A was micronized by grinding with mortar and pestle and sieving through a 20 μm sieve. However, this process resulted in heterogeneous powder size (Figure 2.1A) and the resulting microsphere formulations exhibited poor and variable drug loading and encapsulation efficiency (Table 2.1). Therefore, a cryo-mill (Retsch®, PA, USA) was used to obtain a homogenous powder size less than 10 μm (Figure 2.1B). The encapsulation of this milled powder greatly improved encapsulation efficiency, decreased variability in drug loading, and lowered initial burst in PBST pH 7.4 (Table 2.1). The incorporation of homogeneously sized Tr-A powder into microspheres resulted in encapsulation efficiencies slightly higher than 100%. This slight excess loading was likely caused by discarding the fine fraction below 63 μm sieve size, which are expected to contain a lower drug loading. Accordingly, microspheres formulated using the cryo-milled Tr-A were used for all studies discussed herein.

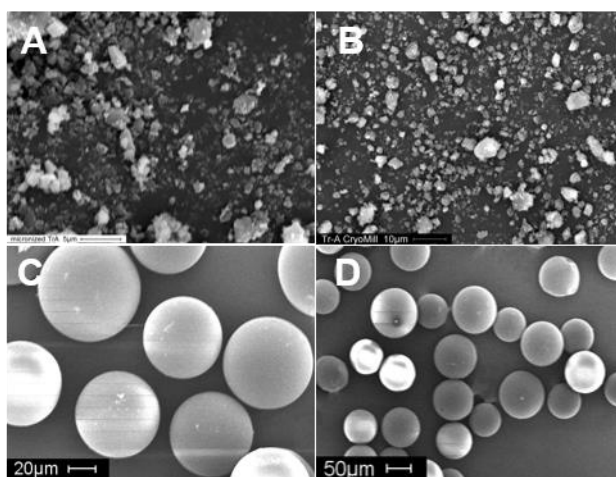


Figure 2.1 SEM micrographs of Tr-A micronized by mortar and pestle (A) and after by Retsch® cryo-mill (B). Micronized Tr-A powder was then encapsulated in Tr-A_1 (C) and Tr-A_2 (D) microspheres.

Table 2.1: Characterization of microsphere formulations prepared using unmilled and milled Tr-A. All values are reported as mean \pm SEM, n=3.

	Unmilled Tr-A		Milled Tr-A	
	Tr-A_1	Tr-A_2	Tr-A_1	Tr-A_2
Tr-A loading (w/w %)	3.2 \pm 0.3	4.2 \pm 0.1	5.4 \pm 0.2	5.2 \pm 0.1
Encapsulation Efficiency (%)	64 \pm 6	84 \pm 3	108 \pm 4	104 \pm 1
Initial Burst in PBST pH 7.4 (%)	9.8 \pm 2.2	6.6 \pm 0.4	1.9 \pm 0.3	2.8 \pm 0.4

Following successful microsphere preparation and characterization, Tr-A release was determined in several types of release media to determine the effect of media composition on release kinetics. Release in each media was compared to what was observed in PBST pH 7.4, as this condition is commonly used throughout the literature for conducting *in vitro* release tests. Release from Tr-A_1 was generally continuous over 35 days, with a slight lag observed in the first 7 days in 3 of the 4 media. Release from Tr-A_2 was slower and could be described as tri-phasic. A low initial burst was observed in the first day, followed by a lag phase in all four media. Following the lag phase, drug release was continuous in the third phase and lasted approximately 63 days in 3 of the 4 media. As seen in Figure 2.2A, release from Tr-A_1 microspheres was accelerated in two media: PBST pH 6.5 and PBS + 1.0% TC. Release from this formulation in PBST pH 7.4 and 6.5 and in HBST pH 7.4 followed a typical tri-phasic profile with low initial burst on day one followed by a short lag phase corresponding to polymer degradation. Following the lag phase, which lasted approximately 7 days, a secondary apparent zero order release occurred faster at the slightly lower pH with complete release occurring after one month. This result is expected, as a more acidic pH is may catalyze hydrolysis of the polymer to cause accelerated release [11, 24, 25]. In the presence of the plasticizer triethyl citrate (TC) a slightly higher initial burst (%) was followed by no apparent lag phase and complete

release in just 3 weeks. The presence of TC also resulted in accelerated release from Tr-A₂ (Figure 2.2B). Release from this microsphere formulation prepared from a higher MW ester end-capped PLGA (54 kDa) showed slower overall release than Tr-A₁ and a lag phase was noticeable in all four media, though it lasted only approximately 14 days in PBS + 1.0% TC versus approximately 21 days in the other three media.

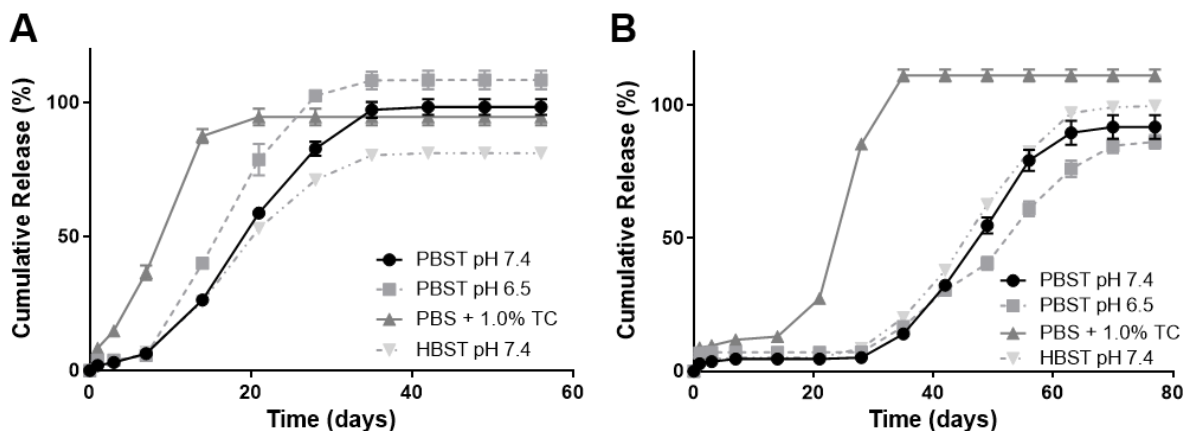


Figure 2.2: *In vitro* release from Tr-A₁ (A) and Tr-A₂ (B) microspheres in various media. Data represent mean \pm SEM, n=3. Note: in some cases, release average release was slightly greater than 100% due to slight error in measurement.

After the initial burst, drug release of poorly soluble small molecules such as Tr-A from low molecular weight PLGAs is expected to be dominated by erosion, while release from moderate molecular weight PLGAs is expected to occur via erosion and/or diffusion through the polymer matrix, though erosion is expected to be the predominant mechanism [2, 26]. Erosion-controlled release from PLGA microspheres typically exhibits a tri-phasic release. An initial burst of drug (usually due to surface-associated drug particles) is followed by a lag phase, during which the polymer chains degrade by hydrolysis until a critical chain length is reached. Following the lag phase, the duration of which is dependent on polymer characteristics (e.g.

MW, lactic acid : glycolic acid ratio, etc.), an erosion controlled, continuous release phase continues until all encapsulated drug has been released. [2, 3, 26-31]

In order to understand the underlying factors which cause accelerated release in some *in vitro* conditions, mechanisms of drug release from each formulation in all four media were studied and the major mechanism(s) of release in each condition was determined. Kinetics of PLGA hydrolysis during *in vitro* release is shown in Figure 2.3 and the associated initial first order rate constants over 14 d are reported in Table 2.2. As expected, the slightly acidic pH caused significantly faster degradation than standard conditions (0.163 ± 0.003 versus $0.125 \pm 0.018 \text{ day}^{-1}$) in PLGA 502H (Tr-A_1). Degradation of the higher molecular weight, ester terminated polymer (Tr-A_2) was significantly faster in PBS + 1.0% TC than in other media (0.121 ± 0.012 vs. $0.034 \pm 0.001 \text{ day}^{-1}$). PLGA hydrolysis results in the formation of water-soluble low molecular weight monomers and oligomers which are expected to diffuse out of the polymer matrix into the bulk media. The result of this process is overall erosion of the solid microspheres which can be measured by mass loss. As expected due to the accelerated hydrolysis, Tr-A_2 microsphere mass loss was accelerated in PBS + 1.0% TC (Figure 2.4). The plasticizer can increase the mobility of the polymer chains, allowing for increased mobility of water, which can lead to accelerated hydrolysis. The increased chain mobility can also cause increased diffusion of the low molecular weight degradation products out of the microspheres, causing the observed increase in overall mass loss [7].

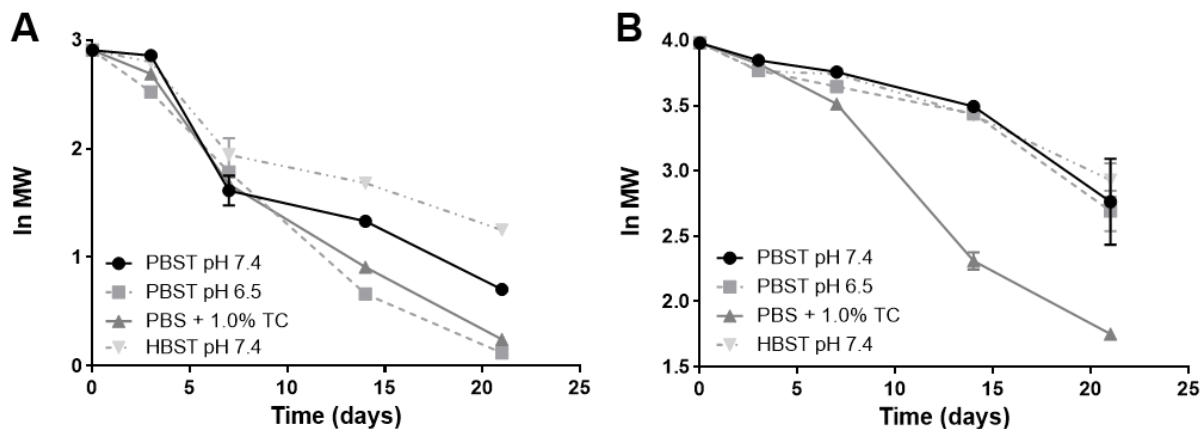


Figure 2.3: Decline of molecular weight of PLGA in Tr-A_1 (A) and Tr-A_2 (B) microspheres in various in vitro release media. Data represent mean \pm SEM, $n=3$.

Table 2.2: Initial first order rate constants (day^{-1}) of PLGA hydrolysis in Tr-A_1 and Tr-A_2 microspheres as determined by linear regression analysis of data shown in Figure 2.3. Values were taken from regression over the first 14 days.

	PBST pH 7.4	PBST pH 6.5	PBS + 1.0% TC	HBST pH 7.4
Tr-A_1	0.125 \pm 0.018	0.163 \pm 0.003*	0.151 \pm 0.009	0.095 \pm 0.013
Tr-A_2	0.034 \pm 0.001	0.037 \pm 0.003	0.121 \pm 0.012*	0.037 \pm 0.004

* $p < 0.05$ compared to PBST pH 7.4

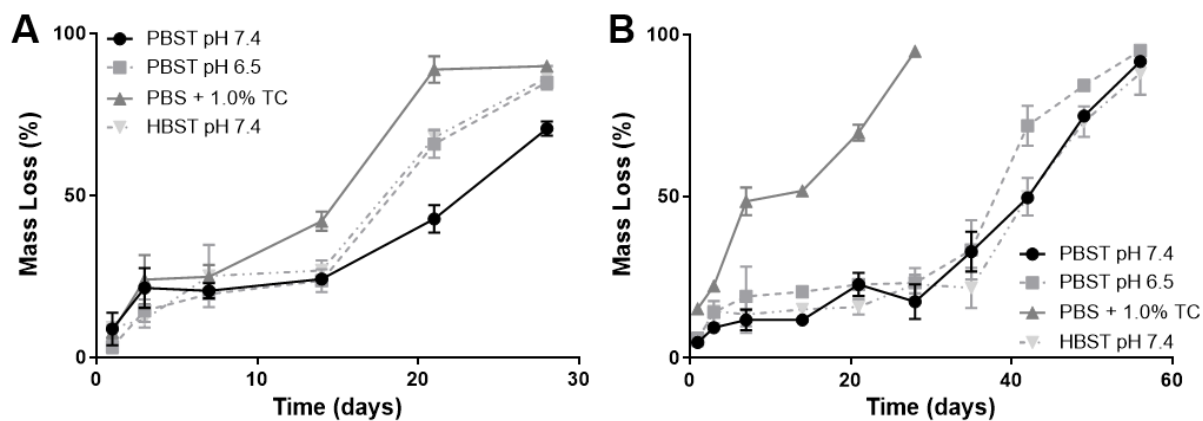


Figure 2.4: Mass loss of Tr-A_1 (A) and Tr-A_2 (B) microspheres in various in vitro release media. Data represent mean \pm SEM, $n=3$.

Erosion (i.e. polymer mass loss), one of the major mechanisms of drug release from PLGA microspheres, can be further described by determining the time-scale over which mass loss of the polymer matrix occurs. Mass loss curves shown in Figure 2.4 were fit using four-parameter logistic nonlinear or linear regressions (Figures S2.6 and S2.7), and the time to 50% mass loss ($t_{50,erosion}$) was determined in each media. The same process was also applied to release curves to determine the 50% release time ($t_{50,release}$) (Figures S2.4 and S2.5). The contribution of this mechanism to overall drug release can be estimated by comparing these two defining parameters of the time scales of erosion and release. For example, if $t_{50,release}/t_{50,erosion} \approx 1$, one can conclude that erosion is the dominant mechanism responsible for drug release in a given condition, as erosion and release happen over the same time scale. These values are reported in Table 2.3, and the same trends are shown in Figure 2.5, where release in each media was plotted vs. mass loss and compared to the line plotted to represent release = mass loss. In the standard conditions (PBST pH 7.4), erosion-controlled drug release was observed in both formulations. In the case of Tr-A_1, release occurred faster than erosion in PBS + 1.0% TC ($t_{50,release}/t_{50,erosion} = 0.52$), indicating that another mechanism was contributing to, and likely controlled, accelerated Tr-A release in that media. Although release was slightly accelerated in PBST pH 6.5, this appeared to be due to accelerated erosion and the predominant mechanism of release in this instance was unchanged. As discussed, the only media which caused a significant increase in the rate of Tr-A release from Tr-A_2 microspheres was PBS + 1.0% TC and erosion was increased in this media as well ($t_{50,erosion} = 8 \pm 0.4$ days).

Table 2.3: Characteristic times (in days) of release and erosion from Tr-A_1 and Tr-A_2 microspheres. Values represent mean \pm SEM, n=3. T_{50} ratios were calculated from mean values of $t_{50,release}$ and $t_{50,erosion}$ in each media.

		PBST pH 7.4	PBST pH 6.5	PBS + 1.0% TC	HBST pH 7.4
Tr-A_1	$t_{50,release}$	19.0 \pm 0.4	16.6 \pm 0.4	8.0 \pm 0.4*	17.6 \pm 0.2
	$t_{50,erosion}$	25 \pm 8	18.6 \pm 0.8	15 \pm 1	18 \pm 2
	$t_{50,release} / t_{50,erosion}$	0.77	0.89	0.52	0.96
Tr-A_2	$t_{50,release}$	46.8 \pm 0.6	50.1 \pm 0.8	25.0 \pm 0.3*	46.1 \pm 0.3
	$t_{50,erosion}$	46 \pm 3	39 \pm 2	18 \pm 2*†	43 \pm 2
	$t_{50,release} / t_{50,erosion}$	1.02	1.28	1.43	1.06

* $p < 0.05$ compared to PBST pH 7.4

† linear regression was used

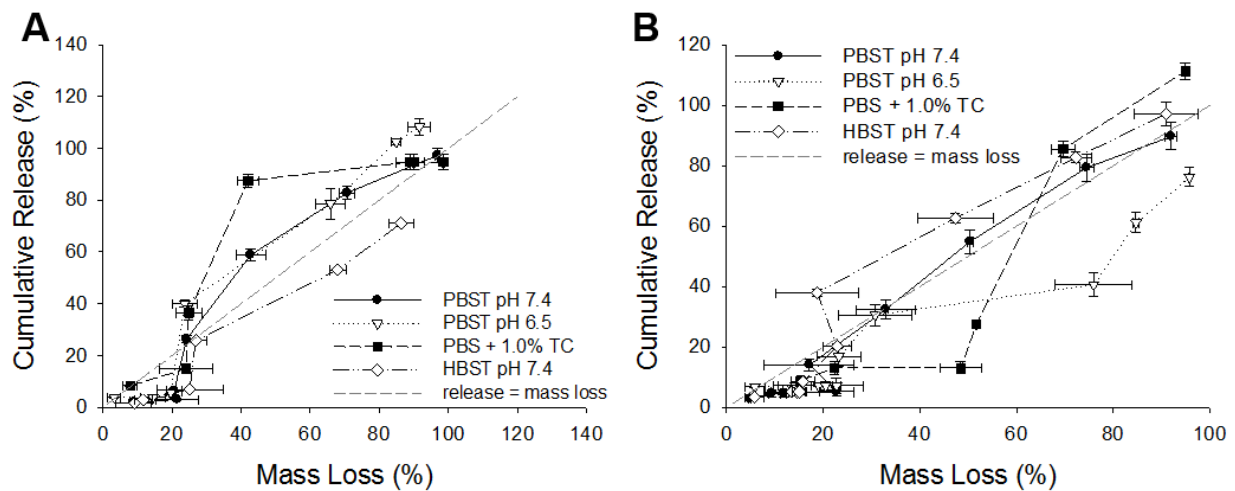


Figure 2.5: Release vs. mass loss of Tr-A_1 (A) and Tr-A_2 (B) microspheres. Dashed line represents release = mass loss, indicating pure erosion controlled release. X and Y data represent mean \pm SEM, n=3.

Further investigation into the mechanisms of release of Tr-A from PLGA microspheres included measurement of water uptake into the polymer matrix (Figure 2.6). HBST pH 7.4 caused noticeably more water uptake than the other three media in Tr-A_1 and Tr-A_2 at later time points. This may be due to the potential interaction between the cationic species of the

zwitterionic HEPES molecule interacting with free carboxylic acids present in Tr-A_1 at all times during release, and in Tr-A_2 as degradation causes production of acidic oligomers. The electrostatic interaction would presumably increase osmotic pressure, resulting in increased water uptake and microsphere swelling. However, given no clear trend in these data as related to the release kinetics of either formulation suggest that water-mediated processes likely do not play a significant role in Tr-A release.

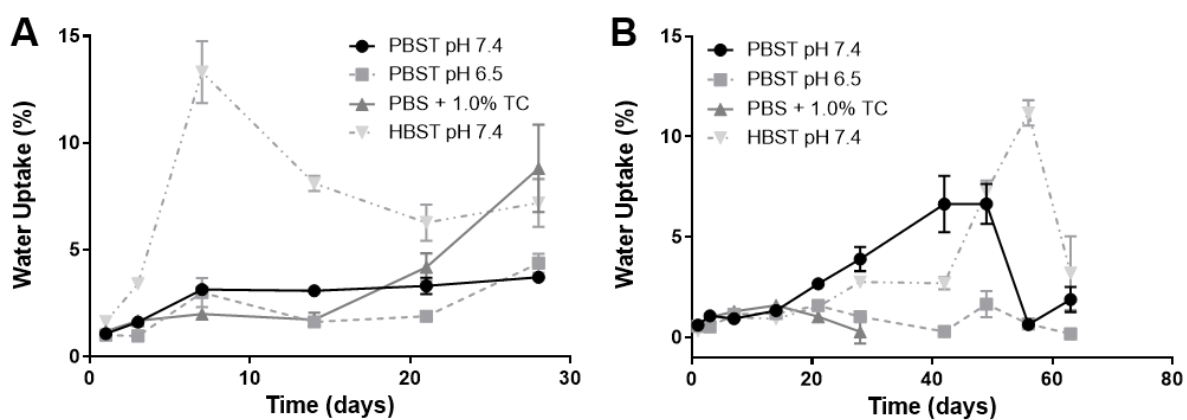


Figure 2.6: Water uptake Tr-A_1 (A) and Tr-A_2 (B) microspheres in various in vitro release media. Data represent mean \pm SEM, $n=3$.

Finally, degrading particle morphology and diffusion through the polymer matrix, controlled primarily by the solid polymer phase, was studied using the fluorescent probe, bodipy. This small, pH insensitive dye partitions preferentially into the polymer phase and thus is a suitable marker for solid state diffusion [21]. As the probe is also water soluble, it can be used to view the larger pore structure in the polymer as well. Representative images of Tr-A_1 and Tr-A_2 particles during release can be seen in Figure 2.7 (additional images are shown in Figures S2.8 and S2.9). These confocal micrographs show the morphology of degrading microspheres and provide visual evidence of the previously discussed mechanisms of drug release.

Micrographs of particles incubated in PBST pH 6.5, PBS + 1.0% TC, and HBST pH 7.4 were compared to those incubated in PBST pH 7.4 to determine the effects of these non-standard conditions on particle morphology. Incubation in PBST pH 6.5 caused a noticeable increase in the penetration of the dye from the surface of Tr-A_1 microspheres. This effect can be explained by the slightly reduced pH of the buffer and thus a reduced pH at the surface of the microspheres. As previously mentioned, this increases the hydrolysis of PLGA and thus allows for increased penetration of molecules such as bodipy into the regions of degraded polymer. The presence of TC increased mobility of the polymer in Tr-A_1 microspheres, resulting in a loss of spherical morphology and formation of large pores on the surface at early time points and swelling and dye saturation at later time points. This increase in polymer chain mobility resulted in a significant increase in the effective diffusion coefficient in the polymer matrix (Figure 2.8A) following 3 days in release media, though this was the latest time point diffusion could be measured at the uptake time point selected in three of the four *in vitro* conditions due to rapid polymer degradation in this low molecular weight PLGA. Tr-A_1 microspheres swelled dramatically in HBST pH 7.4 as early as three days.

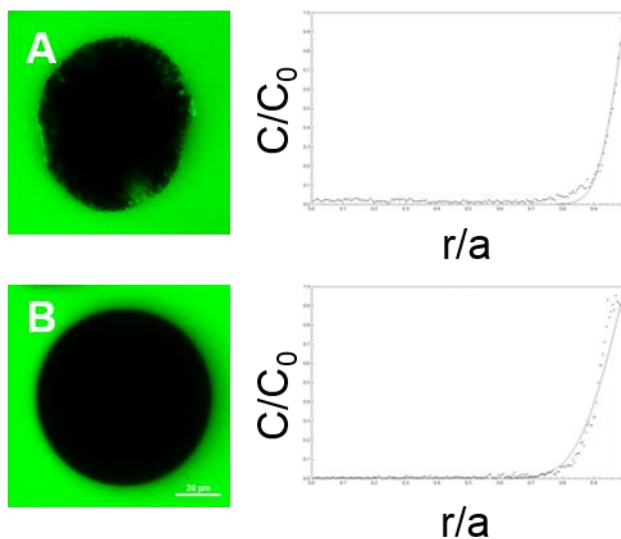


Figure 2.7: Representative images of Tr-A_1 (A) and Tr-A_2 (B) microspheres following 3 days release in PBST pH 7.4 and 3 hours in 5µg/mL bodipy in PBST pH 7.4 and resulting bodipy concentration gradient plots shown at right.

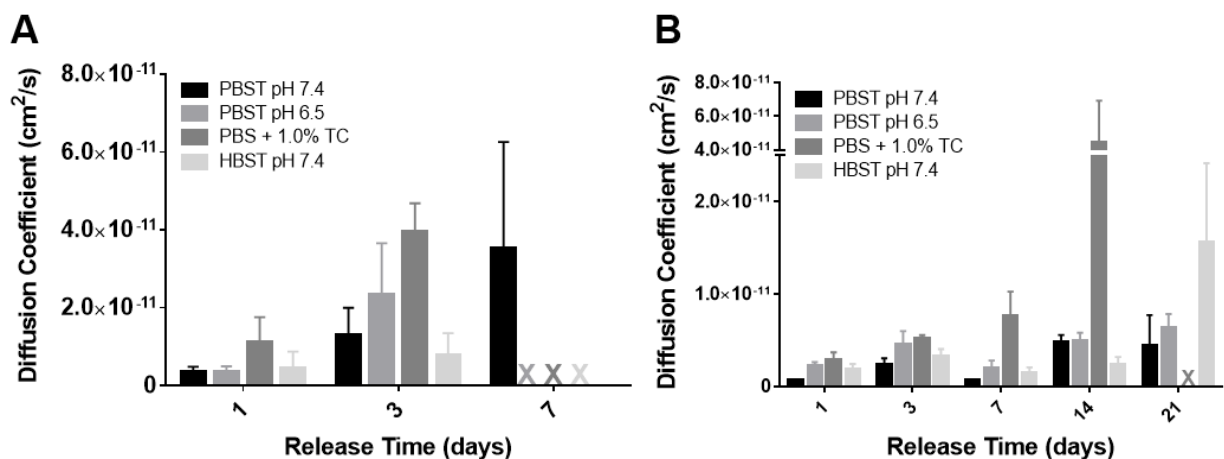


Figure 2.8: BODIPY diffusion coefficients in degrading Tr-A_1 (A) and Tr-A_2 (B) microspheres in varying release media. Data represent mean \pm SEM, $n=6$. X indicates no diffusion coefficient could be determined due to agglomeration and/or saturation of microspheres.

The PLGA used for formulation of Tr-A_2 microspheres was a higher molecular weight (54 kDa) with ester end capping and thus, these particles bioeroded at a slower rate than was observed in Tr-A_1 particles. Particles incubated in PBST pH 6.5 exhibited some preferential surface erosion similar to what was observed in Tr-A_1. The presence of triethyl citrate also created a visible bodipy diffusion front as a result of polymer chain flexibility caused by plasticization. This mobilization also had a significant impact on bodipy diffusion after 7 and 14 days, while PBST pH 6.5 and HBST pH 7.4 buffer solutions exhibited no effect on solid state diffusion as compared to PBST pH 7.4 at any measurable time point (Figure 2.8B).

In order to estimate the overall contribution of diffusion to release, we estimated Tr-A diffusion coefficients using a D_{Tr-A}/D_{bodipy} ratio determined experimentally as described in the supplementary information. Tr-A uptake data and models are shown in Figure S2.10. Representative D_{Tr-A} values were chosen for both formulations and release profiles were modeled, shown in Figure 2.9. Given the distinct differences in D_{bodipy} values in the presence and absence of plasticizer, we chose to use these values at early times and at later times during

release to develop release models to comprehensively represent the range of conditions studied herein. Theoretical $t_{50,diffusion}$ values were then estimated for purely diffusion-controlled release processes (Table 2.4). Note that the effective diffusion coefficients estimated, as indicated by their very low order of magnitude ($\sim 10^{-12} - 10^{-11} \text{ cm}^2/\text{s}$), are primarily based on solid-state diffusion, although isolated pores are also important by instantaneously advancing the diffusion front (see Kang and Schwendeman [21] for discussion). It is also known that steroids can diffuse through membranes of PLGA [32]. The calculated t_{50} values resulting from D_{Tr-A} values representative of plasticizer-containing media conditions in both formulations suggest that diffusion contributes to the overall release, as these values correspond to the accelerated release times observed in this media. In other media not containing the plasticizer, diffusion at early times during release (i.e. 1-3 days) is very slow and thus this process does not likely contribute to release which is slow and controlled by hydrolysis and erosion. Following the lag phase, however, diffusion increases and the resulting models suggest diffusion occurring at times similar to release, as the polymer chains have become more flexible.

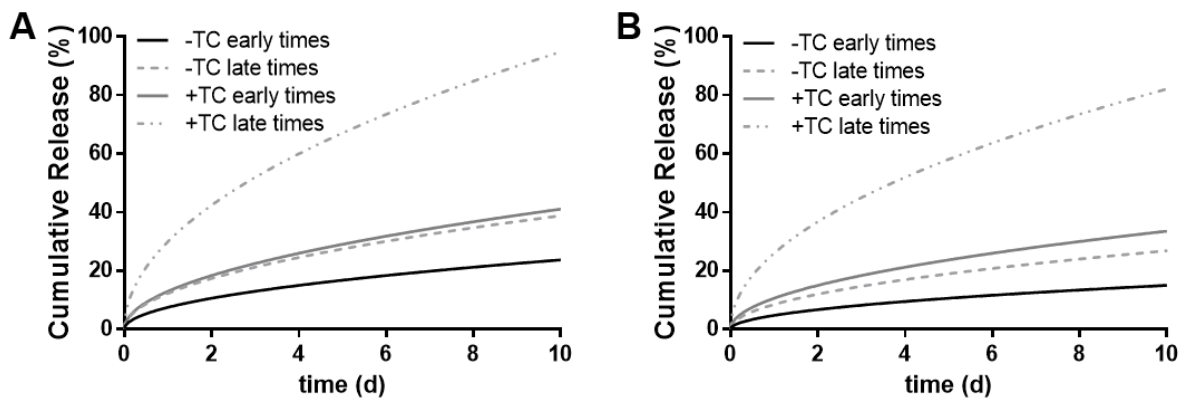


Figure 2.9: Theoretical Tr-A release profiles from Tr-A_1 (A) and Tr-A_2 (B) microspheres for diffusion-controlled release. Profiles were generated using representative diffusion coefficients with and without the plasticizer triethyl citrate that were determined at early (1-3 days) and late times (7+ days) during the release incubation.

Table 2.4: $T_{50,diffusion}$ estimated using diffusion-controlled release models shown in Figure 2.9.

	-TC early times	-TC late times	+TC early times	+TC late times
Tr-A_1	45 days	17 days	15 days	2.8 days
Tr-A_2	110 days	35 days	22 days	3.7 days

2.6 Conclusions

In closing, this study shows how *in vitro* release conditions affect not only the release rate of Tr-A, but also the mechanisms by which these microsphere formulations release the encapsulated drug. Release from low molecular weight acid-capped PLGA 50/50 microspheres (Tr-A_1) was accelerated at slightly acidic pH 6.5 and in media containing the plasticizer triethyl citrate. Drug release from this formulation was dominated by erosion in three of the four conditions studied, including PBST pH 6.5, where the rate of polymer hydrolysis was faster than in standard conditions. In the presence of TC, however, release was triggered not only by accelerated erosion, but also by increased diffusion in the polymer matrix with the latter as the principal controlling mechanism. Triethyl citrate also caused accelerated release from moderate molecular weight ester-capped PLGA 50/50 microspheres (Tr-A_2) by accelerating PLGA hydrolysis and causing accelerated erosion. Solid state diffusion was also increased in this media, indicating that polymer plasticization caused by TC decreases tortuosity and allows for increased drug diffusion. This effect increases the contribution of diffusion to overall release of drug from both formulations. These data further lay the foundation for comparing the release mechanism *in vivo* and developing mechanistic strategies for IVIVCs.

2.7 References

1. Jain, R.A., *The manufacturing techniques of various drug loaded biodegradable poly(lactide-co-glycolide) (PLGA) devices*. Biomaterials, 2000. **21**(23): p. 2475-2490.
2. Wischke, C. and S.P. Schwendeman, *Principles of encapsulating hydrophobic drugs in PLA/PLGA microparticles*. International Journal of Pharmaceutics, 2008. **364**(2): p. 298-327.
3. Schwendeman, S.P., et al., *Progress and challenges for peptide, protein, and vaccine delivery from implantable polymeric systems*, in *Controlled Drug Delivery: Challenges and Strategies*, K. Park, Editor. 1997, The American Chemical Society: Washington, D.C. p. 229-267.
4. Martinez, M., et al., *In vitro and in vivo considerations associated with parenteral sustained release products: A review based upon information presented and points expressed at the 2007 Controlled Release Society Annual Meeting*. Journal of Controlled Release, 2008. **129**(2): p. 79-87.
5. Zolnik, B.S., *In Vitro and In Vivo Release Testing of Controlled Release Parenteral Microspheres*, in *Pharmaceutics*. 2005, University of Connecticut: Storrs.
6. Conti, B., et al., *Testing of "In Vitro" Dissolution Behaviour of Microparticulate Drug Delivery Systems*. Drug Development and Industrial Pharmacy, 1995. **21**(10): p. 1223-1233.
7. Kranz, H., et al., *Physicomechanical properties of biodegradable poly(D,L-lactide) and poly(D,L-lactide-co-glycolide) films in the dry and wet states*. Journal of Pharmaceutical Sciences, 2000. **89**(12): p. 1558-1566.
8. D'Souza, S. and P. DeLuca, *Methods to Assess In Vitro Drug Release from Injectable Polymeric Particulate Systems*. Pharmaceutical Research, 2006. **23**(3): p. 460-474.
9. Zolnik, B.S., P.E. Leary, and D.J. Burgess, *Elevated temperature accelerated release testing of PLGA microspheres*. J Control Release, 2006. **112**(3): p. 293-300.
10. Sansdrap, P. and A.J. Moës, *In vitro evaluation of the hydrolytic degradation of dispersed and aggregated poly(-lactide-co-glycolide) microspheres*. Journal of Controlled Release, 1997. **43**(1): p. 47-58.
11. Shameem, M., H. Lee, and P. DeLuca, *A short-term (accelerated release) approach to evaluate peptide release from PLGA depot formulations*. The AAPS Journal, 1999. **1**(3): p. 1-6.
12. *In vitro and In vivo Evaluations of Dosage Forms, United States Pharmacopeia <1088>*.
13. *Food and Drug Administration Guidance for Industry. Extended Release Oral Dosage Forms: Development, Evaluation, and Application of In Vitro/In Vivo Correlations, CDER 09, 1997*.
14. Zolnik, B.S. and D.J. Burgess, *In Vitro–In Vivo Correlation on Parenteral Dosage Forms*, in *Biopharmaceutics Applications in Drug Development*, R. Krishna and L. Yu, Editors. 2008, Springer US. p. 336-358.
15. Young, D., C. Farrell, and T. Shepard, *In Vitro/In Vivo Correlation for Modified Release Injectable Drug Delivery Systems*, in *Injectable Dispersed Systems: Formulation, Processing and Performance*, D. Burgess, Editor. 2005, Taylor & Francis Group: Boca Raton. p. 159-176.

16. Martinez, M.N., et al., *Breakout session summary from AAPS/CRS joint workshop on critical variables in the in vitro and in vivo performance of parenteral sustained release products*. Journal of Controlled Release, 2010. **142**(1): p. 2-7.
17. Burgess, D.J., et al., *Assuring quality and performance of sustained and controlled release parenterals: AAPS workshop report, co-sponsored by FDA and USP*. Pharm Res, 2002. **19**(11): p. 1761-8.
18. Burgess, D., et al., *Assuring quality and performance of sustained and controlled release parenterals: EUFEPS workshop report*. The AAPS Journal, 2004. **6**(1): p. 100-111.
19. Higuchi, T., *Mechanism of sustained-action medication. Theoretical analysis of rate of release of solid drugs dispersed in solid matrices*. Journal of Pharmaceutical Sciences, 1963. **52**(12): p. 1145-1149.
20. Liu, Y. and S.P. Schwendeman, *Mapping Microclimate pH Distribution inside Protein-Encapsulated PLGA Microspheres Using Confocal Laser Scanning Microscopy*. Molecular Pharmaceutics, 2012. **9**(5): p. 1342-1350.
21. Kang, J. and S.P. Schwendeman, *Determination of Diffusion Coefficient of a Small Hydrophobic Probe in Poly(lactide-co-glycolide) Microparticles by Laser Scanning Confocal Microscopy*. Macromolecules, 2003. **36**(4): p. 1324-1330.
22. Crank, J., *The Mathematics of Diffusion*. 1956: Clarendon Press.
23. Desai, S.J., A.P. Simonelli, and W.I. Higuchi, *Investigation of factors influencing release of solid drug dispersed in inert matrices*. J Pharm Sci, 1965. **54**(10): p. 1459-64.
24. Holy, C.E., et al., *In vitro degradation of a novel poly(lactide-co-glycolide) 75/25 foam*. Biomaterials, 1999. **20**(13): p. 1177-1185.
25. Zolnik, B.S. and D.J. Burgess, *Effect of acidic pH on PLGA microsphere degradation and release*. Journal of Controlled Release, 2007. **122**(3): p. 338-344.
26. Fredenberg, S., et al., *The mechanisms of drug release in poly(lactic-co-glycolic acid)-based drug delivery systems—A review*. International Journal of Pharmaceutics, 2011. **415**(1–2): p. 34-52.
27. Siegel, R.A. and M.J. Rathbone, *Overview of Controlled Release Mechanisms: Fundamentals and Applications of Controlled Release Drug Delivery*, J. Siepmann, R.A. Siegel, and M.J. Rathbone, Editors. 2012, Springer US. p. 19-43.
28. Uhrich, K.E., et al., *Polymeric Systems for Controlled Drug Release*. Chemical Reviews, 1999. **99**(11): p. 3181-3198.
29. Alexis, F., *Factors affecting the degradation and drug-release mechanism of poly(lactic acid) and poly[(lactic acid)-co-(glycolic acid)]*. Polymer International, 2005. **54**(1): p. 36-46.
30. Allison, S.D., *Analysis of initial burst in PLGA microparticles*. Expert Opin Drug Deliv, 2008. **5**(6): p. 615-28.
31. Wang, J., B.M. Wang, and S.P. Schwendeman, *Characterization of the initial burst release of a model peptide from poly(d,l-lactide-co-glycolide) microspheres*. Journal of Controlled Release, 2002. **82**(2–3): p. 289-307.
32. Pitt, C.G., et al., *Sustained drug delivery systems. I. The permeability of poly(epsilon-caprolactone), poly(DL-lactic acid), and their copolymers*. J Biomed Mater Res, 1979. **13**(3): p. 497-507.

2.8 Supplementary Information

2.8.1 Selection of Tr-A/PLGA Microspheres

Initial control studies were performed with various PLGA microsphere formulations encapsulating Tr-A to select two formulations for extensive mechanistic analysis. Microspheres were formulated using un-milled Tr-A incorporated as a solid (s/o/w, discussed in detail in section 2.4.1) or co-dissolved with PLGA in the oil phase using dimethylformamide as a co-solvent. As shown in Table S 2.1, other formulation parameters were varied, such as the initial polymer concentration and the theoretical loading. In these initial selection experiments, the effect of these formulation variables was studied by measuring in vitro release in PBST pH 7.4 (Figure S 2.1). One microsphere formulation of each type of PLGA was selected for the studies discussed in this chapter: G (Tr-A_1) and I (Tr-A_2), although cryo-milling to reduced drug particle size was performed for the encapsulation of Tr-A_1 and Tr-A_2 formulations in the main text. Both of these formulations were prepared using s/o/w methods, which generally exhibited a more controlled release profile than the microspheres prepared using DMF as a co-solvent. Both formulations selected had moderate drug loading, as high drug loading was not the focus of this mechanistic analysis, and good encapsulation efficiency.

Table S 2.1: Initial Tr-A/PLGA microsphere formulation parameters and characterization.

Formulation	Solvent DMF:CH ₂ Cl ₂	polymer	Polymer conc. (mg/ml)	L _T (%)	L _A (%)	EE (%)	method
A	1:3	502H	800	5%	2.8±0.1	57±1	O/W
B	1:3	502H	1000	5%	3.1±0.2	63±3	O/W
C	1:3	Ester-end capped PLGA	400	10%	4.2±0.2	42±2	O/W
D	1:3	Ester-end capped PLGA	400	20%	13.4±0.4	67±2	O/W
E	1:3	PLA	320	20%	8.2±1.2	41±6	O/W
F	CH ₂ Cl ₂	502H	800	5%	3.6±0.2	71±5	S/O/W
G	CH ₂ Cl ₂	502H	1000	5%	3.4±0.1	67±2	S/O/W
H	CH ₂ Cl ₂	502H	1000	10%	7.3±0.3	73±3	S/O/W
I	CH ₂ Cl ₂	Ester-end capped PLGA	400	5%	3.4±0.4	68±7	S/O/W
J	CH ₂ Cl ₂	Ester-end capped PLGA	400	10%	7.8±0.4	78±4	S/O/W
K	CH ₂ Cl ₂	Ester-end capped PLGA	400	20%	19±3	96±14	S/O/W

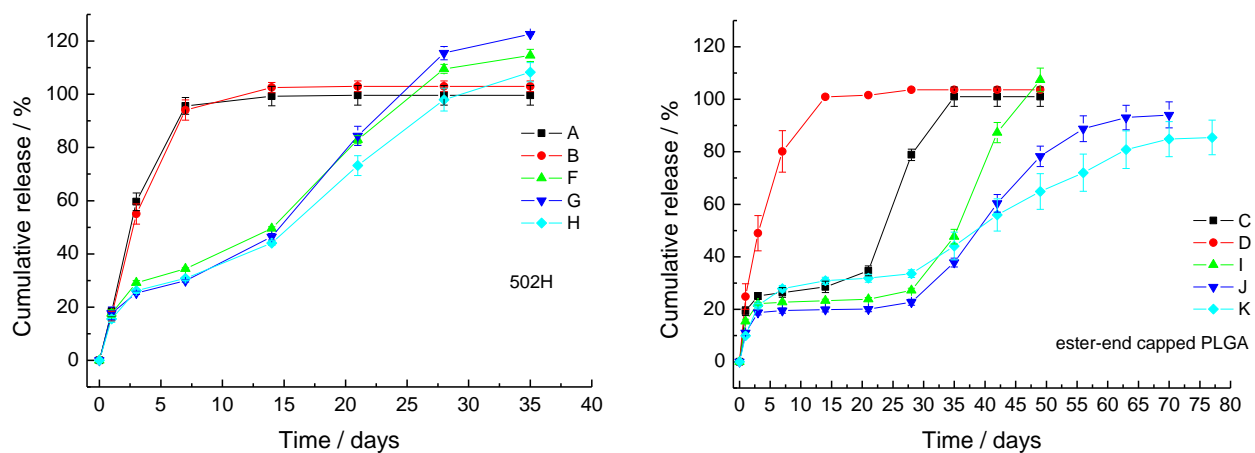


Figure S 2.1: In vitro release of initial Tr-A/PLGA microsphere formulations using PLGA 502H (A) and ester end-capped, moderate molecular weight PLGA (B). Data represent mean ± SEM, n=3.

2.8.2 Regression Analysis

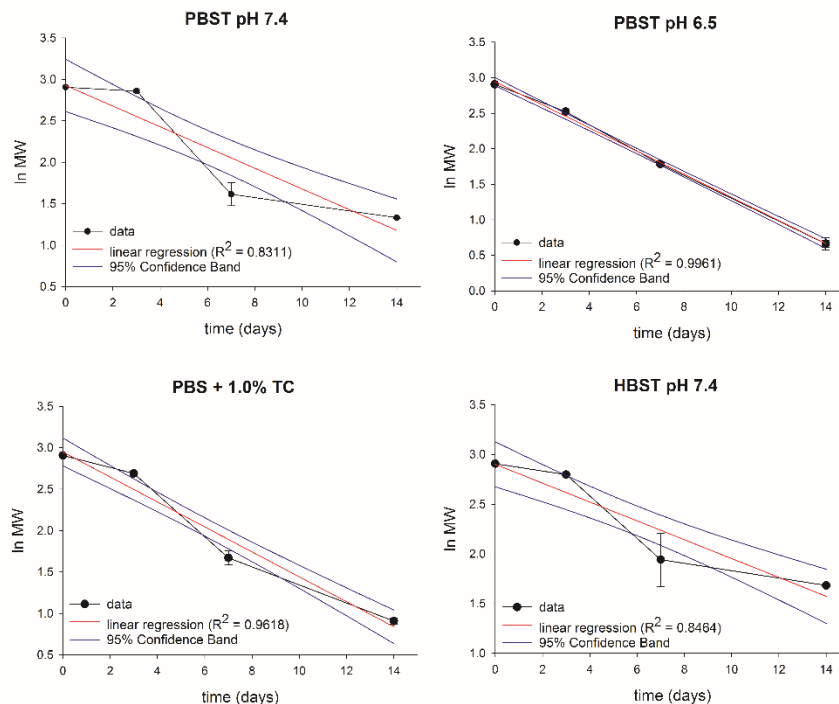


Figure S 2.2: Linear regression fits of $Tr-A_1$ hydrolysis data. Rate constants shown in Table 2.2 were determined from these regressions.

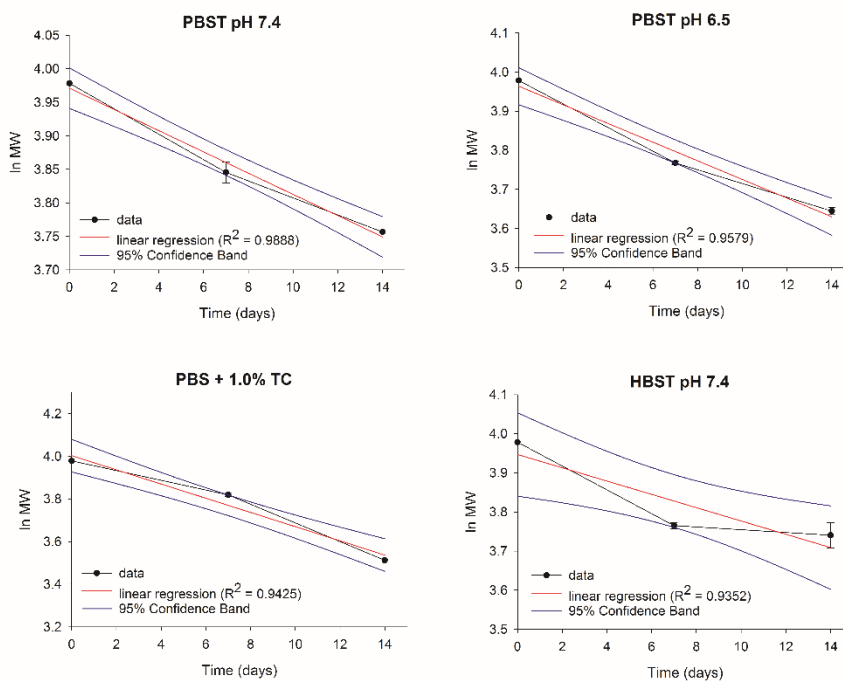


Figure S 2.3: Linear regression fits of $Tr-A_2$ hydrolysis data. Rate constants shown in Table 2.2 were determined from these regressions.

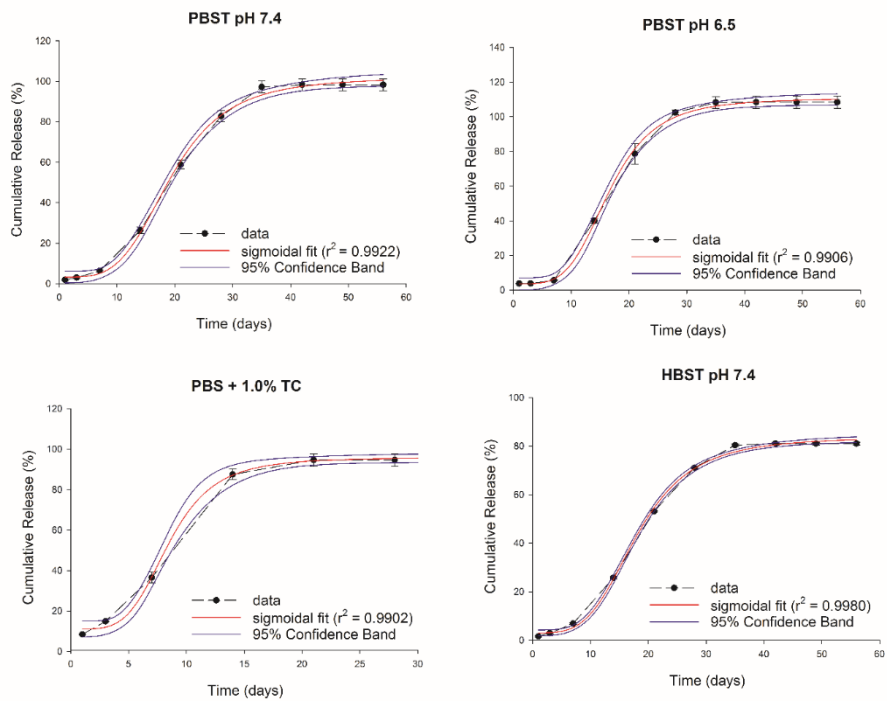


Figure S 2.4: Four parameter logistic nonlinear fits of Tr-A_1 release data. $T_{50,release}$ values and associated errors were determined from the associated equations.

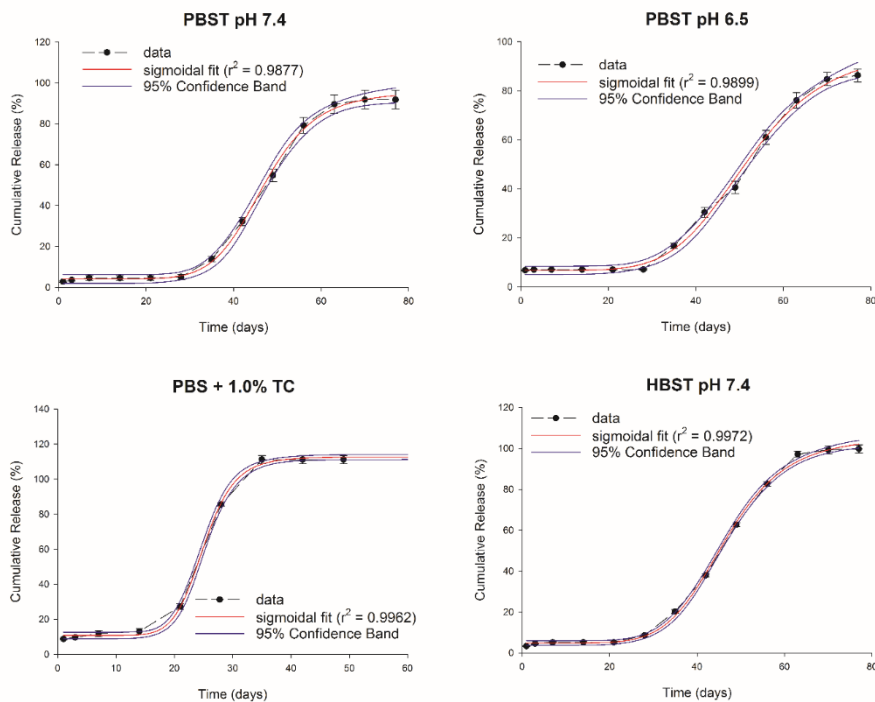


Figure S 2.5: Four parameter logistic nonlinear fits of Tr-A_2 release data. $T_{50,release}$ values and associated errors were determined from the associated equations.

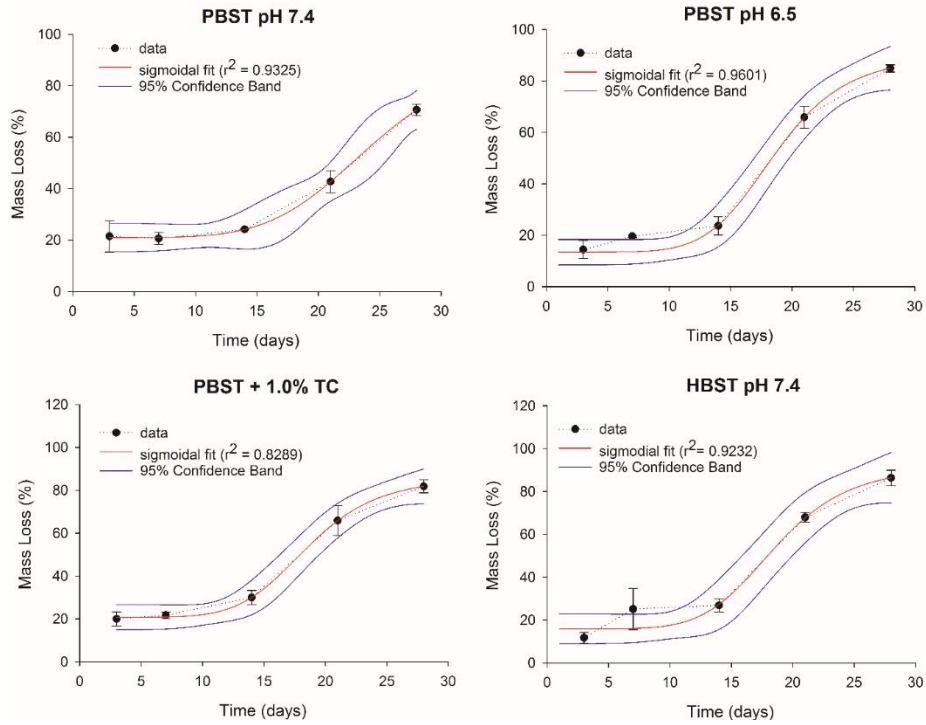


Figure S 2.6: Four parameter logistic nonlinear fits of Tr-A_1 mass loss data. $T_{50,erosion}$ values and associated errors were determined from the associated equations.

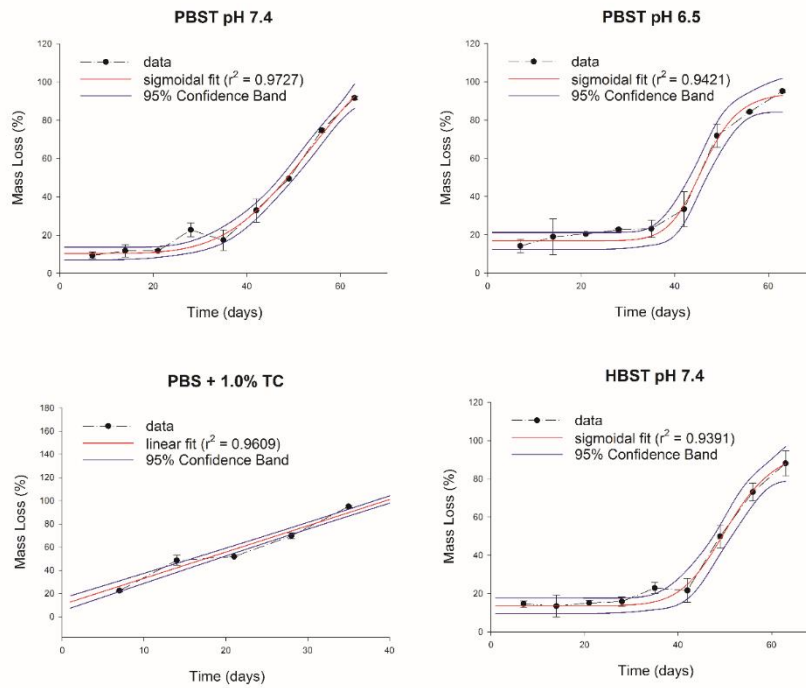


Figure S 2.7: Four parameter logistic nonlinear fits of Tr-A_2 mass loss data. $T_{50,erosion}$ values and associated errors were determined from the associated equations.

2.8.3 Additional LCSM images of Tr-A_1 and Tr-A_2 microspheres

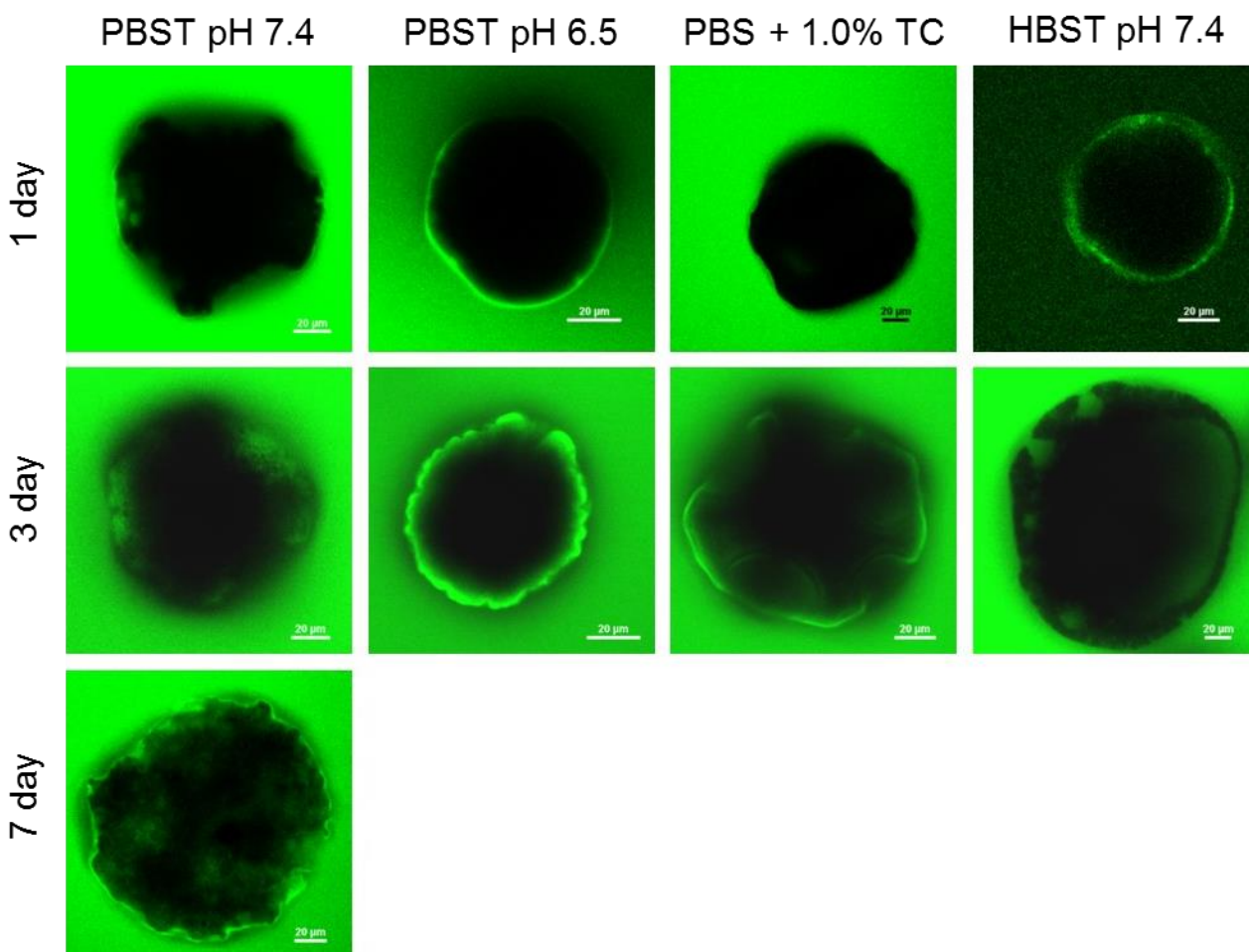


Figure S 2.8: Confocal images of Tr-A_1 microspheres following 1, 3, and 7 days incubation in various release media. Microspheres incubated in PBST pH 6.5, PBS + 1.0% TC and HBST pH 7.4 are not pictured at 7 days due to complete dye saturation and/or agglomeration at this and future time points.

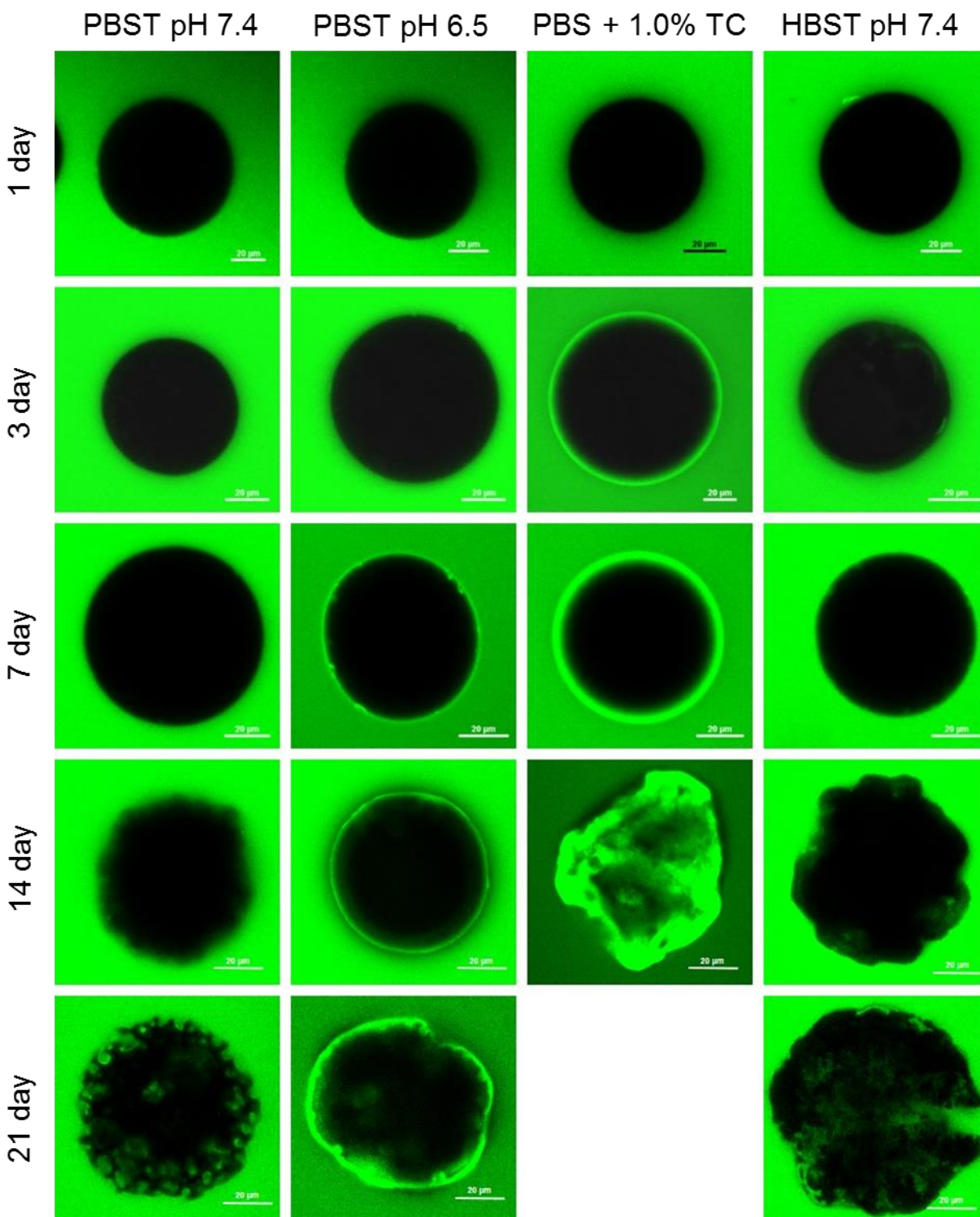


Figure S 2.9: Confocal images of Tr-A_2 microspheres following 1, 3, 7, 14, and 21 days incubation in various release media. Microspheres incubated in PBS + 1.0% TC are not pictured at 21 days due to complete dye saturation and/or agglomeration at this and future time points.

2.8.4 Development of diffusion-controlled release models

Tr-A uptake was measured in blank PLGA microspheres as described in the main paper. The data was then fit to Crank's solution for uptake into particles of spherical morphology to determine a diffusion coefficient (D):

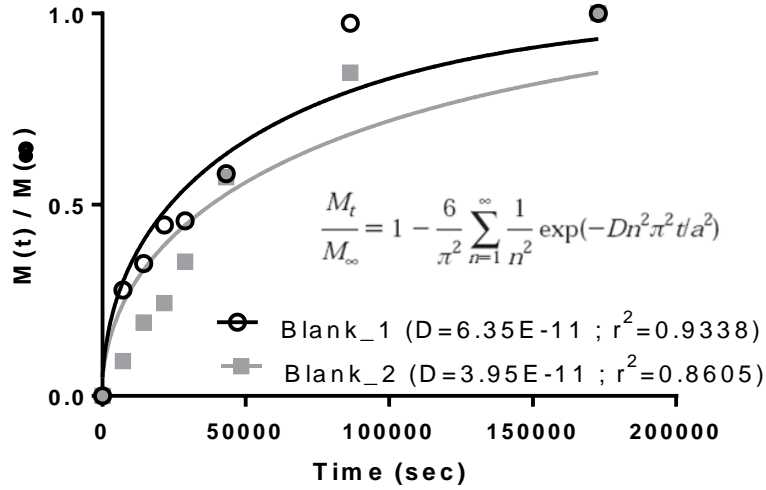


Figure S 2.10: Tr-A uptake in blank PLGA microspheres and resulting fits to Crank's solution (shown). Estimated diffusion coefficients resulting from these fits are shown in the legend.

Then, blank PLGA microspheres (Blank_1 and Blank_2) were suspended in PBST pH 7.4 for one day, then incubated in bodipy solution for 3 hours before imaging using confocal microscopy. The images were then analyzed as previously described to determine D_{bodipy} .

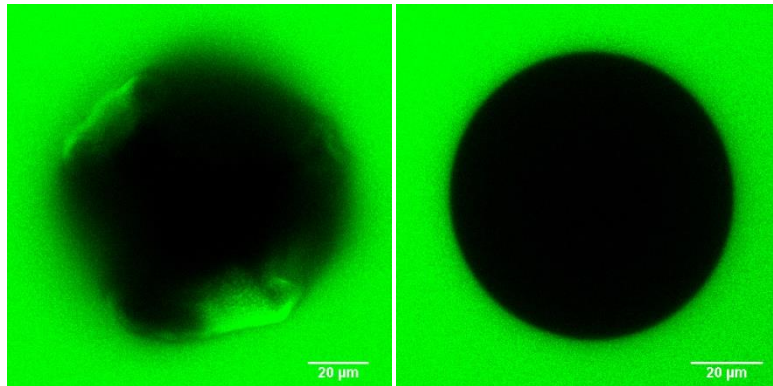


Figure S 2.11: Representative confocal images of Blank_1 (A) and Blank_2 (B) microspheres following 1 day incubation in PBST pH 7.4 and 3 hours in bodipy solution.

Table S 2.2: Estimated diffusion coefficients of Tr-A and bodipy in blank microspheres.

Polymer	D_{Tr-A}	D_{bodipy}	D_{Tr-A}/D_{bodipy}
502H (18 kDa) Blank_1	6.30E-11	3.30E-12	19.1
e.t. PLGA (54 kDa) Blank_2	3.95E-11	6.07E-13	65.1

Using the D_{Tr-A}/D_{bodipy} ratios, D_{Tr-A} values were estimated at each time point in each media from D_{bodipy} ratios shown in Figure 2.8. Representative diffusion coefficients were then chosen (with or without TC at early and late times during release) to build diffusion-controlled release models using the Higuchi equation solved for spherical systems:

$$M_t = A\sqrt{2DC_sC_0t}$$

A = area of the microsphere
 D = estimated D_{Tr-A}
 C_s = Tr-A solubility in PLGA
 C_0 = Tr-A loading in microsphere
 t = time

The solubility of Tr-A in the two types of PLGA was determined experimentally. At the end of the Tr-A uptake study described above, a partition coefficient for the drug in polymer was determined $[(Tr-A)_{PLGA,final} / PLGA] / [(Tr-A)_{PBST,final} / H_2O]$. Then, the polymer solubility was estimated from the solubility of Tr-A in PBST (25.9 μ g/mL) and the experimentally determined partition coefficients.

Table S 2.3: Estimated partition coefficients and solubilities of Tr-A in PLGA.

Polymer	Partition coefficient	C_s (μg/mL)
502H (18 kDa) Blank_1	0.84	21.8
e.t. PLGA (54 kDa) Blank_2	0.22	5.7

Chapter 3 : Cage Implant System for Assessing *in vivo* Controlled Release Performance of Long-acting Release PLGA Microspheres

3.1 Abstract

Here we describe development of a silicone rubber/stainless steel mesh cage implant system, much like that used to assess biocompatibility of biomaterials [1] for easy removal of microspheres *in vivo*. The cage has a stainless steel mesh size (38 μm) large enough for cell penetration and free fluid flow *in vivo* but small enough for microsphere retention, and a silicone rubber shell for injection of the microspheres. Two model drugs, the poorly soluble small molecule triamcinolone acetonide and the short peptide leuprolide, were encapsulated in PLGA microspheres large enough to be restrained by the cage implant *in vivo*. The *in vitro* release from both formulations was followed with and without the cage in PBS + 0.02% Tween 80 + 0.05% sodium azide at 37 °C by UPLC. Pharmacokinetics in rats was assessed after SC injection or SC in-cage implantation of microspheres with plasma analysis by LC-MS/MS or EIA. Tr-A and leuprolide *in vitro* release was equivalent irrespective of the cage or test tube incubation vessel and release was much slower than observed *in vivo* for both drugs. Moreover, Tr-A and leuprolide pharmacokinetics (PK) with and without the cage were highly similar during the 2-3 week release duration before a significant inflammatory response was caused by the cage implant. Hence, the PK-validated cage implant provides a simple means to recover and evaluate the microsphere drug carriers *in vivo* during a time window of at least a few weeks in order to characterize the polymer microspheres and release mechanisms of microspheres *in vivo*. This approach may facilitate development of mechanism-based *in vitro/in vivo* correlations and enable development of more accurate and useful *in vitro* release tests.

3.2 Introduction

Currently, no FDA guideline exists for establishing *in vitro-in vivo* correlation (IVIVC) models to predict *in vivo* performance of controlled release poly(lactic-co-glycolic acid) (PLGA) microparticles [2-4]. For these formulations, *in vitro* release tests often do not accurately predict drug release *in vivo* [5-14]. The lack of predictive release testing methods creates a significant challenge during development of these drug products and related generics, an issue which has persisted even now more than 25 years after the first commercial microsphere products were approved. The environment at the site of microparticle administration *in vivo* is complex and its effects on polymer degradation and drug release are poorly understood [15]. Without a clear understanding of the mechanisms of release from these formulations *in vivo*, it is difficult to design *in vitro* release systems to accurately predict the rate and mechanism(s) of drug release following administration. In fact, most recent discussion on the need for developing IVIVCs for CR products has focused on developing a mechanistic understanding of drug release *in vivo* [3, 16-18].

At least three principal mechanisms contribute to drug release from PLGA microspheres: water uptake-related phenomena, hydrolysis and bioerosion of the polymer, and pore- and solid-state diffusion [19, 20]. Methods have been developed to study these mechanisms and their contribution to drug release *in vitro*, but a mechanistic understanding of release from microspheres *in vivo* is still lacking [15, 19, 21]. This is mainly due to the difficulty of retrieving micro-scale biodegradable formulations following administration. Microspheres are typically suspended in an injection medium then administered either intramuscularly (IM) or subcutaneously (SC) using a needle with sufficiently large inner diameter to freely inject microspheres. The particles are then free to migrate away from the injection site, making it

extremely difficult to then retrieve them after even just one day. Drug release can be quantified by measuring drug concentrations in blood samples, but without retrieval of the formulation itself there is no simple way to determine exactly what mechanisms are at play over the time course of drug release.

A portion of microspheres has been recovered from tissue during *in vivo* evaluation to allow measurement of biodegradation kinetics [15] although removal from tissue causes damage to the microspheres to limit the useful analysis of the polymer matrix. Similarly, pharmacokinetics can be used to estimate drug release *in vivo*, but this method again does not allow analysis of the release mechanism. Previous authors have used a cage implant to restrain polymer implants and films while concurrently studying the inflammatory response resulting from the administration of these materials [1, 22-25]. A similar approach was used to study SC and IM degradation and release of PLGA microspheres in rats [26]. Using these devices as a framework, we have designed a cage implant using stainless steel wire mesh with openings small enough to restrain microspheres of a certain size, yet large enough to allow free contact with fluids and cells at the administration site. This cage will allow for the retrieval of microparticles from the subcutaneous site for a more detailed analysis of the intact microspheres in the *in vivo* environment.

The purpose of this work was to design and construct a cage implant for microsphere retrieval, and to study the effect of the cage on the release of drugs *in vitro* and *in vivo* in order to understand the utility of the cage for *in vivo* microsphere evaluation. The inflammatory response of the cage was also evaluated. Two model drugs were chosen to demonstrate the utility of this system; the small hydrophobic molecule corticosteroid triamcinolone acetonide (Tr-A) and the peptide leuprolide. Tr-A has previously been successfully encapsulated and studied extensively

in vitro and has very few if any drug instability issues, has low susceptibility to polymorphism and solubility changes upon microencapsulation, can be measured easily using conventional release methods and analytical techniques, and exhibits anti-inflammatory properties. Leuprolide was chosen to be used as a model peptide because the hydrophilic LHRH agonist is well characterized in PLGA microspheres, is used in one of the most successful long-term controlled release products, the Lupron Depot, and has very few instability issues [27-32].

3.3 Materials

PLGA RESOMER® 503H (i.v. = 0.37 dL/g, free acid terminated), triamcinolone acetonide (Tr-A), betamethasone (BMZ), carboxymethyl cellulose (CMC), and polyvinyl alcohol (PVA, 80% hydrolyzed, MW ~ 10,000) were purchased from Sigma Aldrich. Polyvinyl alcohol (PVA, 88% hydrolyzed, MW ~ 25,000) was purchased from Polysciences, Inc. (Warrington, PA). PLGA (i.v. = 0.61 dL/g, ester terminated) was purchased from Lactel. Leuprolide was purchased from SHJNJ Pharmaceuticals (Shanghai, China) and leuprolide EIA kits were purchased from AB Biolabs (Ballwin, MO). Stainless steel wire cloth (type 316 , 400 mesh; 38 µm openings) was purchased from Grainger Industrial Supply (Lake Forest, IL). Dow Corning Pharma-80 FDA compliant silicone tubing (0.95 cm outer diameter x 0.64 cm inner diameter, MFR# 3257177) was purchased from Cole Parmer (Vernon Hills, IL). Medical grade liquid silicone rubber (MED-4940) was purchased from NuSil Technology (Carpinteria, CA). 7-9 week old male Sprague-Dawley (SD) rats were purchased from Charles River Laboratories (Wilmington, MA). All solvents used were HPLC grade and were purchased from Fisher Scientific and unless otherwise noted, all other chemicals were purchased from Sigma-Aldrich.

3.4 Methods

3.4.1 *Microsphere Preparation*

PLGA microspheres encapsulating Tr-A were prepared as previously described (Tr-A₂; see Chapter 2.4.1). Leuprolide microspheres were prepared from PLGA 503H using a double-emulsion-solvent evaporation technique. Briefly, PLGA was dissolved in methylene chloride (400 mg in 1.75 mL) and an aqueous solution containing leuprolide (55 mg in 170 μ L) at 60 °C was added and homogenized at 10,000 rpm for 1 min (Tempest IQ², VirTis, Warminster, PA) to form a w/o emulsion. Then, this emulsion was cooled to 15 °C, to increase encapsulation efficiency and reduce initial burst [33] and then 5% PVA (80% hydrolyzed) was added and vortexed to form a w/o/w emulsion. The complex emulsion was stirred in 0.5% PVA bath for 3 h to allow methylene chloride evaporation. Particles were screened to 63-90 μ m and then freeze-dried with approximately 13% w/w mannitol to prevent aggregation [33]. Microspheres were stored at -20°C until use.

3.4.2 *Determination of Loading and Encapsulation Efficiency*

Tr-A microspheres (~5 mg) were dissolved in 20 mL acetonitrile. The resulting solution was filtered and analyzed for Tr-A content by ultra-performance liquid chromatography (UPLC), as described below. Loading of leuprolide was determined by two-phase extraction. Leuprolide microspheres (~5 mg) were dissolved in 750 μ L of methylene chloride and then 750 μ L of 50 mM sodium acetate buffer at pH 4.0 was added and vortexed for 1 min. After centrifugation at 3,400 g for 4 minutes, 500 μ L of the aqueous phase was collected and replaced with the same volume of the buffer. This extraction was repeated with 50 mM sodium acetate buffer 5 times and then with 50 mM sodium acetate buffer containing 1 M sodium chloride 6 times [28]. The amount of leuprolide was determined by UPLC as described below. Drug loading was calculated

from the ratio of the mass of drug in the microspheres to the mass of the microspheres.

Encapsulation efficiency was calculated by the measured drug loading divided by theoretical loading.

3.4.3 *Cage Construction and Preparation*

Silicone tubing was cut into segments 0.5 cm in height and stainless steel wire mesh (38 μm openings) was cut to form circles of the same dimensions as the tubing segments (outer diameter = 1.59 cm) (see Figure 3.1A) for schematic). The mesh was then applied to both sides of the tubing using silicone elastomer spread on the edges of the tubing, which was vulcanized by autoclaving at 121°C to seal the cage shut. Microspheres were loaded into the cage following construction. Microspheres were suspended in a sterile injection medium (0.9% saline + 3.0% CMC) and injected through the silicone tubing into the cage using a 20 g needle. The tubing resealed following needle withdrawal, confining the microspheres to the cage. Cages were then filled with sterile saline until the time of implantation (< 1 h) with little escape of fluid before placing in the animal.

3.4.4 *In vitro Release*

In vitro release of Tr-A and leuprolide was measured in phosphate buffer + 0.02% Tween 80 + 0.05% sodium azide pH 7.4 (PBST pH 7.4). Microspheres were suspended freely in buffer or loaded into cages as described above, and then the cages were suspended in the same volume of buffer (1 mL for leuprolide, 30 mL for Tr-A). At each time point, the media was completely removed and replaced. Tr-A or leuprolide content was measured by ultra-performance liquid chromatography (UPLC), as detailed below.

3.4.5 *Quantification of Tr-A and Leuprolide in vitro*

Tr-A concentration in release media was determined by UPLC (Acquity UPLC, Waters, USA). The mobile phase was composed of 70 : 30 v/v (methanol : water) and the flow rate was set to 0.5 mL/minute. Samples and standards prepared in PBST were injected onto a C18 (Acquity BEH C18, 1.7 μ m, 2.1 x 100 mm) column maintained at 30 °C. Tr-A was detected at 254 nm. Leuprolide was detected using the same UPLC column. The initial mobile phase composition was 25 : 75 v/v (0.1% trifluoroacetic acid in acetonitrile : 0.1% trifluoroacetic acid in ddH₂O) and a linear gradient was used to achieve final composition of 35 : 65 over 2 min. Leuprolide was detected and quantified at 280 nm.

3.4.6 *Surgical Procedures*

The treatment of experimental animals was in accordance with the terms of the University Committee on Use and Care of Animals (University of Michigan UCUCA). Male SD rats were housed in cages and given free access to food and water, and were allowed 1-2 weeks to acclimate prior to study initiation. Rats were anesthetized with 2-4% isoflurane gas administered by a vaporizer (Midmark, Orchard Park, NY) before surgical preparation including shaving and sterilizing the surgical area using repeated, alternating swabs of alcohol and betadine solutions. An incision approximately 2 cm in length was made across the back of each rat and a pocket was formed in the subcutaneous space using surgical scissors. The cage was placed into this pocket, then the incision was closed using ETHILON[®] nylon sutures. Animals were allowed to recover from anesthesia on a heated water pad then returned to their cages where they were monitored until suture removal 7 days after surgery. At each time point, animals were euthanized using CO₂ overdose prior to cage retrieval and tissue excision.

3.4.7 *Pharmacokinetic Studies*

SD Rats were separated into two groups per microsphere formulation: SC injection or cage implant. The SC injection groups received a total dose of 4.5 mg/kg Tr-A or 5.6 mg/kg leuprolide as a suspension in 500-800 μ L injection medium (0.9% normal saline + 3.0% CMC) injected subcutaneously with a 20 g needle. The cage implant groups received the same total dose of microspheres using the surgical procedures described above. At each time point, the rats were anesthetized and 500 μ L whole blood was drawn via the jugular vein and transferred to a BD Microtainer[®] tube coated with EDTA. Following centrifugation at 1500 g at 4 °C for 10 minutes, plasma was aspirated and immediately frozen at -80 °C for storage.

3.4.8 *Tr-A Quantification in Plasma*

Twenty μ L internal standard solution (2 μ g/mL) was added to 200 μ L plasma and vortexed for 10 s. Then, 10 μ L of acetonitrile was added and vortexed for an additional 10 s. Three mL of an extraction solvent (4 : 3 : 3 ethyl acetate : methylene chloride : methylene chloride) was added, vortexed for 60 s and then centrifuged at 4°C for 6 minutes at 3400 rpm. 2.4 mL of the organic layer was then removed and dried at 40°C under nitrogen stream. Standards and QC samples were prepared by spiking blank plasma with 10 μ L of the appropriate Tr-A solution prepared in acetonitrile and then extracting according to the procedure above. The dried extracts were reconstituted in 1 : 1 acetonitrile : mobile phase (55 : 45 acetonitrile : 2 mM ammonium acetate pH 3.2 adjusted with formic acid) and analyzed by LC-MS/MS. Mobile phase consisted of 2 mM ammonium acetate (pH 3.2) adjusted with formic acid : acetonitrile (55:45). Flow rate was set to 1.0 mL/min and samples were injected onto a C18 column (Xbridge, 50mm x 4.6 mm, 3 μ m particle size) maintained at 35°C. Mass spectrometer was set at positive mode for data acquisition; collision energy was 13.4eV for Tr-A and 12eV for BMZ.

3.4.9 *Leuprolide Quantification in Plasma*

Plasma samples were diluted with 4 times volume of assay buffer included in the EIA kit and then was incubated in a 96-well plate in the presence of competitive biotinylated leuprolide and anti-leuprolide antibody at 4°C for 48 h. After washing wells, the samples were incubated with streptavidin-conjugated horseradish peroxidase at room temperature for 1 h, followed by color development using tetramethylbenzidine (TMB) solution. Absorbance of the samples was read at 450 nm. Leuprolide standards were prepared at 0, 0.3, 1, 3, 10, 30, 100 and 300 ng/mL in the presence of plasma.

3.4.10 *In vivo release from Microspheres*

Following cage removal from the subcutaneous space, the cage was opened using fine scissors and the microspheres were collected onto a 20- μ m sieve. The particles were washed thoroughly with ddH₂O to remove cellular debris and exudate then dried to constant weight under vacuum. Remaining Tr-A or leuprolide was then determined using the extraction procedures used to determine loading, described above.

3.4.11 *Histology*

At the time of euthanasia, tissue surrounding the cage implant was removed and fixed in 10% neutral buffered formalin for 24 h. For the SC injection groups, the injection site was marked at the time of administration and the surrounding tissue was excised at each time point. The fixed tissue was stored in 70% ethanol until time of paraffin embedding. Sections were then cut and stained with hematoxylin and eosin (H&E) stain. Images were taken by a Canon Rebel XS DSLR camera (Canon, Melville, NY) affixed to a Zeiss AxioLab.A1 light microscope (Zeiss, Oberkochen, Germany) using EOS utility software (Canon, Melville, NY).

3.5 Results and Discussion

Drug release from PLGA microspheres can occur due to a number of mechanisms such as hydrolysis, erosion, water uptake, diffusion, and combinations thereof. These processes have been studied extensively and are well understood *in vitro*, but the same comprehensive analysis has not been performed *in vivo*. To determine the overall contribution of each of these processes to overall drug release, the microspheres need to be retrievable for analysis. Hence, we designed a cage implant to restrain microspheres during release *in vivo*. Similar devices were first designed for studying the inflammatory response resulting from implantation of polymer films and implants, and were constructed to have openings large enough for aspiration of fluid out of the cage via 22 g needles. Thus, the openings and the implant itself was very large and not suitable for study with microspheres [1, 22-24, 34]. The cage described and used herein was designed to be able to prevent microspheres from migrating far from the site of administration but still allow for contact with fluids and cells present in the subcutaneous space. The cages are loaded with microspheres of a larger size than the openings in the material and then implanted in the backs of rats, which tolerate these implants well. As shown Figure 3.1E, once the cage is removed the microspheres can be collected, washed, and then subjected to mechanistic analysis.

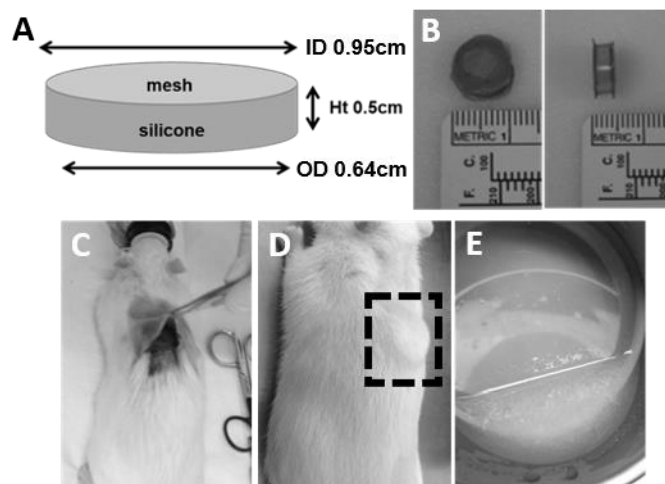


Figure 3.1: Cage implant design and use in rats. (A) Schematic of cage design and dimensions. (B) Top view (left) and side view (right) of a cage implant. Cages are implanted in the subcutaneous space in rats (C and D). Following euthanasia, cages are retrieved and the microspheres are retrieved and rinsed on a sieve prior to analysis (E).

In order for this cage model to be used as a tool for studying mechanisms of release *in vivo*, it needed to be evaluated in a series of experiments to ensure the cage itself does not have a significant impact on drug release. One may expect that the cage could be a physical barrier for drug diffusion, slowing the release, or for diffusion of PLGA degradation products, potentially increasing autocatalysis to result in increased hydrolysis and subsequent release. Additionally, the introduction of a large implant may alter the microsphere contacts with incoming cells and/or induce a severe inflammatory response, the latter of which could affect not only the rate of release but also the release mechanisms. For example, it has been suggested that inflammation would cause a slightly acidic pH in the local administration environment, which catalyzes hydrolysis [15, 21, 35-37]. To address these and other concerns over use of this system to study PLGA microspheres *in vivo*, several *in vitro* and *in vivo* experiments were performed.

Microspheres encapsulating Tr-A or leuprolide were successfully prepared and characterized prior to the following *in vitro* and *in vivo* studies. Tr-A loading in microspheres was 5.2 ± 0.1 w/w % and leuprolide loading was 5.79 ± 0.1 w/w % with corresponding 104 ± 1

% and 56 ± 1 % encapsulation efficiency. First, to ensure that the presence of the cage does not affect drug release from microspheres, drug release was quantified *in vitro* from microspheres freely suspended in buffer and from microspheres restrained in cages that were then incubated in the same volume of buffer.

As shown in Figure 3.2, there were no differences in the caged microspheres as compared to the suspended microspheres for both formulations. Similarity between the two *in vitro* release profiles for each formulation was determined by calculating the F2 value, a metric used to compare the dissolution profiles of the test and reference formulations and suggested by the Food and Drug Administration (FDA) [38-41]. The F2 value is a logarithmic reciprocal square root transformation of the sum of the squared error between reference and test data at each time point during dissolution, or in this case, release. These values were found to be 76.9 and 64.4 for Tr-A and leuprolide, respectively; both above the F2 value threshold of 50, which indicates similarity of the two curves. This result suggests that the presence of the cage does not strongly change the release rate of the small molecule or the peptide. To confirm this data and demonstrate the *in vivo* utility of this system, the plasma concentration of Tr-A and leuprolide following the administration of microspheres as a subcutaneous injection of suspended particles and as an implant in the cage model was measured (Figure 3.3). Other than a delayed burst in the case of Tr-A microspheres and a decreased burst in the case of leuprolide microspheres, no apparent differences were observed between the groups. The AUCs of both drugs were similar between groups, as shown in Table 3.1. This analysis shows that the presence of the cage *in vivo* does not result in a significant change in the release kinetics. It also suggests that although some inflammatory response may occur as a result of implantation, it does not cause an observable change in drug release over the release window studied.

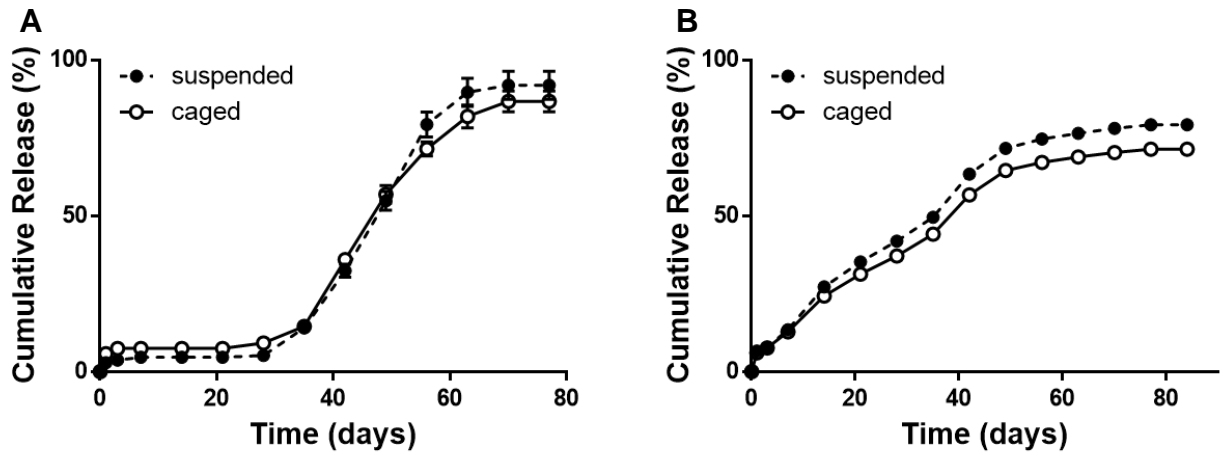


Figure 3.2: Release of Tr-A (A) and leuprolide (B) in vitro in PBST pH 7.4. Solid symbols represent release from suspended microspheres, open symbols represent release from microspheres restrained in cages. Data represent mean \pm SEM, $n=3$.

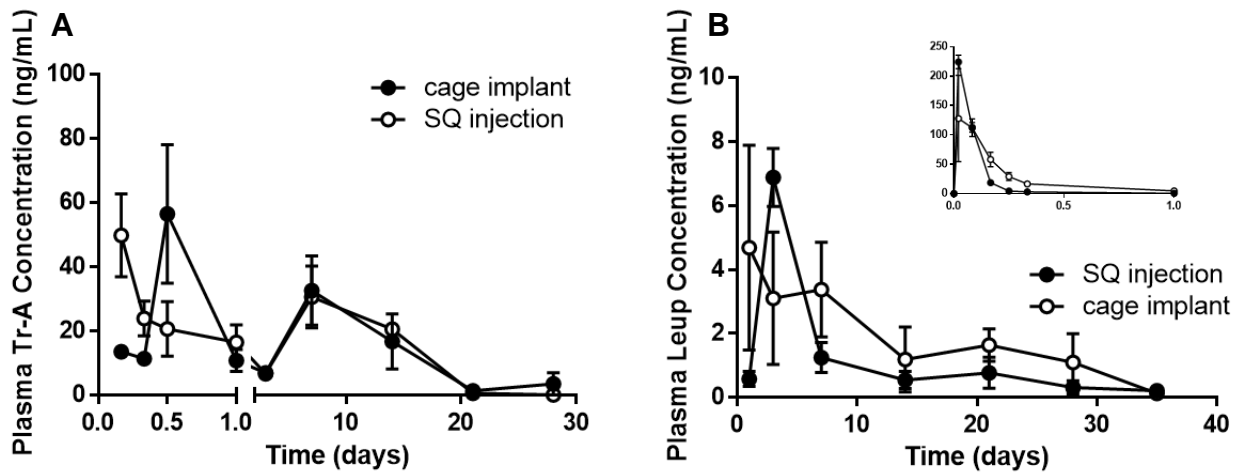


Figure 3.3: Pharmacokinetics of Tr-A (A) and leuprolide (B) following administration in rats as a suspension (open symbols) or in a cage implant (solid symbols). Inset in panel B shows leuprolide concentrations in plasma for the first 24 hours after administration, units are the same as the parent graph. Data represent mean \pm SEM, $n=2-4$.

Table 3.1: AUC and F2 similarity factor values for Tr-A and leuprolide following microspheres administration in rats.

	Tr-A microspheres		Leuprolide microspheres	
	SC injection	cage implant	SC injection	Cage implant
AUC (0-28d) (ng/ml/day)	374.04	374.52	60.82	88.81
SD	7.95	75.87	12.62	9.09
F2 (0-24h)	66.0		78.4	
f2 (0-28d)	84.5		90.2	

Using the cage, drug release from both microsphere formulations was directly assessed *in vivo* by extraction at time points following administration. Faster drug release was observed from PLGA microspheres encapsulating Tr-A and leuprolide *in vivo* than was expected following *in vitro* release tests (Figure 3.4). This phenomenon has been reported in the literature and raises concerns over what causes these discrepancies. Tr-A release from PLGA microspheres *in vitro* was controlled over 10 weeks, with a low initial burst occurring during the first day of release followed by a lag phase, which lasted through 5 weeks. PLGA erosion began at the end of this lag phase and Tr-A release was slow and continuous for the remainder of the study through 7-8 weeks. Leuprolide release occurred in a similar fashion, though the lag phase was less obvious in this case. Leuprolide was released continuously until completion after approximately 7-8 weeks. *In vivo* release directly measured from both Tr-A and leuprolide microspheres occurred much faster than was predicted from the *in vitro* results. Tr-A release was complete after just 2 weeks and leuprolide release was complete after 30 days. These results are supported by the PK data, as plasma concentrations of leuprolide were very low after 30 days and Tr-A plasma concentrations were low after 14 days. As previously mentioned, these differences have been shown previously but a definitive mechanistic analysis of drug release *in vitro* and *in vivo* has not been reported in an effort to determine the underlying causes for the

observed changes in release rate. The cage model described and validated here will be used in future studies to perform these analyses.

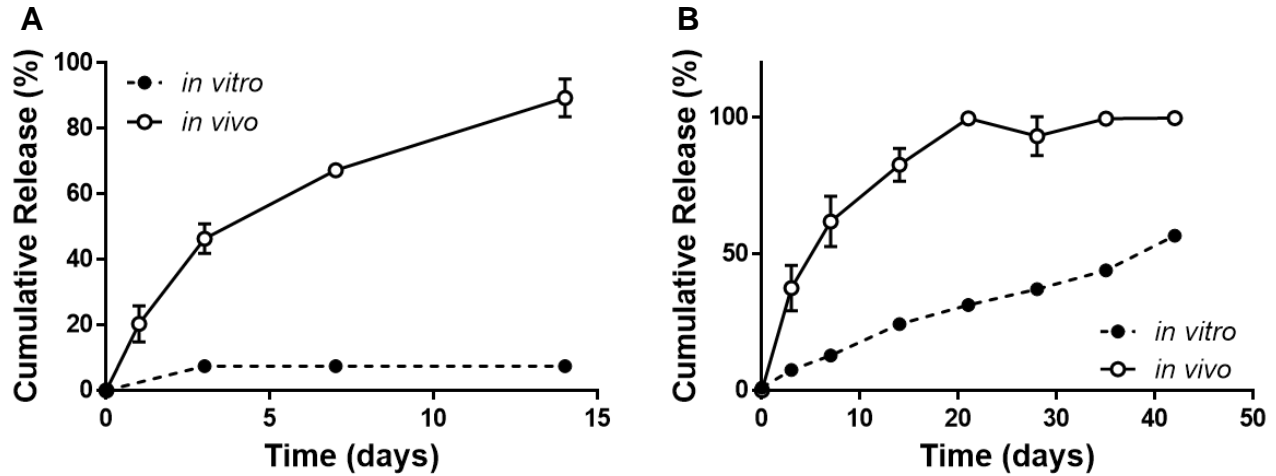


Figure 3.4: Release of Tr-A (A) and leuprolide (B) in vitro in PBST pH 7.4 and in vivo. Data represent mean \pm SEM, $n=3$.

To further examine the inflammation that occurs due to the introduction of the cage in the subcutaneous site, tissue surrounding the cage was removed at the time of euthanasia and retrieval then fixed and treated with H&E stains (Figure 3.5). Implantation of empty cages resulted in an obvious inflammatory response, with infiltration of lymphocytes occurring in the first three days as part of the acute inflammatory response. Leuprolide-containing cages exhibited a similar inflammatory response to the empty cages, and fibroblasts and neovascularization was observed on day 7. Macrophage infiltration was observed at day 14 and further evidence of the chronic phase of inflammation was seen at days 21 where there was deposition of collagenous fibers. Decreased leukocyte presence at later time points indicated the remission of inflammation. It is also important to note that at late times (56 d), there was some purulent in response to the prolonged presence of the cage. However, at such late time points it is unlikely that this component of the inflammatory response affects the implanted microspheres, as

the release data indicate complete release after 35 d. The presence of Tr-A microspheres ameliorated the inflammatory response, as very little inflammatory cell infiltration was seen at any point during the study. This is due to the anti-inflammatory properties of the steroid. There was no obvious acute inflammation through 3 days. There is evidence of very slight fibrogenesis at day 7 followed by collagenase deposition at days 14 and 21, part of the chronic phase of inflammation occurring due to the near complete release of Tr-A at these time points. The pus observed in leuprolide-containing cages was not evident in any cages containing Tr-A microspheres, though these studies were not extended to time points past 21 days due to the rapid release of this drug.

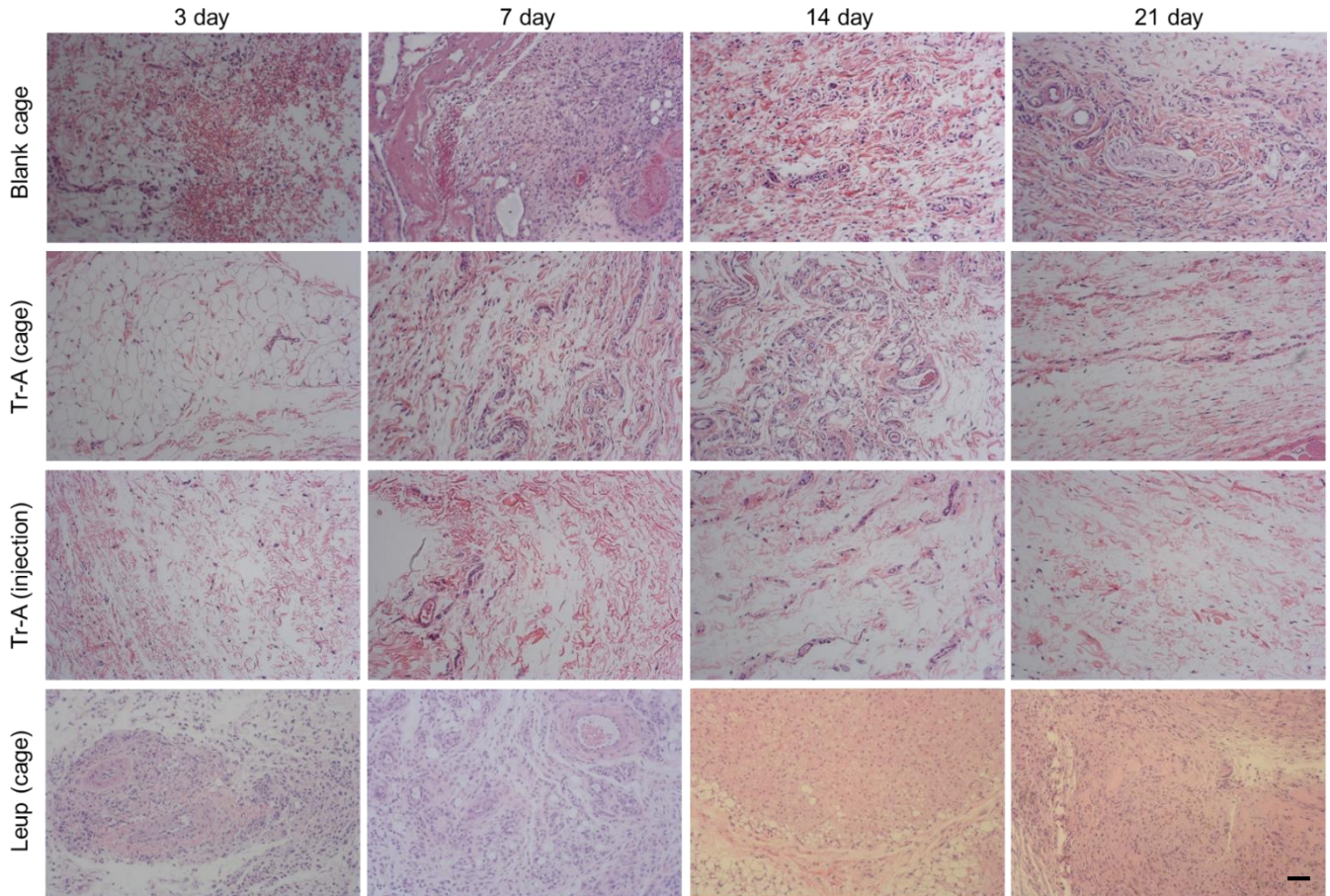


Figure 3.5: H&E stained images of tissue samples taken from the site of cage implantation or SC injection. Tissue was removed at the time of euthanasia. Scale bar represents 50 μ m.

One of the reasons Tr-A was selected as a model drug to use during this initial cage implant development and validation study was because it exhibits anti-inflammatory properties. As was just discussed, the release of this steroidal molecule from PLGA microspheres greatly diminished any sign of inflammation caused due to the implantation of the cage. Leuprolide, however, does not have the same effect and the inflammatory response is still evident. The results discussed earlier show that release of both drugs was faster *in vivo* than *in vitro*, as determined by using the cage. The lack of inflammation resulting from Tr-A cage implantation shows that this faster release is not likely due to inflammation, but some other biological components accelerating release. This also suggests that although initial implantation may cause

an inflammatory response, it is unlikely that this has an effect on overall drug release and thus the cage serves as a good tool for studying release and the release mechanisms *in vivo*. Further studies may employ the use of anti-inflammatory compounds to ameliorate the inflammatory response when evaluating microspheres containing drugs which do not exhibit these properties. Additionally, the presence of pus and tissue infiltration in the cage may need to be considered in these studies and strategies such as microsphere treatment with collagenases following cage excision could be employed if deemed necessary and if validated through a series of *in vitro* experiments to ensure there is no effect on the formulation.

To date, two other implantable devices have been discussed in the literature for restraint of polymeric implants *in vivo*. Our cage implant was modelled after a cage designed by Marchant et al. for studying the biocompatibility of polymeric films, hydrogels and implants [1, 22, 23, 34]. In these studies, large samples were loaded into cages made of stainless steel type 316, similar to the mesh we have used in the previously described experiments. These cages, however, were much larger than ours (3.5 cm in length, 1 cm in diameter) with openings large enough to allow penetration of a 22 g needle (0.8 mm x 0.8 mm). The authors implanted the cages in SD rats, aspirated exudate from inside the cage during the study, and then analyzed the fluid for concentrations of enzymes known to be released from inflammatory cells. Cell infiltration was also quantified and used as a marker for inflammation. Empty cages did result in a noticeable inflammatory response, including elevated counts of inflammatory cells and enzyme activity [22]. The morphology and cellular adhesion of the biomaterial was also studied in an effort to understand the effects the SC environment has on the material, which is our intent for future studies using our cage implant. In later studies, the corticosteroid hydrocortisone was included in a polymer film then implanted using the same cage, which resulted in decreased

inflammation, similar to our results with the steroid Tr-A [1]. The cage originally described was later modified by other authors to have smaller openings for the study of smaller poly (lactic acid) particles, though these studies focused only on exudate analysis and did not contain information on the effects of implantation on the polymer [25]. It is important to note that these initial cage implants were designed to study biocompatibility of polymeric implants and not drug release or release mechanisms, as is our overall goal.

More recently, another device was designed for the study of PLGA and poly(fumaric-co-sebacic acid) (P(FASA)) microspheres following SC, intramuscular (IM) and intraperitoneal (IP) administration [26]. This study is a more similar application to the studies discussed herein as the focus was on microsphere degradation rather than biocompatibility, although the device itself was a pouch made of porous polyethylene rather than surgical grade stainless steel. The major findings from the use of the pouch were that polymer degradation *in vivo* was accelerated in the IM site, and that the inflammatory response at the other two sites (SC and IP) was more robust than IM. Several *in vitro* experiments were also described wherein hydrolysis, mass loss and drug release were measured in PLGA microspheres with and without the pouch in an effort to show the effect of the pouch itself on these processes independent from the different administration environments. The results indicated that the pouch slightly increased mass loss, hydrolysis, and drug release *in vitro* as compared to microspheres tested without the pouch. Our cage implant, however, has been shown to not impede drug release in two highly different PLGA formulations. By using two drugs, the water-soluble peptide leuprolide and the hydrophobic small molecule Tr-A ($\log P \approx 2.4$ [42]), and two PLGAs (i.v. = 0.37 dL/g, free acid terminated and i.v. = 0.61 dL/g, ester terminated) we have successfully validated the use of this cage with two very different microspheres, suggesting its utility for a wide range of formulations.

Furthermore, we were able to confirm the accelerated release of both drugs *in vivo* measured by direct extraction following implantation by performing PK studies which also suggest complete release over 3 weeks in the case of Tr-A and 5 weeks in the case of leuprolide both with and without the cage. These data suggest that even *in vivo*, the cage does not significantly affect the release of either drug.

Hence, although previous authors have employed similar devices for studying biocompatibility and bio-erosion of implantable polymeric devices, we have presented a rigorous evaluation and validation of a cage designed to study polymeric formulation behavior *in vivo*. These experiments will serve as the framework for future studies involving more detailed analysis of implanted microspheres.

3.6 Conclusions

The cage implant designed here serves as a useful tool to study PLGA microspheres *in vivo*. This novel system allows for free contact with the administration space, while restraining the microspheres so they can be recovered at any time. This is especially important for the study of release mechanisms *in vivo*. Future studies will employ the cage implant to determine what mechanisms of release control drug release from polymeric microspheres *in vivo*. These studies will ultimately lead to a better understanding of *in vivo* microsphere behavior, and thus will help to design better *in vitro* release systems for testing these formulations to develop IVIVCs.

3.7 References

1. Marchant, R.E., *The cage implant system for determining in vivo biocompatibility of medical device materials*. Fundamental and Applied Toxicology, 1989. **13**(2): p. 217-227.
2. Young, D., C. Farrell, and T. Shepard, *In Vitro/In Vivo Correlation for Modified Release Injectable Drug Delivery Systems*, in *Injectable Dispersed Systems: Formulation, Processing and Performance*, D. Burgess, Editor. 2005, Taylor & Francis Group: Boca Raton. p. 159-176.
3. Zolnik, B.S. and D.J. Burgess, *In Vitro–In Vivo Correlation on Parenteral Dosage Forms*, in *Biopharmaceutics Applications in Drug Development*, R. Krishna and L. Yu, Editors. 2008, Springer US. p. 336-358.
4. *Guidance for Industry: Dissolution testing of immediate release solid oral dosage forms*. Food and Drug Administration Center for Drug Evaluation and Research. 1997.
5. Blanco-Prieto, M.a.J., et al., *In vitro and in vivo evaluation of a somatostatin analogue released from PLGA microspheres*. Journal of Controlled Release, 2000. **67**(1): p. 19-28.
6. Liu, W.H., et al., *Preparation and in vitro and in vivo release studies of Huperzine A loaded microspheres for the treatment of Alzheimer's disease*. Journal of Controlled Release, 2005. **107**(3): p. 417-427.
7. Heya, T., et al., *Controlled release of thyrotropin releasing hormone from microspheres: evaluation of release profiles and pharmacokinetics after subcutaneous administration*. J Pharm Sci, 1994. **83**(6): p. 798-801.
8. Heya, T., et al., *In vitro and in vivo evaluation of thyrotrophin releasing hormone release from copoly (dl-lactic/glycolic acid) microspheres*. Journal of Pharmaceutical Sciences, 1994. **83**(5): p. 636-640.
9. Kostanski, J.W., et al., *Evaluation of Orntide microspheres in a rat animal model and correlation to in vitro release profiles*. AAPS PharmSciTech, 2000. **1**(4): p. E27.
10. Negrin, C.M., et al., *In vivo-in vitro study of biodegradable methadone delivery systems*. Biomaterials, 2001. **22**(6): p. 563-70.
11. Rawat, A., U. Bhardwaj, and D.J. Burgess, *Comparison of in vitro-in vivo release of Risperdal((R)) Consta((R)) microspheres*. Int J Pharm, 2012. **434**(1-2): p. 115-21.
12. Kim, T.-K. and D.J. Burgess, *Pharmacokinetic characterization of I4C-vascular endothelial growth factor controlled release microspheres using a rat model*. Journal of Pharmacy and Pharmacology, 2002. **54**(7): p. 897-905.
13. Morita, T., et al., *Evaluation of in vivo release characteristics of protein-loaded biodegradable microspheres in rats and severe combined immunodeficiency disease mice*. J Control Release, 2001. **73**(2-3): p. 213-21.
14. Zolnik, B.S. and D.J. Burgess, *Evaluation of in vivo-in vitro release of dexamethasone from PLGA microspheres*. Journal of Controlled Release, 2008. **127**(2): p. 137-145.
15. Tracy, M.A., et al., *Factors affecting the degradation rate of poly(lactide-co-glycolide) microspheres in vivo and in vitro*. Biomaterials, 1999. **20**(11): p. 1057-62.
16. Clark, B. and P. Dickinson, *Case Study: In Vitro/In Vivo Release from Injectable Microspheres*, in *Injectable Dispersed Systems: Formulation, Processing and Performance* D. Burgess, Editor. 2005, Taylor & Francis Group: Boca Raton, FL. p. 543-570.

17. Martinez, M., et al., *In vitro and in vivo considerations associated with parenteral sustained release products: A review based upon information presented and points expressed at the 2007 Controlled Release Society Annual Meeting*. Journal of Controlled Release, 2008. **129**(2): p. 79-87.
18. Martinez, M.N., et al., *Breakout session summary from AAPS/CRS joint workshop on critical variables in the in vitro and in vivo performance of parenteral sustained release products*. Journal of Controlled Release, 2010. **142**(1): p. 2-7.
19. Alexis, F., *Factors affecting the degradation and drug-release mechanism of poly(lactic acid) and poly[(lactic acid)-co-(glycolic acid)]*. Polymer International, 2005. **54**(1): p. 36-46.
20. Uhrich, K.E., et al., *Polymeric Systems for Controlled Drug Release*. Chemical Reviews, 1999. **99**(11): p. 3181-3198.
21. Anderson, J.M. and M.S. Shive, *Biodegradation and biocompatibility of PLA and PLGA microspheres*. Advanced Drug Delivery Reviews, 1997. **28**(1): p. 5-24.
22. Marchant, R., et al., *In vivo biocompatibility studies. I. The cage implant system and a biodegradable hydrogel*. Journal of Biomedical Materials Research, 1983. **17**(2): p. 301-325.
23. Marchant, R.E., K.M. Miller, and J.M. Anderson, *In vivo biocompatibility studies. V. In vivo leukocyte interactions with biomer*. Journal of Biomedical Materials Research, 1984. **18**(9): p. 1169-1190.
24. Kim, J., et al., *In vivo biodegradation and biocompatibility of PEG/sebacic acid-based hydrogels using a cage implant system*. Journal of Biomedical Materials Research Part A, 2010. **95A**(1): p. 191-197.
25. Bergsma, J.E., et al., *Biocompatibility study of as-polymerized poly(L-lactide) in rats using a cage implant system*. Journal of Biomedical Materials Research, 1995. **29**(2): p. 173-179.
26. Sandor, M., J. Harris, and E. Mathiowitz, *A novel polyethylene depot device for the study of PLGA and P(FASA) microspheres in vitro and in vivo*. Biomaterials, 2002. **23**(22): p. 4413-4423.
27. Reinhold, S.E., et al., *Self-Healing Microencapsulation of Biomacromolecules without Organic Solvents*. Angewandte Chemie International Edition, 2012. **51**(43): p. 10800-10803.
28. Sophocleous, A.M., et al., *The nature of peptide interactions with acid end-group PLGAs and facile aqueous-based microencapsulation of therapeutic peptides*. Journal of Controlled Release, 2013. **172**(3): p. 662-670.
29. Ogawa, Y., et al., *Controlled Release of LHRH Agonist, Leuprolide Acetate, from Microcapsules: Serum Drug Level Profiles and Pharmacological Effects in Animals*. Journal of Pharmacy and Pharmacology, 1989. **41**(7): p. 439-444.
30. Ogawa, Y., et al., *Controlled-release of leuprolide acetate from polylactic acid or copoly(lactic/glycolic) acid microcapsules: influence of molecular weight and copolymer ratio of polymer*. Chem Pharm Bull (Tokyo), 1988. **36**(4): p. 1502-7.
31. Okada, H., Y. Doken, and Y. Ogawa, *Persistent suppression of the pituitary-gonadal system in female rats by three-month depot injectable microspheres of leuprorelin acetate*. J Pharm Sci, 1996. **85**(10): p. 1044-8.
32. Okada, H., et al., *Pharmacokinetics of once-a-month injectable microspheres of leuprolide acetate*. Pharm Res, 1991. **8**(6): p. 787-91.

33. Ogawa, Y., S. Takada, and M. Yamamoto, *US Patent No. 5,330,767*. 1994.
34. Marchant, R.E., J.M. Anderson, and E.O. Dillingham, *In vivo biocompatibility studies. VII. Inflammatory response to polyethylene and to a cytotoxic polyvinylchloride*. *J Biomed Mater Res*, 1986. **20**(1): p. 37-50.
35. Ali, S.A.M., P.J. Doherty, and D.F. Williams, *Molecular biointeractions of biomedical polymers with extracellular exudate and inflammatory cells and their effects on the biocompatibility, in vivo*. *Biomaterials*, 1994. **15**(10): p. 779-785.
36. Anderson, J.M., *In Vitro and In Vivo Monocyte, Macrophage, Foreign Body Giant Cell, and Lymphocyte Interactions with Biomaterials*, in *Biological Interactions on Materials Surfaces*, D.A. Puleo and R. Bizios, Editors. 2009, Springer New York. p. 225-244.
37. Anderson, J.M., A. Rodriguez, and D.T. Chang, *Foreign body reaction to biomaterials*. *Seminars in Immunology*, 2008. **20**(2): p. 86-100.
38. Duan, J., K. Riviere, and P. Marroum, *In Vivo Bioequivalence and In Vitro Similarity Factor (f₂) for Dissolution Profile Comparisons of Extended Release Formulations: How and When Do They Match?* *Pharmaceutical Research*, 2011. **28**(5): p. 1144-1156.
39. Shah, V., et al., *In Vitro Dissolution Profile Comparison—Statistics and Analysis of the Similarity Factor, f₂*. *Pharmaceutical Research*, 1998. **15**(6): p. 889-896.
40. Liu, J.-p., M.-C. Ma, and S.-C. Chow, *Statistical Evaluation of Similarity Factor f₂ as a Criterion for Assessment of Similarity between Dissolution Profiles*. *Drug Information Journal*, 1997. **31**(4): p. 1255-1271.
41. HH, M.J.F., *Mathematical Comparison of Curves with an Emphasis on Dissolution Profiles*. *Pharmaceutical Research*, 1994(11).
42. Phillips, C.A. and B.B. Michniak, *Transdermal delivery of drugs with differing lipophilicities using azone analogs as dermal penetration enhancers*. *Journal of Pharmaceutical Sciences*, 1995. **84**(12): p. 1427-1433.

3.8 Supplementary Information

3.8.1 *Tr-A* release *in vivo* (*Tr-A_1*)

A second PLGA microsphere formulation encapsulating *Tr-A* (*Tr-A_1*) was prepared as described previously (Chapter 2.4.1). These microspheres were prepared using a lower molecular weight, acid terminated PLGA. Preliminary studies showed that drug release from this formulation was much faster *in vivo* than *in vitro*, as was reported for the other *Tr-A* microsphere formulation (*Tr-A_2*; data reported in the main body of this chapter). Release from *Tr-A_1* *in vivo* reached 99.1% by day 21, however, only 52.9% of drug had been release *in vitro* at the same time point. This, in conjunction with the data previously discussed, highlights the need to study release mechanisms which cause accelerated drug release *in vivo*.

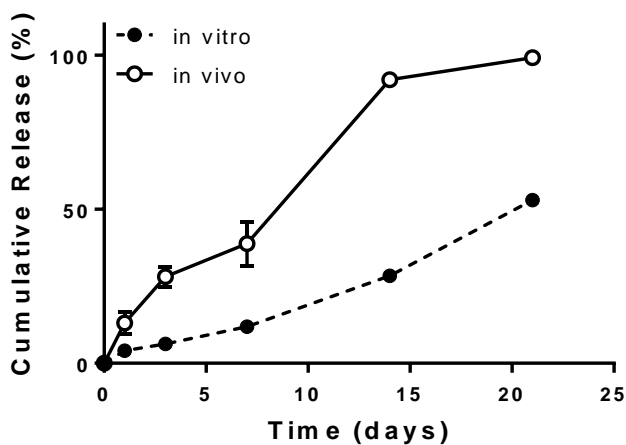


Figure S 3.1: Release of *Tr-A* from *Tr-A_1* microspheres *in vitro* in PBST pH 7.4 and *in vivo*. Data represent mean \pm SEM, $n=3$.

3.8.2 *In vitro* release and Pharmacokinetics (Tr-A_1)

Tr-A release from Tr-A_1 was measured *in vitro* in PBST pH 7.4, as described in detail in the main text of this chapter. Release was similar from suspended and caged microspheres (F2 value of similarity = 94.9). The pharmacokinetics of Tr-A was also measured in male SD rats over one month following administration as a either SC injection or in the cage implant. Again, the plasma concentration vs. time curves were similar in the two treatment groups, F2 = 88.6. This provides further validation that the cage can be used to study release and release mechanisms, as the cage does not affect drug release *in vitro* nor *in vivo*.

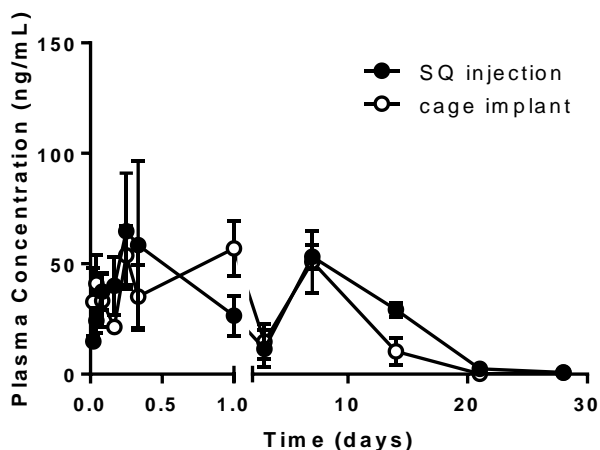


Figure S 3.2: Pharmacokinetics of Tr-A_1 following Tr-A_1 administration in rats as a suspension (open symbols) or in a cage implant (solid symbols). Data represent mean \pm SEM, n=2-4.

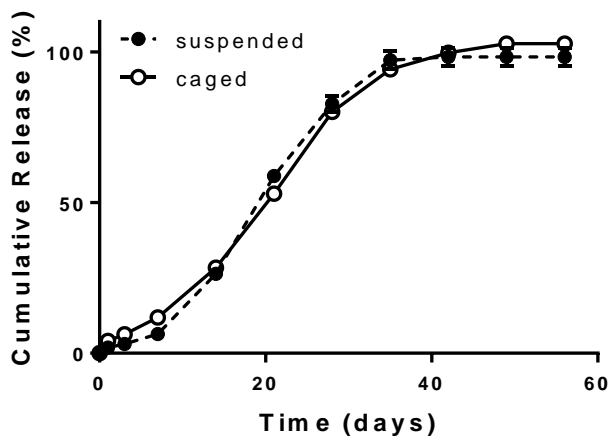


Figure S 3.3: Release of Tr-A from Tr-A_1 microspheres restrained in cages or suspended in PBST pH 7.4. Data represent mean \pm SEM, n=3.

3.8.3 *Bodipy Diffusion in vitro*

There is some concern that restraining microspheres in a cage during *in vivo* release will affect release and release mechanisms. The previously discussed *in vitro* and *in vivo* experiments show that there is no impact on drug release, but there is still the possibility that the cage will cause a change in the formulation that will not result in a significant change in release rate. For example, the restraint of the microspheres may also restrain low molecular weight acidic byproducts, leading to increase autocatalysis, degradation and subsequent erosion. To determine whether our cage model has a significant impact on degradation of microspheres and mechanisms of release, we studied the morphology of both Tr-A_1 and Tr-A_2 microspheres during *in vitro* release either suspended or caged in PBST pH 7.4. Using these confocal images, we calculated diffusion coefficients of bodipy in the degrading Tr-A_2 microparticles as previously described (Chapter 2.4.8). These experiments showed no significant difference between drug diffusion in microspheres suspended in PBST pH 7.4 and microspheres caged in PBST pH 7.4 (Figure S 3.4 and Figure S 3.5). This is further evidence that the presence of the cage itself does not affect formulation behavior. In particular, there is no evidence that the cage causes accumulation of acidic byproducts which cause increased particle degradation, and has no effect on drug diffusion in the polymer matrix.

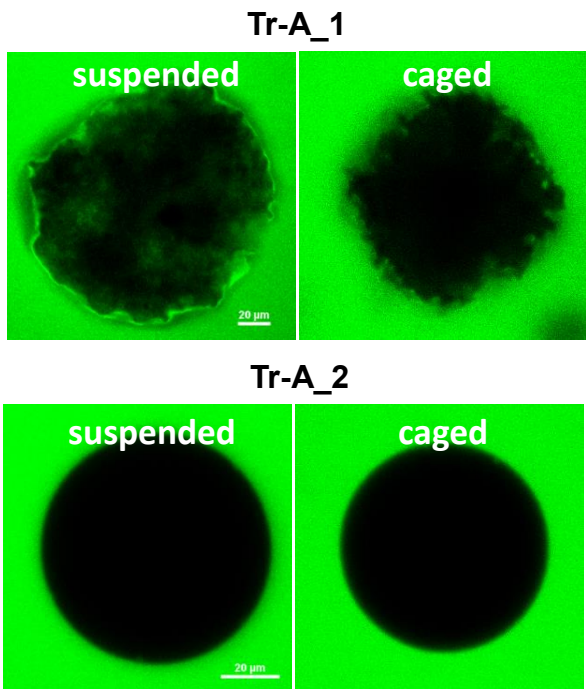


Figure S 3.4: LCSM images of microspheres following one week incubation in PBST.

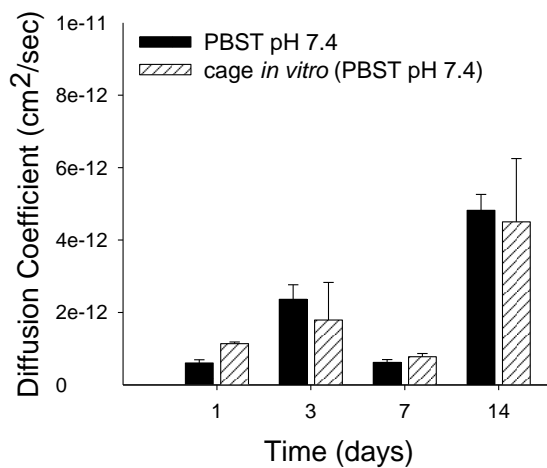


Figure S 3.5: Diffusion coefficients of BODIPY in degrading microspheres either freely suspended or caged in PBST pH 7.4. There is no significant difference between the two conditions at any time point. Data represent mean + SEM, n=6.

Chapter 4 : Mechanisms of Release of Triamcinolone Acetonide from PLGA Microspheres *in vivo*

4.1 Abstract

In vitro-in vivo correlations for PLGA microspheres have been extremely limited in the literature due to a lack of a mechanistic understanding of drug release *in vivo*. Most reports of IVIVC are empirical in nature, typically based on a mathematical relationship between *in vitro* drug release and *in vivo* drug release, which is often estimated using deconvolution from pharmacokinetic data. In order to improve *in vitro* release tests to better predict microsphere behavior *in vivo*, the *in vivo* release mechanisms must be elucidated. Here, two PLGA microsphere formulations encapsulating the model drug triamcinolone acetonide (Tr-A) were implanted subcutaneously in rats using a previously validated cage model to allow for microsphere retrieval during *in vivo* release. Release of Tr-A from both formulations was greatly accelerated *in vivo* compared to *in vitro* (PBST pH 7.4), including rate of PLGA hydrolysis, mass loss and water uptake. Both microsphere formulations exhibited erosion-controlled release *in vitro*, but only Tr-A_1 exhibited the same mechanism *in vivo*. The release of Tr-A_2 *in vivo* displayed an osmotically induced/pore diffusion mechanism not previously observed *in vitro*. This research indicates the need to develop *in vitro* release tests which cause these same mechanisms to be operative in causing drug release. In this way, mechanistic IVIVCs can be developed by accurately predicting and simulating *in vivo* performance.

4.2 Introduction

Although biodegradable polymers such as poly (lactic-*co*-glycolic acid) (PLGA) are widely used in the literature to achieve controlled drug release, and are even used in several FDA-approved controlled release (CR) drug products, very little is known about the behavior of these formulations *in vivo* [1-4][1-4]. Typical analysis of these products includes extensive characterization and *in vitro* release, followed by *in vivo* pharmacokinetic and efficacy studies. Surprisingly, *in vivo* analysis of the polymer during drug release is rarely reported and instead, only plasma drug concentrations and therapeutic endpoint markers are discussed [5-14][5-14]. This is an issue especially because the *in vitro* tests used to estimate kinetics of *in vivo* release from CR formulations rarely result in accurate predictions. Thus, to date, no FDA guideline exists for establishing *in vitro-in vivo* correlation (IVIVC) models to predict *in vivo* performance of CR PLGA formulations, and in particular, microspheres [15, 16][15, 16].

An IVIVC has been defined by the FDA as a “predictive mathematical model describing the relationship between an *in vitro* property of dosage form and a relevant *in vivo* response” [17, 18][17, 18]. Generally, the *in vitro* property is the rate or extent of drug dissolution or release while the *in vivo* response is the plasma drug concentration or amount of drug absorbed. Five levels of IVIVC are described in the FDA guidelines: A, B, C, multiple level C, and D [19]. Level A correlates point-by-point an *in vitro* dissolution profile with an *in vivo* plasma drug level pharmacokinetics profile. This most stringent correlation defines that measurement of dissolution rate alone is sufficient to assure *in vivo* bioequivalence. There have been some attempts in the literature to establish IVIVCs for polymeric CR formulations, but many of these studies have been based on building mathematical relationships between drug release *in vitro* and the *in vivo* pharmacokinetics, not a direct measurement of drug release *in vivo* [5, 7-11, 14, 20][5, 7-11, 14,

20]. Therefore, while claiming that these are level A IVIVCs, there is still some deconvolution of the data to estimate release rates, making these attempts to establish IVIVC for CR products empirical in nature. Furthermore, there has been little attempt to date to understand not only rates of drug release *in vivo*, but how the *in vivo* environment affects release mechanisms from CR formulations [2, 15, 21, 22][2, 15, 21, 22].

Release from PLGA microspheres can be controlled by at least three major mechanisms, or combinations thereof: 1) diffusion through the polymer matrix, 2) water-mediated transport processes, and 3) polymer hydrolysis and erosion. While these processes are well studied and understood in the context of *in vitro* systems, it is unknown whether the same mechanisms are responsible for release *in vivo*. Given the reported discrepancies between *in vitro* and *in vivo* release data, it is likely the *in vivo* environment changes the rates of the mechanistic processes, resulting in differences in release rates. From the data presented in Chapter 2 of this thesis, it is clear that *in vitro* tests can be designed to alter release mechanisms and release rates. Thus, a mechanistic understanding of drug release *in vivo* can lead to the design of *in vitro* tests which will accurately predict *in vivo* performance, resulting in mechanism-based IVIVC.

One of the major reasons the *in vivo* release mechanisms of PLGA microspheres are not well understood is due to the difficulty of retrieving the particles following administration, as they are required for mechanistic analyses. Thus, we previously developed a cage implant to restrain PLGA microspheres during *in vivo* release. The cage system was validated both by the similar release and *in vivo* pharmacokinetics in the presence and absence of the cage. Using this system, discussed in detail in Chapter 3, microspheres can be readily retrieved and analyzed at any point during the window of release before significant inflammation results from the presence of the cage, and such inflammation is strongly inhibited by the presence of released steroid. This

chapter discusses the mechanisms of release from PLGA microspheres encapsulating the model drug triamcinolone acetonide (Tr-A). These microspheres have been extensively characterized *in vitro* (Chapter 2) and here were subjected to the same mechanistic analyses during *in vivo* release to understand the reason for the previously reported accelerated *in vivo* release.

4.3 Materials

Triamcinolone acetonide (Tr-A), PLGA RESOMER® 502H (i.v. = 0.19 dL/g, free acid terminated), and carboxymethyl cellulose (CMC) were purchased from Sigma-Aldrich. Poly vinyl alcohol (PVA, 88% hydrolyzed, MW ~ 25,000) was purchased from Polysciences, Inc. (Warrington, PA). PLGA (i.v. = 0.61 dL/g, ester terminated) was purchased from Lactel. BODIPY® FL (4,4-Difluoro-5,7-Dimethyl-4-Bora-3a,4a-Diaza-s-Indacene-3-Propionic Acid) was purchased from Life Technologies. Stainless steel wire cloth (type 316 , 400 mesh; 38 µm openings) was purchased from Grainger Industrial Supply (Lake Forest, IL). Dow Corning Pharma-80 FDA compliant silicone tubing (1.9 cm outer diameter x 1.3 cm inner diameter, MFR# 4008433) was purchased from Cole Parmer (Vernon Hills, IL). Medical grade liquid silicone rubber (MED-4940) was purchased from NuSil Technology (Carpinteria, CA). 7-9 week old male Sprague-Dawley (SD) rats were purchased from Charles River Laboratories (Wilmington, MA). All solvents used were HPLC grade and were purchased from Fisher Scientific and unless otherwise noted, all other chemicals were purchased from Sigma-Aldrich.

4.4 Methods

Methods for microsphere preparation (Section 2.4.1), cage construction/microsphere loading (Section 3.4.3), and in vitro release and mechanistic analyses (Sections 2.4.5-2.4.9) are described in detail in Chapters 2 and 3.

4.4.1 *Surgical Procedures*

The treatment of experimental animals was in accordance with the terms of the University Committee on Use and Care of Animals (University of Michigan UCUCA). Male SD rats were housed in cages and given free access to food and water, and were allowed 1-2 weeks to acclimate prior to study initiation. Rats were anesthetized with 2-4% isoflurane gas administered by a vaporizer (Midmark, Orchard Park, NY) before surgical preparation including shaving and sterilizing the surgical area using repeated swabs of alcohol and betadine solutions. An incision approximately 2 cm in length was made across the back of each rat and a pocket was formed in the subcutaneous space using surgical scissors. The cage was placed into this pocket, then the incision was closed using ETHILON[®] nylon sutures. Animals were allowed to recover from anesthesia on a heated water pad then returned to their cages where they were monitored until suture removal 7 days after surgery. At each time point, animals were euthanized by CO₂ overdose prior to cage retrieval.

4.4.2 *Assessment of Drug Release in vitro from Cage Implant*

In vitro drug release and mechanistic analyses of Tr-A_1 and Tr-A_2 microspheres was carried out in PBS (137mM NaCl, 3mM KCl, 7.74 mM Na₂HPO₄, 2.26 mM NaH₂PO₄) + 0.02% Tween 80 + 0.05% NaN₃ (PBST pH 7.4). Microspheres (~50 mg) were loaded in cage implant as previously described (see Chapter 3.4.3) and the cage was then placed in 30 ml of media and shaken mildly at 37°C for the duration of the experiment. At each time point (1, 3, 7 days and weekly thereafter), the cage was transferred into fresh media and drug content in the media was measured by UPLC, as previously described.

4.4.3 Release and Mechanistic Analyses *in vivo*

During *in vitro* release; PLGA molecular weight, mass loss, water content, and bodipy diffusion were determined weekly. These methods were previously developed and reported in Chapter 2 of this thesis. Following cage removal from the subcutaneous space, the cage was opened using fine scissors and the microspheres were collected onto a 20 μm sieve. The particles were washed thoroughly to remove cellular debris and exudate then dried to constant weight under vacuum. A small aliquot of dried microparticles (3-5 mg) was then dissolved in 20 mL acetonitrile to determine the remaining Tr-A content, measured by UPLC. Mechanistic analyses were also performed on the particles retrieved by the cage using the methods previously described (*see Chapter 2.4.6-2.4.9*).

4.4.4 Statistical and Regression Analysis

Statistical analyses and regressions were performed using Prism (Graphpad, San Diego, CA). Rate constants, t_{50} values, and diffusion coefficients *in vivo* were compared to *in vitro* results (PBST pH 7.4) using unpaired student t-tests to determine two-tailed P-values. The level of significance was established at the 95% confidence interval ($\alpha < 0.05$).

4.5 Results and Discussion

Tr-A release from both PLGA microsphere formulations was much faster *in vivo* than *in vitro* (Figure 4.1). *In vitro*, Tr-A_1 exhibited mostly continuous release lasting approximately 35 days. Release *in vivo* was also continuous, but release was 99.1 ± 0.4 % complete after just 21 days. Release was similarly fast from Tr-A_2 *in vivo*, with 95.1 ± 2.4 % drug released in 21 days vs just 7.4 ± 1.0 % release at the same time point in PBST pH 7.4. The lag phase observed in this formulation *in vitro* was absent *in vivo*, resulting in continuous release until completion. It is also interesting to note that although there were distinct differences in the release rate and profile

between the two formulations *in vitro*, *in vivo* release was very similar from the low molecular weight, acid-terminated PLGA and the moderate molecular weight, ester end-capped PLGA. Given the drastic differences observed between *in vitro* and *in vivo* release kinetics for both of these microsphere formulations, it is important to understand what mechanisms of release are responsible for the accelerated release and how these may be different from the operative mechanisms *in vitro*.

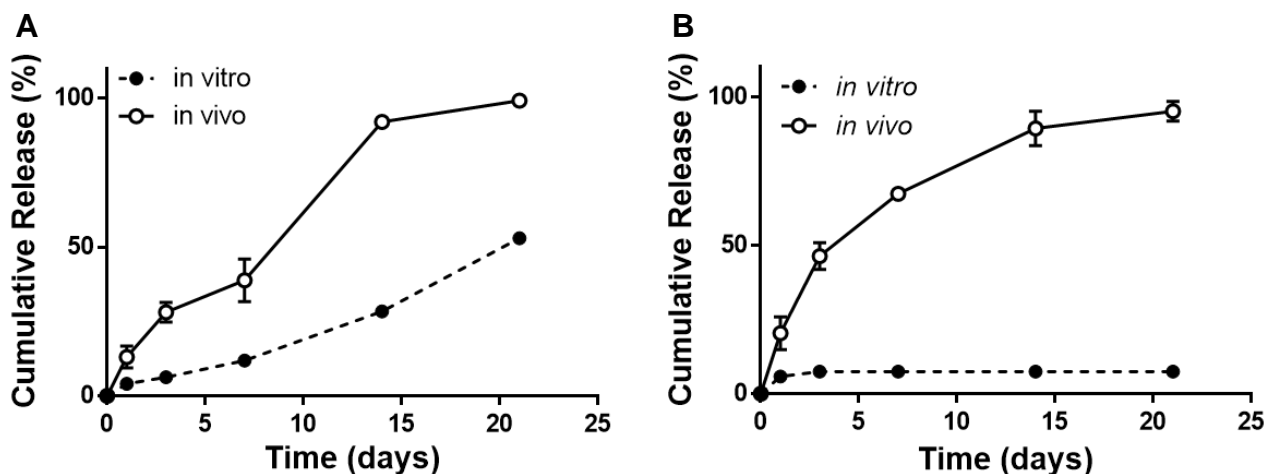


Figure 4.1: *in vitro* and *in vivo* release from Tr-A_1 (A) and Tr-A_2 (B) microspheres. Release was measured using cage model. Data represent mean \pm SEM, $n=3-4$.

Using the cage model previously developed and validated, mechanistic analyses were performed on microspheres during *in vivo* release. First, the degradation kinetics were determined by measuring the PLGA molecular weight at each time point. Hydrolysis was significantly faster *in vivo* than *in vitro* (Figure 4.2), as seen by the first order degradation rate constants listed in Table 4.1. Total erosion of microspheres was also accelerated *in vivo* (Figure 4.3). Erosion was found to be the major mechanism of release from microspheres *in vitro* as release and mass loss occurred generally on the same time scale. This was determined by performing nonlinear regression analysis on release and mass loss data to determine t_{50} values, or

the time taken to reach 50% release ($t_{50,release}$) and 50% mass loss ($t_{50,erosion}$). As previously discussed, if these two processes occur generally on the same time scale ($t_{50,release}/t_{50,erosion} \approx 1$), erosion is likely the dominant mechanism of release. Table 4.2 shows the estimated t_{50} values as well as the ratios of these values both in PBST pH 7.4 and *in vivo*. In the case of Tr-A_1, both the $t_{50,release}$ and the $t_{50,erosion}$ are both significantly lower *in vivo* than *in vitro*, but the ratio does not change (0.77 vs. 0.72). This suggests that although release is accelerated *in vivo*, erosion is likely still the major cause of release and this process is also accelerated. This is supported by the degradation kinetics, as the rate of hydrolysis *in vivo* is nearly double that *in vitro*. The rapid production of shorter, lower molecular PLGA chains leads to faster transport of these oligomers out of the microsphere, causing overall erosion of the polymer matrix. Tr-A release from Tr-A_2 microspheres was greatly accelerated *in vivo* ($t_{50,release} \approx 7$ d vs. 47 d), as was erosion ($t_{50,erosion} \approx 15$ d vs. 46 d). In this formulation, however, the $t_{50,release}/t_{50,erosion}$ did not stay the same *in vivo* (1.01 vs. 0.46), as release occurred on a faster time scale than erosion *in vivo*. This suggested that some other mechanism was contributing to release *in vivo* more prominently than *in vitro*.

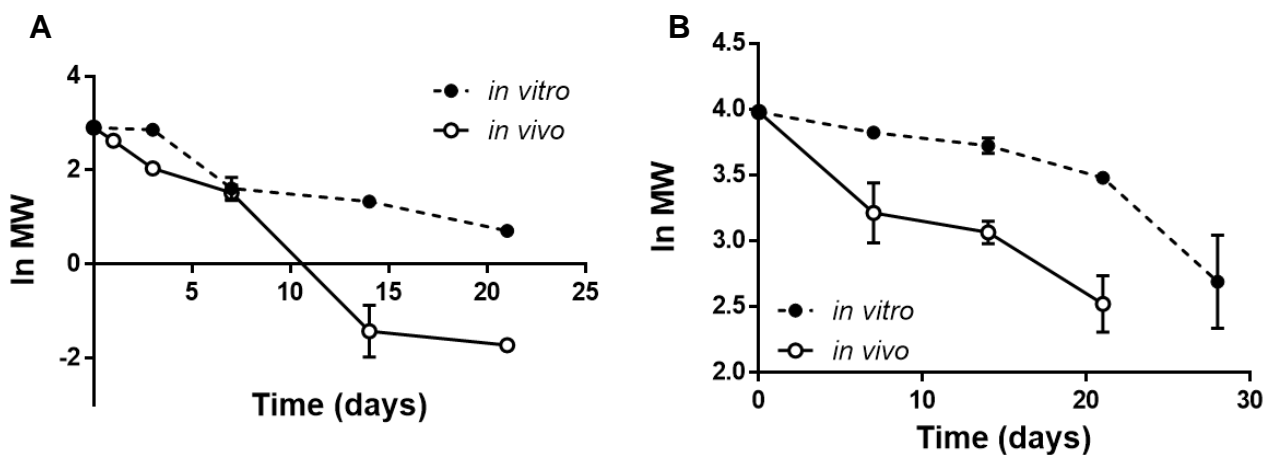


Figure 4.2: *in vitro* and *in vivo* PLGA hydrolysis kinetics in Tr-A_1 (A) and Tr-A_2 (B) microspheres. Data represent mean \pm SEM, $n=3-5$.

Table 4.1: Initial first order rate constants (day^{-1}) of PLGA hydrolysis in Tr-A_1 and Tr-A_2 microspheres as determined by linear regression analysis of data shown in Figure 4.2. Values were taken from regression over the first 14 days.

	<i>in vitro</i>	<i>in vivo</i>
Tr-A_1	0.125 ± 0.018	$0.301 \pm 0.022^\dagger$
Tr-A_2	0.034 ± 0.001	$0.065 \pm 0.010^*$

* $p < 0.05$; $^\dagger p < 0.0001$

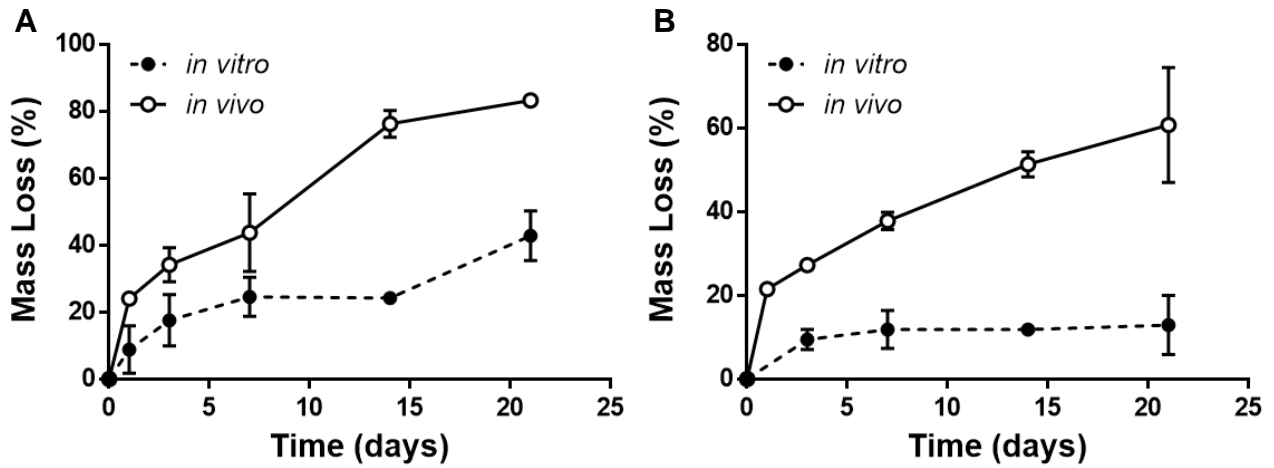


Figure 4.3: *in vitro* and *in vivo* mass loss of Tr-A_1 (A) and Tr-A_2 (B) microspheres. Data represent mean \pm SEM, $n=3-5$.

Table 4.2: Characteristic times (in days) of release and erosion from Tr-A_1 and Tr-A_2 microspheres. Values represent mean \pm SEM, $n=3$. T_{50} ratios were calculated from mean values of $t_{50,release}$ and $t_{50,erosion}$.

	Tr-A_1		Tr-A_2	
	<i>in vitro</i>	<i>in vivo</i>	<i>in vitro</i>	<i>in vivo</i>
$t_{50,release}$	19.0 ± 0.4	$7.9 \pm 0.8^*$	46.8 ± 0.6	$6.8 \pm 4.4^*$
$t_{50,erosion}$	25 ± 8	$11 \pm 1^*$	46 ± 3	$15 \pm 2^*$
$t_{50,release} / t_{50,erosion}$	0.77	0.72	1.01	0.46

* $p < 0.05$

Further investigation into the mechanisms causing accelerated Tr-A release *in vivo* included measurement of water content in the microspheres. Water content was dramatically increased at each time point *in vivo* relative to that observed *in vitro* (Figure 4.4). Increased water uptake into the microspheres likely facilitates PLGA hydrolysis and subsequent erosion, and so these data fit the previously reported hydrolysis kinetics and mass loss data.

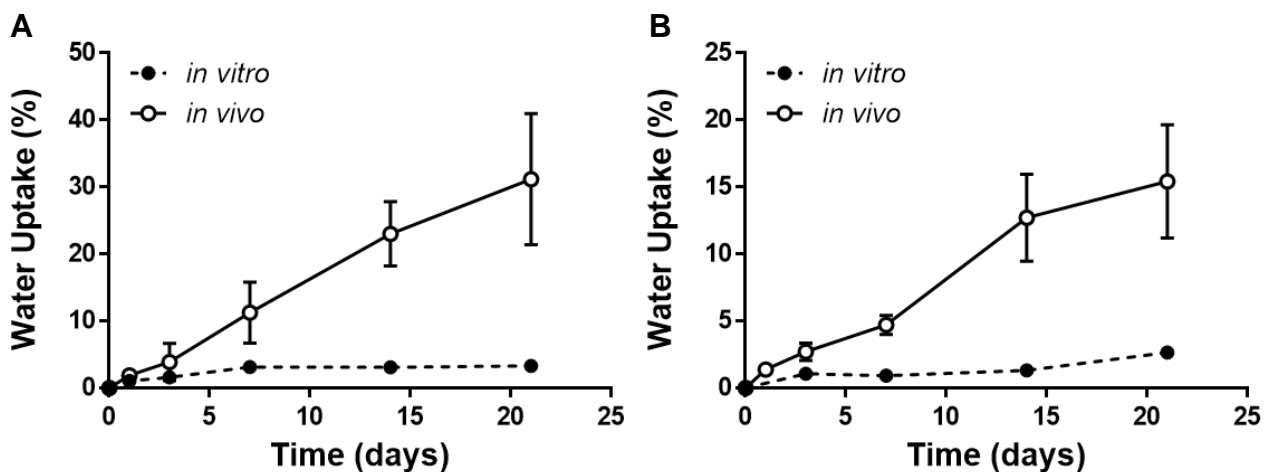


Figure 4.4: *in vitro* and *in vivo* water uptake in Tr-A_1 (A) and Tr-A_2 (B) microspheres. Data represent mean \pm SEM, $n=3-5$.

Finally, for a more complete understanding of how the *in vivo* environment affects the Tr-A/PLGA microspheres, we studied their morphology during release by imaging using confocal microscopy (Figure 4.5). Overall, no major changes in morphology were observed in Tr-A_1 microspheres over 2 weeks. However, one major observation was seen in the Tr-A_2 microspheres implanted subcutaneously for 14 days. These microspheres appear to have developed an internal pore network not evident in microspheres incubated in *in vitro* release media. This pore network suggests higher water penetration in the polymer matrix and the potential for increased aqueous diffusion of Tr-A. This evidence also suggests that Tr-A may also be released by osmotically induced aqueous pore diffusion *in vivo* in this formulation. This hypothesis is supported by the release and erosion kinetics, as $t_{50,release} \ll t_{50,erosion}$, suggesting a

second mechanism causing rapid drug release *in vivo*. The much higher water uptake observed in Tr-A_2 microspheres *in vivo* also supports a water-mediated mechanism causing accelerated release as compared to what was observed *in vitro*.

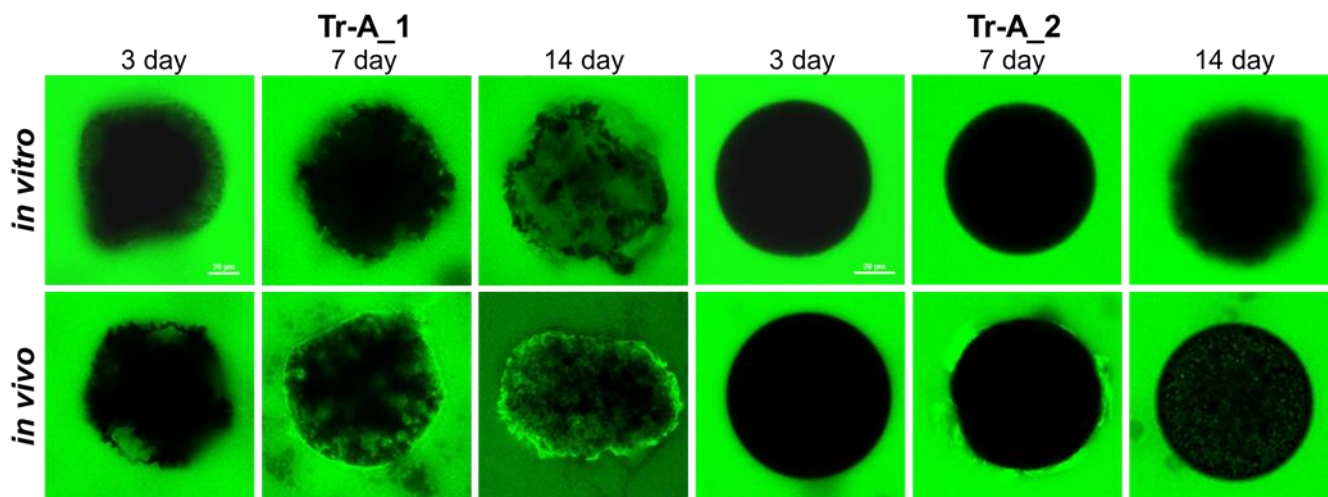


Figure 4.5: Representative confocal images of Tr-A_1 and Tr-A_2 microspheres during *in vitro* and *in vivo* release. Images were taken following incubation in aqueous solution of BODIPY FL for 10 min or 3 h.

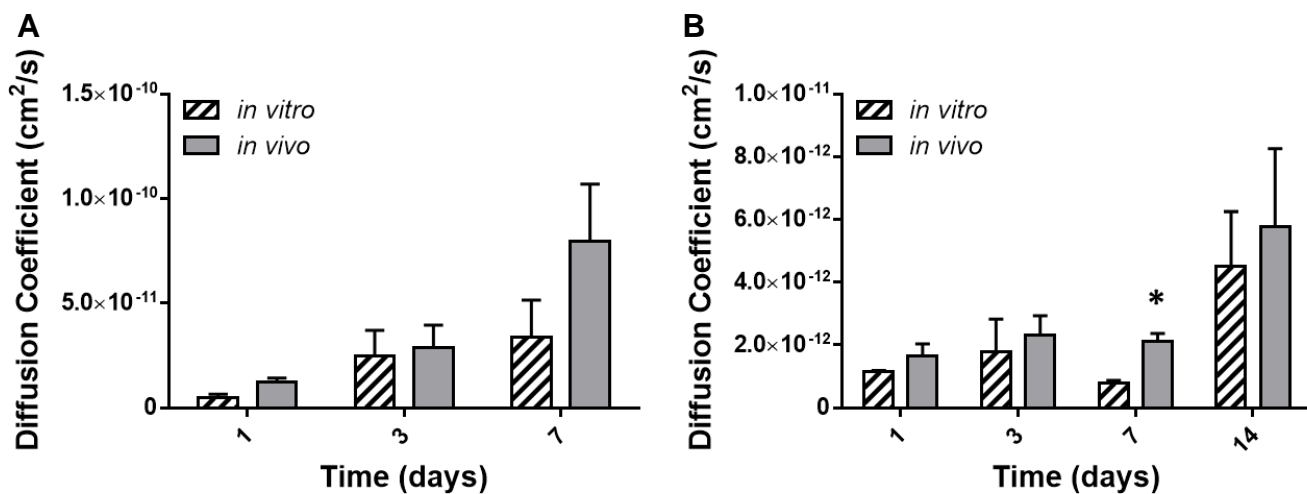


Figure 4.6: BODIPY diffusion coefficients in degrading Tr-A_1 (A) and Tr-A_2 (B) microspheres *in vitro* and *in vivo*. Data represent mean \pm SEM, $n=6$. * $p < 0.05$.

Solid state diffusion was measured through one week in Tr-A_1 microspheres and two weeks in Tr-A_2 microspheres by analyzing the confocal images, as previously described (Figure 4.6). In Tr-A_1, diffusion was slightly increased *in vivo* at 7 days but the difference was not significant. A significant increase ($p < 0.05$) was observed at 7 days in Tr-A_2 microspheres but not at any other time points. Using the D_{bodipy} values estimated using image analysis, $D_{\text{Tr-A}}$ values were estimated from $D_{\text{Tr-A}}/D_{\text{bodipy}}$ ratios determined in each polymer (see section 2.8.4). These estimated $D_{\text{Tr-A}}$ values were used to model theoretical release curves of Tr-A from Tr-A_1 and Tr-A_2 microspheres if diffusion through the polymer matrix were the sole mechanism responsible for release. This process was described in detail in Chapter 2. The theoretical *in vivo* release profiles are shown in Figure 4.7 along with the comparable models developed *in vitro*, in the presence and absence of the plasticizer triethyl citrate. From the equations derived using the Higuchi equation for spherical systems, $t_{50,\text{diffusion}}$ values were estimated to represent the time to reach 50% drug release if diffusion was the primary release mechanism (Table 4.3). The resulting release profiles and estimated $t_{50,\text{diffusion}}$ values fell within the range of conditions tested *in vitro*. Theoretical diffusion-controlled release *in vivo* followed a similar profile to PBST pH 7.4 *in vivo* at times later than 3 days, at which time the polymer is sufficiently wetted and the polymer chains are mobile. The profiles and estimated $t_{50,\text{diffusions}}$ were also similar to those generated from $D_{\text{Tr-A}}$ values at early times (1-3 days) in PBS containing the plasticizer triethyl citrate (TC), which increases polymer chain mobility at early time points relative to microspheres incubated in standard release media without plasticizer. These data suggest that water uptake in the polymer phase is faster and more extensive *in vivo* than *in vitro*, potentially due to some plasticizing lipids and/or osmolytic polymer-penetrating species in the subcutaneous space. Given the previously discussed hydrolysis and mass loss kinetics, however, it is unlikely solid

state diffusion plays a major role in the long-term release of Tr-A from either of these two PLGA microsphere formulations. Nevertheless, the effect of a plasticizing agent is still important to consider. Such an agent could increase PLGA chain mobility, facilitating water transport into the polymer matrix, causing increased hydrolysis, as well as increased transport of monomeric and oligomeric degradation byproducts out of the microsphere, resulting in mass loss.

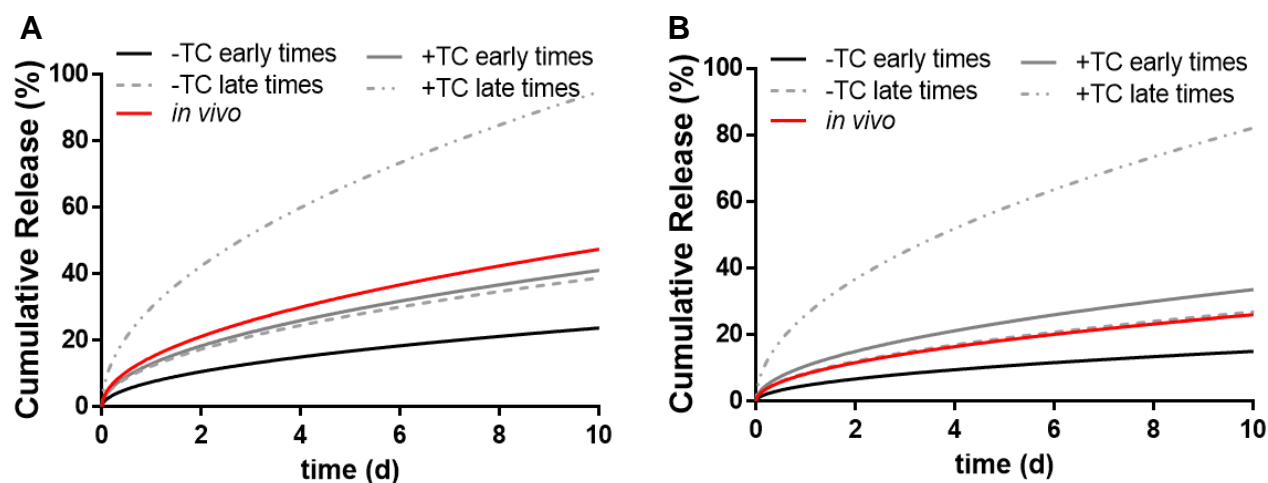


Figure 4.7: Theoretical Tr-A release profiles from Tr-A_1 (A) and Tr-A_2 (B) microspheres for diffusion-controlled release. *In vitro* profiles (in grey) were generated using representative diffusion coefficients with and without the plasticizer triethyl citrate that were determined at early (1-3 days) and late times (7+ days) during the release incubation.

Table 4.3: $T_{50,diffusion}$ values estimated using diffusion-controlled release models shown in Figure 4.7

	-TC early times	-TC late times	+TC early times	+TC late times	<i>in vivo</i>
Tr-A_1	45 days	17 days	15 days	2.8 days	11 days
Tr-A_2	110 days	35 days	22 days	3.7 days	37 days

4.6 Conclusions

In accordance with other literature reports on steroid release from PLGA, Tr-A microspheres exhibited accelerated release from PLGA microspheres *in vivo* as compared to results from standard *in vitro* release tests. Employing a novel cage implant system for

microsphere retrieval, we were able to determine the major mechanisms of release *in vivo* and compare these results directly with data from previously performed analyses of microspheres during *in vitro* release. Rate of PLGA hydrolysis, mass loss and water uptake were all increased *in vivo* compared to in PBST pH 7.4. Both microsphere formulations studied here exhibited erosion-controlled release *in vitro*, but only Tr-A_1 exhibited the same mechanism *in vivo*. The release of Tr-A_2 *in vivo* displayed primarily an osmotically induced/pore diffusion mechanism as indicated by bodipy uptake and polymer mass loss kinetics. Future studies will screen *in vitro* release media including biological components discussed in Chapter 1 to elucidate which of these molecules is/are capable of causing the shifts in release rates and mechanisms shown here. Ultimately, comparison of these data with data gained from further *in vitro* tests will result in the design of a predictive *in vitro* release test from PLGA microspheres.

4.7 References

1. Anderson, J.M. and M.S. Shive, *Biodegradation and biocompatibility of PLA and PLGA microspheres*. *Advanced Drug Delivery Reviews*, 1997. **28**(1): p. 5-24.
2. Clark, B. and P. Dickinson, *Case Study: In Vitro/In Vivo Release from Injectable Microspheres*, in *Injectable Dispersed Systems: Formulation, Processing and Performance* D. Burgess, Editor. 2005, Taylor & Francis Group: Boca Raton, FL. p. 543-570.
3. Tracy, M.A., et al., *Factors affecting the degradation rate of poly(lactide-co-glycolide) microspheres in vivo and in vitro*. *Biomaterials*, 1999. **20**(11): p. 1057-62.
4. Alexis, F., *Factors affecting the degradation and drug-release mechanism of poly(lactic acid) and poly[(lactic acid)-co-(glycolic acid)]*. *Polymer International*, 2005. **54**(1): p. 36-46.
5. Blanco-Prieto, M.a.J., et al., *In vitro and in vivo evaluation of a somatostatin analogue released from PLGA microspheres*. *Journal of Controlled Release*, 2000. **67**(1): p. 19-28.
6. Liu, W.H., et al., *Preparation and in vitro and in vivo release studies of Huperzine A loaded microspheres for the treatment of Alzheimer's disease*. *Journal of Controlled Release*, 2005. **107**(3): p. 417-427.
7. Heya, T., et al., *Controlled release of thyrotropin releasing hormone from microspheres: evaluation of release profiles and pharmacokinetics after subcutaneous administration*. *J Pharm Sci*, 1994. **83**(6): p. 798-801.
8. Heya, T., et al., *In vitro and in vivo evaluation of thyrotrophin releasing hormone release from copoly (dl-lactic/glycolic acid) microspheres*. *Journal of Pharmaceutical Sciences*, 1994. **83**(5): p. 636-640.
9. Kostanski, J.W., et al., *Evaluation of Orntide microspheres in a rat animal model and correlation to in vitro release profiles*. *AAPS PharmSciTech*, 2000. **1**(4): p. E27.
10. Negrin, C.M., et al., *In vivo-in vitro study of biodegradable methadone delivery systems*. *Biomaterials*, 2001. **22**(6): p. 563-70.
11. Rawat, A., U. Bhardwaj, and D.J. Burgess, *Comparison of in vitro-in vivo release of Risperdal((R)) Consta((R)) microspheres*. *Int J Pharm*, 2012. **434**(1-2): p. 115-21.
12. Kim, T.-K. and D.J. Burgess, *Pharmacokinetic characterization of I4C-vascular endothelial growth factor controlled release microspheres using a rat model*. *Journal of Pharmacy and Pharmacology*, 2002. **54**(7): p. 897-905.
13. Morita, T., et al., *Evaluation of in vivo release characteristics of protein-loaded biodegradable microspheres in rats and severe combined immunodeficiency disease mice*. *J Control Release*, 2001. **73**(2-3): p. 213-21.
14. Zolnik, B.S. and D.J. Burgess, *Evaluation of in vivo-in vitro release of dexamethasone from PLGA microspheres*. *Journal of Controlled Release*, 2008. **127**(2): p. 137-145.
15. Martinez, M., et al., *In vitro and in vivo considerations associated with parenteral sustained release products: A review based upon information presented and points expressed at the 2007 Controlled Release Society Annual Meeting*. *Journal of Controlled Release*, 2008. **129**(2): p. 79-87.
16. Zolnik, B.S., *In Vitro and In Vivo Release Testing of Controlled Release Parenteral Microspheres*, in *Pharmaceutics*. 2005, University of Connecticut: Storrs.
17. *Guidance for Industry: Dissolution testing of immediate release solid oral dosage forms*. *Food and Drug Administration Center for Drug Evaluation and Research*. 1997.

18. *In vitro and In vivo Evaluations of Dosage Forms, United States Pharmacopeia <1088>*.
19. *Food and Drug Administration Guidance for Industry. Extended Release Oral Dosage Forms: Development, Evaluation, and Application of In Vitro/In Vivo Correlations, CDER 09, 1997.*
20. Schliecker, G., et al., *In vitro and in vivo correlation of buserelin release from biodegradable implants using statistical moment analysis.* Journal of Controlled Release, 2004. **94**(1): p. 25-37.
21. Martinez, M.N., et al., *Breakout session summary from AAPS/CRS joint workshop on critical variables in the in vitro and in vivo performance of parenteral sustained release products.* Journal of Controlled Release, 2010. **142**(1): p. 2-7.
22. Zolnik, B.S. and D.J. Burgess, *In Vitro–In Vivo Correlation on Parenteral Dosage Forms, in Biopharmaceutics Applications in Drug Development*, R. Krishna and L. Yu, Editors. 2008, Springer US. p. 336-358.

4.8 Supplementary Information

4.8.1 Regression Analysis

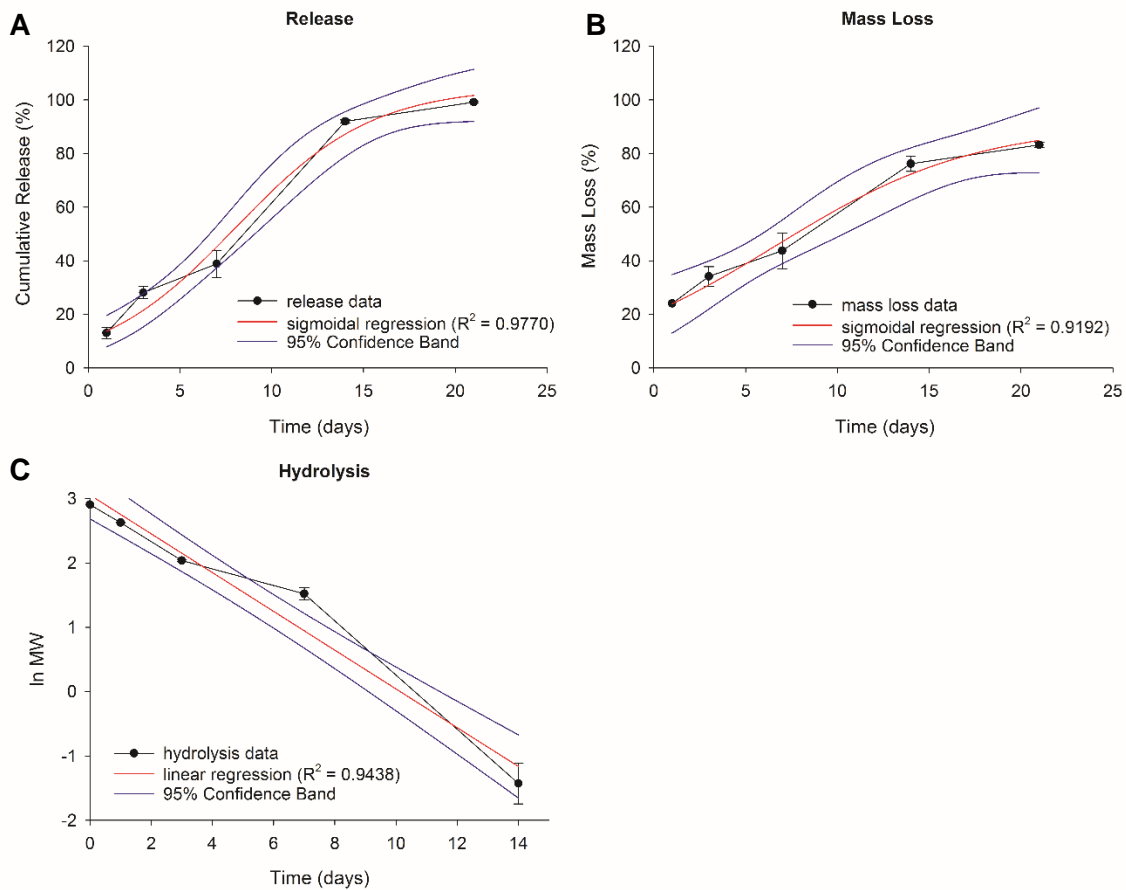


Figure S 4.1: Four parameter logistic nonlinear fits of Tr-A_1 release (A) and mass loss data (B); linear regression fits of Tr-A_1 hydrolysis data (C). Fits were used to estimate relevant t_{50} values and first order rate constant of PLGA hydrolysis.

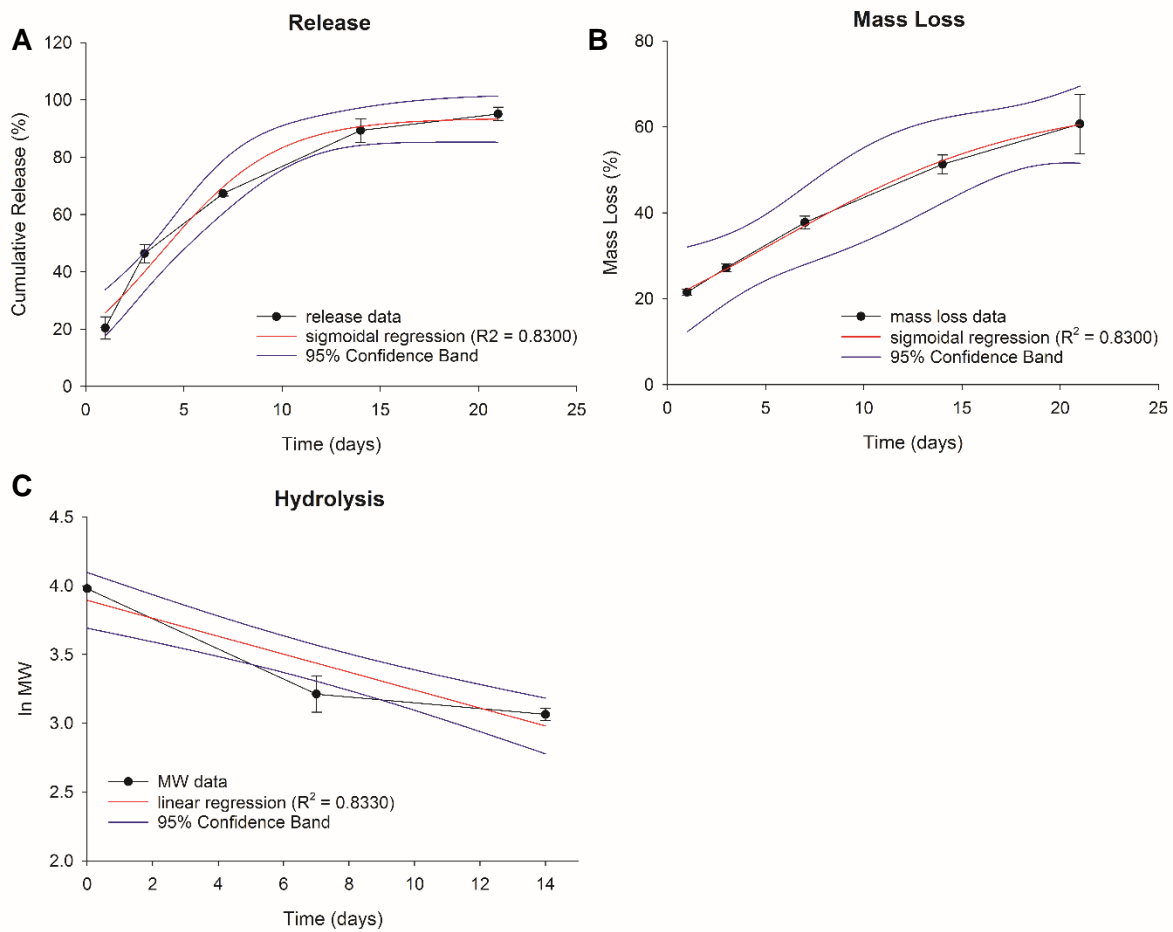


Figure S 4.2: Four parameter logistic nonlinear fits of Tr-A_2 release (A) and mass loss data (B); linear regression fits of Tr-A_2 hydrolysis data (C). Fits were used to estimate relevant t_{50} values and first order rate constant of PLGA hydrolysis.

4.8.2 *In vitro* release under various mixing conditions

One of the potential differences between *in vitro* release tests and actual *in vivo* conditions is mixing/fluid convection. While most release tests are performed with constant agitation, the administration environment (SC or IM) presumably has a much lower degree of mixing. There are several potential effects of low or no mixing during *in vitro* release, specifically: decreased diffusion of drug and decreased diffusion of acidic degradation byproducts, resulting in increased autocatalysis of PLGA hydrolysis. The increase in hydrolysis would be expected to cause increased drug release rates, and could offer a potential explanation for this phenomena observed *in vivo*. To test this hypothesis, release from Tr-A microspheres was measured with and without the cage under varying mixing conditions. It should be noted that the shaker was set to 240 rpm for release measured under “standard conditions”, i.e. those reported in Chapter 2. Somewhat surprisingly, release from both formulations was slower under low (80 rpm) or no mixing (Figure S 4.3 and Figure S 4.4), indicating that the potentially lower agitation the microspheres experience in the SC space is not a factor in causing accelerated release.

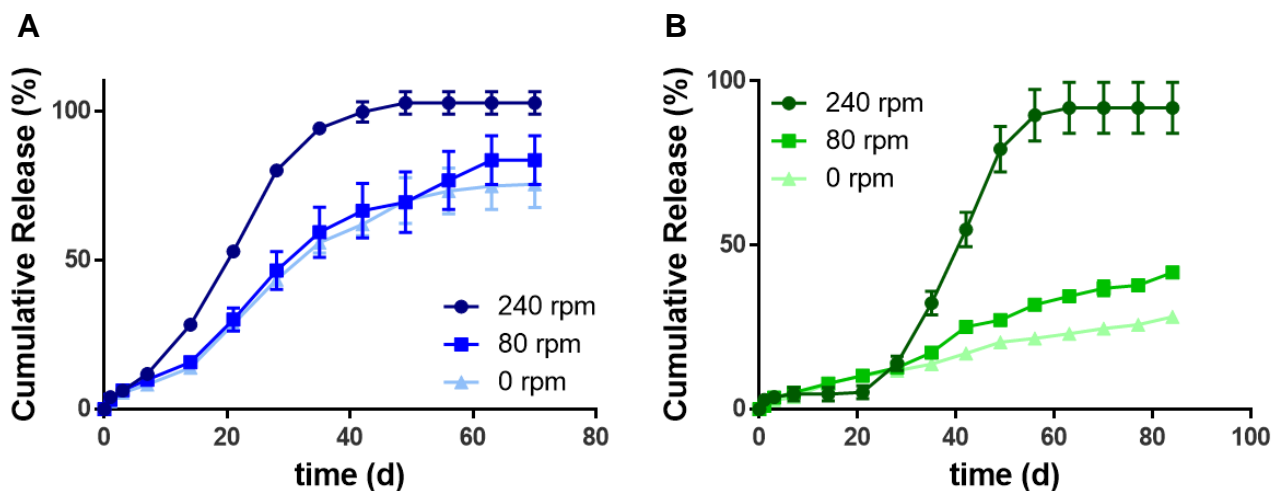


Figure S 4.3: *In vitro* release from Tr-A_1 microspheres caged (A) or suspended freely (B) in PBST pH 7.4 under varying mixing conditions. Data represent mean \pm SEM, $n=3$.

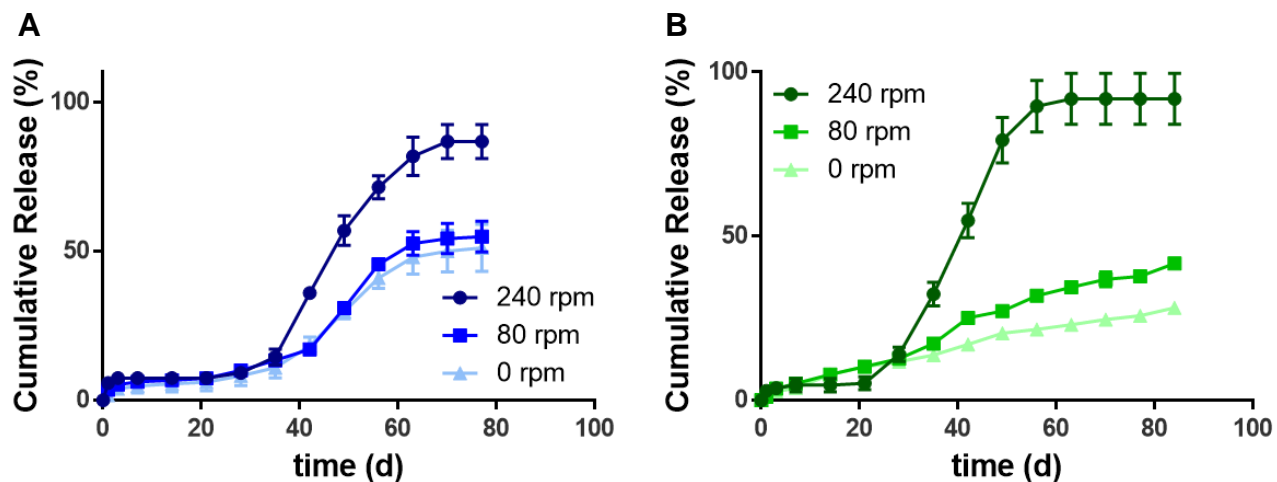


Figure S 4.4: *In vitro* release from Tr-A_2 microspheres caged (A) or suspended freely (B) in PBST pH 7.4 under varying mixing conditions. Data represent mean \pm SEM, n=3.

4.8.3 Subcutaneous pH

As discussed in Chapter 1.4.2, there is the potential for the pH at the subcutaneous administration environment to be slightly acidic. The inflammatory response as well as the buildup of acidic degradation byproducts may potentially decrease the pH lower than 7.4, value at which most *in vitro* release tests are performed. At the time of euthanasia, subcutaneous pH was measured directly by microelectrode at the area of the cage implant. There was no significant deviation from the untreated SC pH at any time point in any of the treatment groups, indicating that pH is not a contributing factor to the observed accelerated release from Tr-A microspheres *in vivo*.

Table S 4.1: Subcutaneous pH values measured during release.

	1 day	3 day	7 day
No treatment	7.38 \pm 0.13	7.47 \pm 0.04	7.45 \pm 0.08
Blank Cage	7.27 \pm 0.14	7.31 \pm 0.16	7.42 \pm 0.03
Tr-A_1 cage	7.32 \pm 0.06	7.35 \pm 0.06	7.31 \pm 0.11
Tr-A_2 cage	7.41 \pm 0.11	7.43 \pm 0.02	7.37 \pm 0.09

Chapter 5 : Conclusions, Implications, and Future Directions

The work presented in this thesis has shown that PLGA microspheres behave differently *in vivo* than in release media typically used during the development of these formulations. A thorough mechanistic analysis of drug release from PLGA microspheres following *in vivo* administration had not been reported prior to this research, which offers an explanation for why drugs, are often released faster than expected based on *in vitro* release tests. In this case, accelerated hydrolysis and subsequent erosion of PLGA microspheres were found to be responsible for the observed increase in release rate of the model drug triamcinolone acetonide. Increased water uptake also resulted in the formation of an aqueous pore network *in vivo*, which was not observed in any of the investigated *in vitro* conditions.

Future studies will investigate the potential causes for the observed changes in water penetration, hydrolysis, and erosion. As was discussed in Chapter 1, there is a plethora of compounds found in the interstitial fluid in the administration space that are not included in currently used *in vitro* release tests. These compounds should be added to standard release media both alone and in combination with others in an effort to find which of these molecules may cause the observed changes in release rates and corresponding release mechanisms. Following this screening process to determine the necessary makeup of predictive *in vitro* release media, the chosen molecules should be validated through *in vivo* studies. Using the cage implant, microspheres can be retrieved and endogenous molecules such as amines and lipids can be extracted and identified. These studies should be performed to prove the relevance and

applicability of the results of the *in vitro* media screening experiments. Once *in vitro* test conditions have been finalized, mechanism-based level A IVIVCs for these formulations. This approach should also be validated by using the newly designed *in vitro* release conditions to test release of a commercial PLGA product, such as Lupron Depot®, to determine the capabilities of predicting the release and pharmacokinetics reported in the literature.

This research has important implications for future development of PLGA microspheres and can also be applied to other biodegradable CR formulations. Specifically, the cage model that was developed in Chapter 3 could be used to study release mechanisms of any biodegradable implant or injectable. As more and more formulations are thoroughly studied *in vivo*, we can begin to develop an understanding of how exactly the administration environment affects any given CR formulation. Using all of these datasets from many formulations encapsulating a variety of drug molecules, generalized IVIVCs can be developed for a range of CR products. This would greatly cut down on product production time and cost, as animal studies would be greatly reduced. IVIVCs will also facilitate generic development for CR products, as mechanism-based IVIVCs can accurately predict drug release and pharmacokinetics without the need to perform large, costly animal studies.

This thesis will provide the framework for other researchers to investigate polymeric formulations *in vivo* to determine the ways in which drug release occurs following administration. By developing a comprehensive understanding of these processes, optimal *in vitro* conditions can be designed to better predict product performance. Future studies which will build on the research presented in this thesis will lead to the development of robust IVIVCs for CR drug formulations.

Appendix A: Remote Loading of Liraglutide in PLGA Microspheres for Controlled Release

A.1 Introduction

Type 2 diabetes (T2D) is a metabolic disease which affects approximately 9% of adults worldwide, and is expected to become the seventh leading cause of death by 2030 [1]. The global market for T2D treatments is estimated to be approximately \$30 billion and growing each year with more diagnoses and the introduction of new products [2-4].

T2D is characterized by hyperglycemia caused by insulin resistance and relative lack of insulin (i.e. insulin production is not sufficient to manage blood glucose) [2]. The current first line of treatment recommended by the International Diabetes Federation (IDF) is metformin, a biguanide taken orally twice a day to inhibit the production of glucose [5]. Other common treatment options include sulfonylureas which increase insulin secretion, thiazolidinediones and PPAR γ agonists which both work increase insulin sensitivity, and α -glucosidase inhibitors which inhibit absorption of glucose from the GI tract [6]. Combination therapy of more than one drug and more than one class of drug is typically used to manage blood sugar levels in T2D patients and after several years on a certain regiment, patients often stop responding and must find a new combination of drugs to manage the disease [2, 6].

In recent years, glucagon-like peptide 1 (GLP-1) has become an area of interest for developing new, more effective T2D treatments. GLP-1 is an endogenous incretin hormone which promotes insulin secretion from pancreatic beta cells and inhibits glucagon release from alpha cells. It is normally secreted following a meal to control blood sugar levels [7]. GLP-1 is

quickly degraded by dipeptidyl peptidase-4 (DPP4) and has a circulating half-life of only 2-3 minutes in humans [7, 8]. Due to this short half-life, additional GLP-1 cannot simply be administered to T2D patients to control blood glucose and thus GLP-1 analogs have been developed by several drug companies. The first to market was the peptide exenatide, which shares approximately 50% sequence homology to GLP-1 and has a half-life of 2.4 hours [9]. Exenatide was first marketed by Amylin (now AstraZeneca) as the twice daily subcutaneous injection Byetta® and later formulated using poly (lactic-*co*-glycolic) acid (PLGA) to create the once weekly injection Bydureon®. Following the launch of Byetta®, Novo Nordisk released their GLP-1 analog, liraglutide (Victoza®) which is a once daily subcutaneous injection [10-12]. This product was quick to capture the majority of the GLP-1 market and has continued to dominate, with its sales representing 70% of \$3 billion annual sales [4]. Although Bydureon® is a once weekly injection rather than daily, the increase in patient comfort has not resulted in an increase in sales and Victoza® continues to hold the majority of the market share [3, 4]. Given the popularity of Victoza®, a controlled release formulation of this peptide that increases patient compliance and comfort could theoretically corner the GLP-1 market for the foreseeable future. Thus, the intent of this work was to develop a once-monthly liraglutide formulation using PLGA.

Based on our group's discovery that peptides can rapidly partition into low molecular weight acid end group PLGAs for later controlled release, we sought to test a remote loading strategy for loading liraglutide into PLGA microspheres [13]. We employed a novel salt-treatment technique to induce electrostatic interaction between PLGA and liraglutide to result in high loading and encapsulation efficiency in microspheres which exhibit controlled release *in vitro* and *in vivo*.

A.2 Materials

PLGA RESOMER® 502H (i.v. = 0.19 dL/g, free acid terminated) and RESOMER® 503H (i.v. = 0.19 dL/g, free acid terminated) were purchased from Sigma Aldrich. Liraglutide was purchased from SHJNJ Pharmaceuticals (Shanghai, China) and liraglutide ELISA kits were purchased from AB Biolabs (Ballwin, MO). Polyvinyl alcohol (PVA, 80% hydrolyzed, MW ~9,000-10,000) was purchased from Sigma Aldrich (MO, USA). 7-9 week old male Sprague-Dawley (SD) rats were purchased from Charles River Laboratories (Wilmington, MA). All solvents used were HPLC grade and were purchased from Fisher Scientific and unless otherwise noted, all other salts and chemicals were purchased from Sigma Aldrich.

A.3 Methods

A.3.1 Salt Treatment of PLGA

PLGA Resomer 502H or Resomer 503H (approximately 1g) was suspended in 25mL of a 1M salt solution (NaCl, CaCl₂, ZnCl₂, MgCl₂) and shaken at room temperature for 24 hours. The resulting polymer was then washed thoroughly with ddH₂O, dried under vacuum, and stored at 20°C for future use.

A.3.2 Liraglutide Sorption to salt-treated PLGA 502H

Liraglutide solution (0.5 mg/mL) was prepared in 10 mM HEPES buffer (pH 7.4). Approximately 10mg of salt-treated PLGA powder was suspended in 1mL liraglutide solution and rotated constantly at 37°C for 24 h. Sorption was determined by total peptide loss from solution, quantified by ultra-performance liquid chromatography (UPLC) as described below.

A.3.3 Liraglutide Release from salt-treated PLGA 502H

Salt-treated PLGA loaded with liraglutide was incubated in 1 mL release media (HEPES-buffered saline pH 7.4) at 37°C and shaken mildly. At each time point, polymer was separated

from media by centrifugation and the media was completely removed and replaced. Media samples were analyzed for liraglutide content by UPLC (see below).

A.3.4 Sorption Isotherm of Liraglutide to salt-treated PLGA 502H

MgCl₂-treated PLGA 502H (Mg-502H). Was incubated in liraglutide solution (0.2, 0.5, 1.0, 5.0 mg/mL in HEPES pH 7.4) and rotated at 37°C for 24 h. Solution samples (10 µL) were taken at 1, 2, 3, 4, 6, 8, 10, 12, 18, and 24 h and concentration was determined by UPLC. Total loss of volume and peptide were corrected for in determining the kinetics of peptide sorption.

A.3.5 Microsphere Formulation

Polymer was dissolved in 1 mL CH₂Cl₂ (800 mg/mL) with or without 3% MgCO₃. An inner water phase containing trehalose (500 mg/mL in ddH₂O) was added to the polymer solution and homogenized for one minute at 10,000 rpm, resulting in an w/o emulsion. An outer water phase of 5% polyvinyl alcohol (PVA) was added and vortexed for one minute to create a w/o/w double emulsion. The resulting porous microspheres were hardened by stirring in 0.5% PVA for three hours, then screened to 20-63 µm and freeze dried. In the cases where Mg-treated PLGAs were used to make microspheres, PVA solutions were prepared in 1M MgCl₂.

A.3.6 Microsphere Imaging

Lyophilized microspheres were mounted by using double sided carbon tape and then coated with a thin layer of gold under vacuum. Scanning electron microcopy (SEM) was performed on a Hitachi S3200N scanning electron microscope (Hitachi, Japan). Images were captured by EDAX® software.

A.3.7 *Liraglutide Loading in Microspheres*

Blank, porous microspheres were incubated in 1 mL liraglutide solution (5.0 mg/mL in HEPES pH 7.4) and rotated at 37°C for 24 h. Following loading, the microspheres were washed with 1 mL ddH₂O then freeze dried.

A.3.8 *Determination of Peptide Loading in Microspheres (mass loss, extraction)*

Peptide loading in microspheres was determined using two methods: mass loss and extraction. Total liraglutide loss was measured by determining the concentration of loading solution following loading and subtracting this value from the original concentration. Peptide removed by washing was corrected for during this calculation. For a direct measurement of peptide content in the microspheres, extraction was performed. Freeze-dried, liraglutide-loaded microspheres were dissolved in 1mL acetonitrile. Peptide was then extracted into an aqueous phase by adding 8 mL ddH₂O and vortexing for 1 min. Centrifugation resulted in phase separation, then total peptide content was determined by UPLC analysis of the aqueous phase, as described below. Loading and encapsulation efficiency were determined by the following two equations:

$$\% \text{ w/w loading } (L_A) = \left(\frac{[\text{liraglutide}]_{\text{initial}} - [\text{liraglutide}]_{\text{final}} + [\text{liraglutide}]_{\text{wash solution}}}{\text{mass of microspheres}} \right) \times 100 \%$$

$$\text{encapsulation efficiency } (\%) = \left(\frac{\text{actual loading } (L_A)}{\text{theoretical loading } (L_T)} \right) \times 100 \%$$

A.3.9 *Ultra Performance Liquid Chromatography (UPLC):*

Liraglutide concentrations in solutions previously mentioned were determined using an ultraperformance liquid chromatography system (Acquity UPLC, Waters, USA). The mobile phase consisted of 0.1% TFA in acetonitrile (solvent A) and 0.1% TFA in ddH₂O (solvent B). Initial conditions were 35:65 (A:B) and a linear gradient was used to achieve final conditions of 95:5 over 3.5 min. The flow rate was set to 0.5 mL/min. Samples and standards in various

aqueous media were injected (5 μ L) onto a C18 (Acquity BEH C18, 1.7 μ m, 2.1 x 100mm) column maintained at 30°C. Liraglutide was detected at 215 and 280 nm.

A.3.10 Loading optimization

In these experiments liraglutide loading solutions were prepared at 1.0 mg/mL in 3.75 mM Na₂HPO₄ at pH 8.1. These conditions were designed using the commercial product, Victoza[®], injection medium as a model in order to ensure stability and solubility of the peptide [14].

A.3.11 Liraglutide Release from Microspheres

Loaded microspheres were suspended in release medium (HEPES-buffered saline or phosphate-buffered saline + 0.2% Tween 80 at pH 7.4) at 37°C with mild agitation. At each time point, microspheres were separated from solution by centrifugation and the release media was completely removed and replaced. Liraglutide release was measured by UPLC.

A.3.12 Stability of Liraglutide in Release Media—appendix?

The stability of liraglutide was measured in three release media: HEPES-buffered saline (HBS), HBS + 0.02% Tween 80 (HBST) and HBS + 1.4% propylene glycol. Liraglutide was dissolved in each medium at relevant concentrations (100 μ g/mL and 50 μ g/mL) which were determined from media samples taken during *in vitro* release tests. The solution was analyzed by UPLC at 1, 3, 7, and 14 days to monitor peptide loss.

A.3.13 Amino Acid Analysis

At time points during release, microspheres were removed from release media, rinsed with ddH₂O and freeze-dried. Amino acid analysis was then performed at UC Davis Molecular Structure Facility (Davis, California). Briefly, microspheres were hydrolyzed at 110°C using 6N

HCl and 1% phenol. The amino acids were derivatized using phenylisothiocyanate and analyzed by HPLC using norleucine as an internal standard.

A.3.14 Pharmacokinetics

The treatment of experimental animals was in accordance with the terms of the University Committee on Use and Care of Animals (University of Michigan UCUCA). Healthy, male Sprague-Dawley (SD) rats were administered a single dose of liraglutide-loaded Mg-503H + MgCO₃ microspheres. The microspheres were suspended in 500 µL of a sterile injection medium of PBS + 3% CMC and injected subcutaneously via a 20g needle. Rats were divided into two groups (n=5 each group): high dose and low dose. The low dose rats were given 1.96 mg/kg liraglutide and high dose rats were given 4.0 mg/kg [15-17]. Whole blood samples were taken from the jugular vein before dosing, 24 hours following the dose and weekly thereafter. Whole blood was collected in EDTA-coated tubes and centrifuged at 4°C for 6 min. Plasma was then aspirated and stored at -80°C. Liraglutide was extracted from plasma using solid phase extraction. Peptide was eluted from the column using 60% acetonitrile in water + 1% TFA which was then dried. The resulting extract was reconstituted in assay buffer and liraglutide concentration was determined by ELISA according to the manufacturer instructions.

A.4 Results and Discussion

Liraglutide is an acylated GLP-1 analog which contains a C16 fatty acid conjugated to a lysine at position 26 (Figure A. 1). It contains 8 amino acids charged at neutral pH resulting in a net negative charge and has a calculated isoelectric point (pI) of 4.35 [18]. Although the peptide has a very similar sequence to endogenous GLP-1(7-37), the acylation promotes protein binding in the blood and results in a half-life of approximately 11 hours in humans [11, 12, 19].

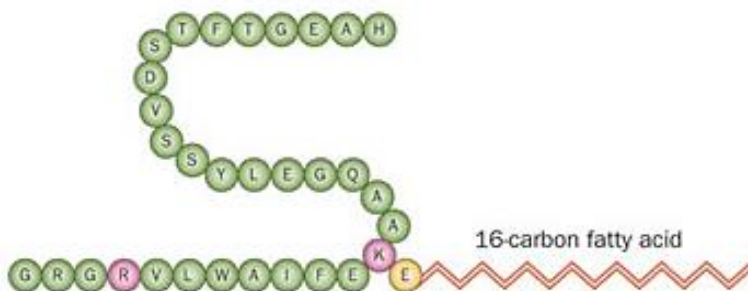


Figure A. 1: Primary structure of liraglutide. Modifications from GLP-1(7-37) are highlighted: K34R and C16 fatty acid conjugated to K20 via a glutamate linker. (Figure from [18])

Previous work in our lab has demonstrated that peptides can partition into moderate molecular weight (MW) PLGAs to result in high loading in microspheres for later controlled release. This phenomenon was demonstrated using the short peptide leuprolide and the electrostatic interaction between the cationic peptide and the free-acid end groups of PLGA Resomer® 502H likely contributed to the high absorption into the polymer [13]. Liraglutide, however, carries an overall net negative charge and thus has very little interaction with the free carboxylic acid end groups of PLGA. In order to induce electrostatic interaction, PLGA 502H was treated with concentrated solutions of salts to create a cationic charge associated with the end groups of the PLGA (Figure A. 2). The salt treatment resulted in increased liraglutide sorption, though there was no difference in sorption among the four salts tested in this preliminary experiment (Figure A. 3).

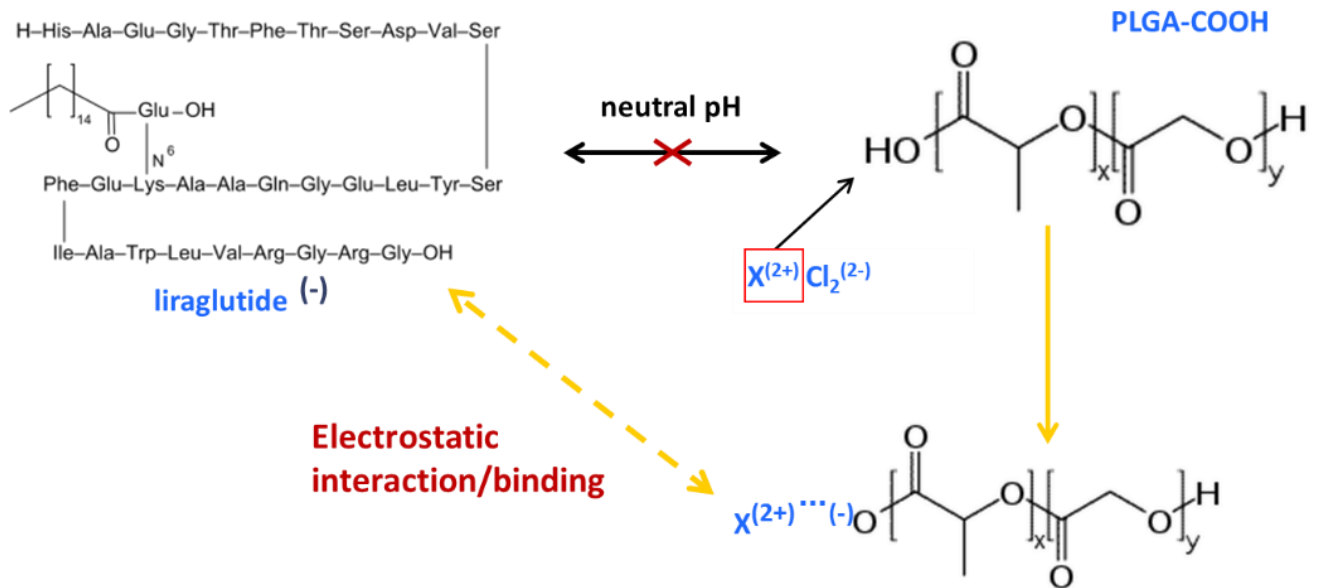


Figure A. 2: Schematic showing salt treatment of PLGA-COOH resulting in electrostatic interaction with liraglutide.

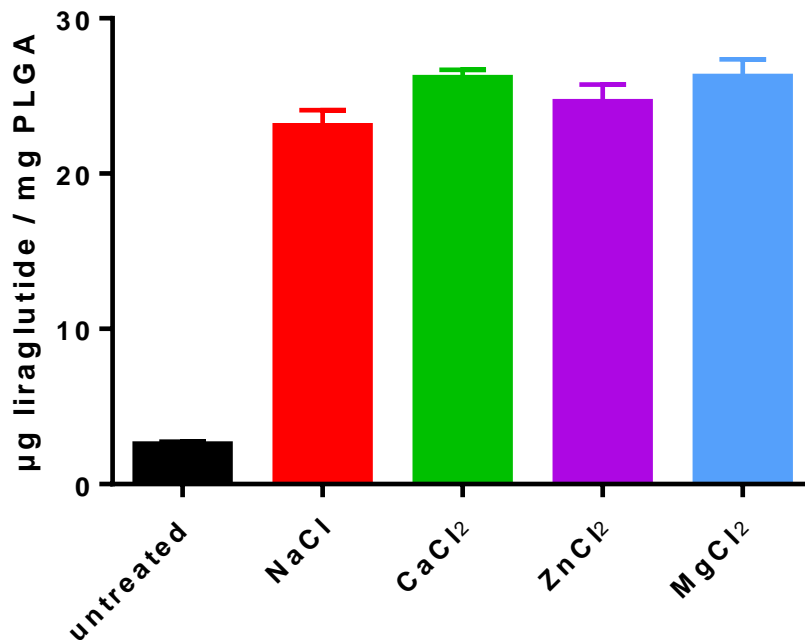


Figure A. 3: Liraglutide sorption to untreated and salt-treated PLGA 502H following 24 hours incubation with peptide solution. Data represent mean \pm SEM, $n=3$.

Based on the promising results from the preliminary sorption experiments, peptide release from the four different salt-treated PLGAs was measured *in vitro* in a low ionic strength buffer, HBS. Controlled release of liraglutide from the treated polymer powder lasted for approximately one week (Figure A. 4), suggesting that upon formulation into microspheres controlled release for longer times could be achieved.

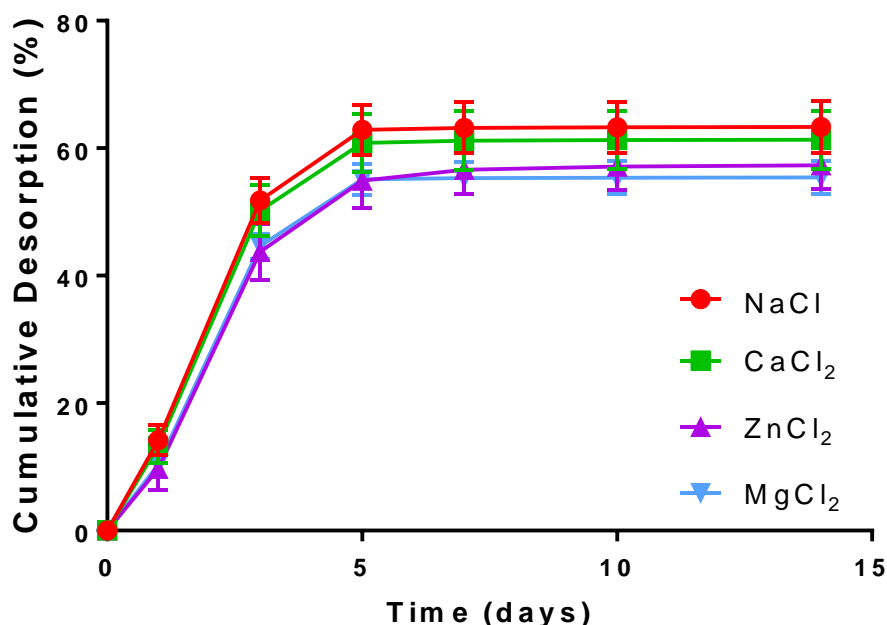


Figure A. 4: Liraglutide release from salt-treated PLGA 502H in HBS pH 7.4. Data represent mean \pm SEM, $n=3$.

To determine the time-dependent and concentration-dependent nature of liraglutide sorption to PLGA, a sorption isotherm experiment was performed using PLGA 502H treated with 1M MgCl₂ (Mg-502H). Liraglutide sorption plateaued following approximately 12 hours of incubation at all four peptide concentrations used (Figure A. 5A), suggesting that this is the time needed for liraglutide content in the polymer to reach equilibrium. Additionally, this experiment showed the concentration-dependent nature of liraglutide sorption (Figure A. 5B). High concentration of the loading solution (5.0 mg/mL) resulted in 8.0 ± 0.6 % w/w peptide content in

Mg-502H. Drawing from these data, liraglutide solutions of 5 mg/mL were used for future loading studies which were carried out for 24 hours.

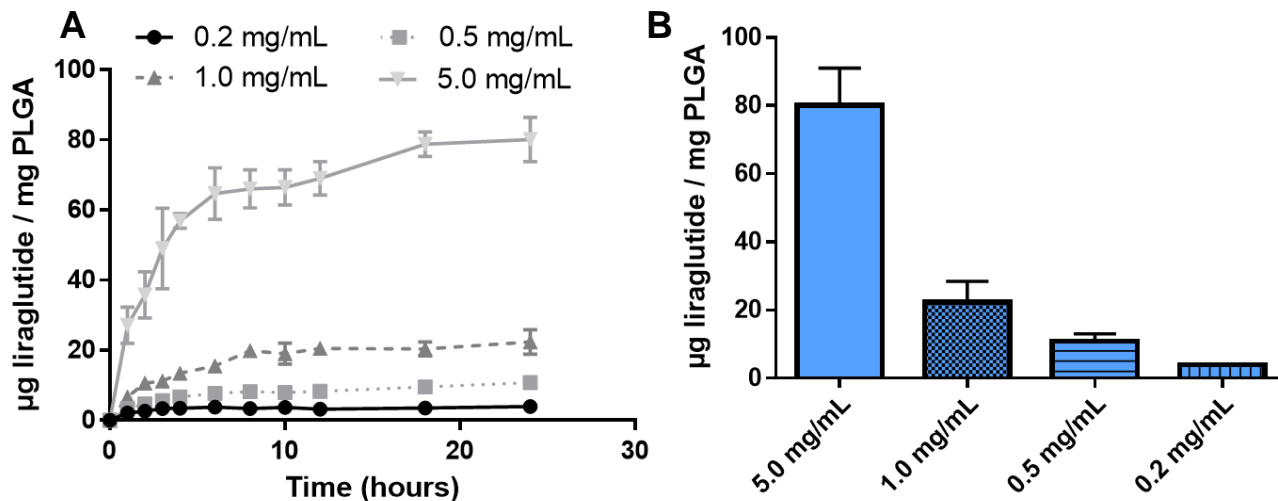


Figure A. 5: (A) Liraglutide sorption isotherm using MgCl₂-treated 502H. Four concentrations of liraglutide were used: 0.2, 0.5, 1.0 and 5.0 mg/mL. Total sorption after 24 hours incubation in each concentration is shown in (B). Data represent mean \pm SEM, n=3.

Given these preliminary results showing that high liraglutide sorption could be achieved in Mg-502H, microspheres using this treated polymer were prepared for loading studies. During formulation, all aqueous solutions (i.e. PVA solutions) were prepared using 1M MgCl₂ to maintain high ion concentration and prevent the ionic polymer from crashing out of solution. The resulting microspheres were well formed and increased loading over untreated 502H microspheres, but following loading the particles lost their integrity (Figure A. 6). The salt treatment caused the polymer to become more brittle, forming some cracks in the microspheres prior to loading and causing their rapid disintegration over 24 hours at 37°C.

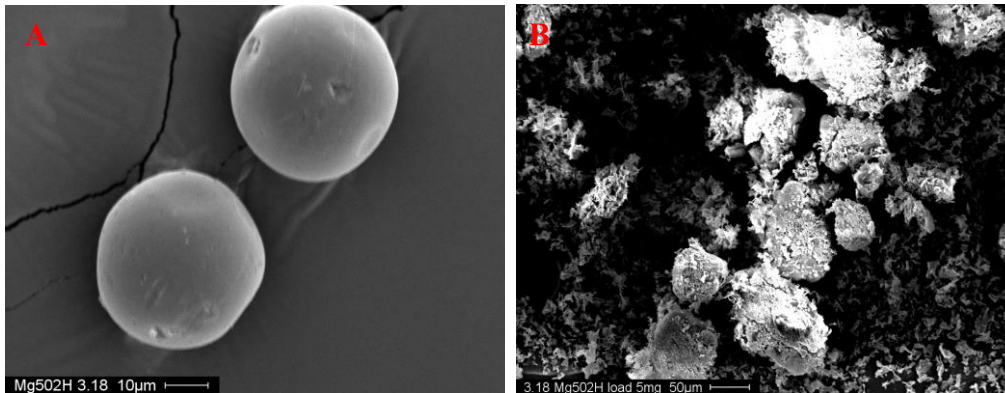
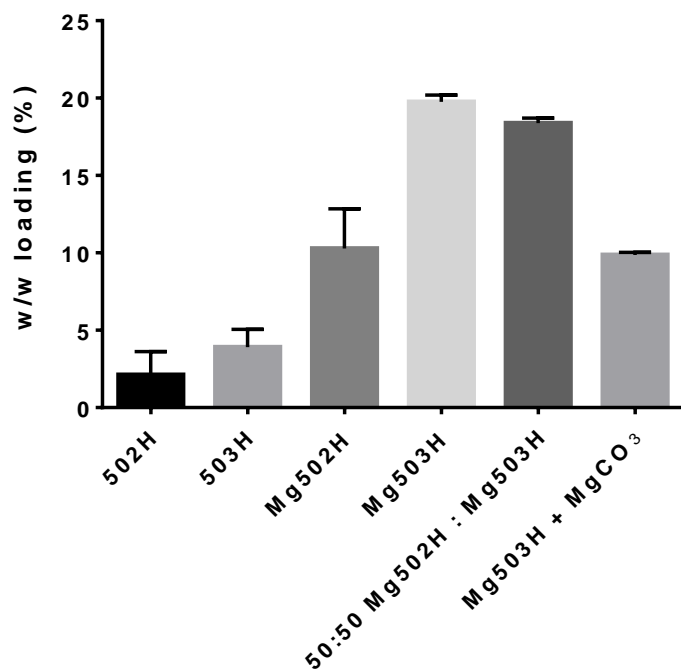


Figure A. 6: SEM images of Mg-502H microspheres before (A) and after (B) liraglutide loading for 24 hours at 37°C.

While the low molecular weight polymer may exhibit high peptide sorption capabilities, the loss of microsphere integrity results in a loss in homogeneity of the formulation and so may not be administered with confidence of product performance. Thus, a higher molecular weight acid end group PLGA (Resomer 503H) was used to prepare additional microspheres. A blend of Mg-502H and Mg-503H was also used with the intent of maintaining the high loading capabilities of the low molecular weight polymer while increasing the integrity of the microspheres with the higher MW 503H. A fourth formulation incorporating the insoluble base MgCO_3 in the polymer phase was also tested due to the physical-chemical properties of liraglutide reported by Novo Nordisk, the manufacturer of Victoza®. In the patents submitted during product development, stability tests were performed and it was reported that liraglutide is stable at high temperature and at slightly basic pH and so the final commercial product is formulated at pH 8.1 [20]. PLGA microspheres, however, develop an acidic microclimate during release due to the buildup of acidic PLGA degradation byproducts [21]. Our lab has shown that incorporation of insoluble bases can modulate this pH during PLGA degradation to improve stability of encapsulated molecules [21-24]. Microspheres prepared using Mg-treated polymers all exhibited higher liraglutide loading than untreated polymeric microspheres; however only the microspheres made of pure Mg-503H maintained their integrity during loading (Figure A. 8).

The higher Mg-503H microspheres also moderated initial burst release after one day *in vitro*

(Figure A. 7).



Microsphere Formulation	Liraglutide Loading (w/w %)	Initial Burst Release (%)
502H	2.11 ± 0.9	50.37 ± 3.2
503H	3.91 ± 0.7	14.76 ± 2.1
Mg502H	10.67 ± 0.09	20.43 ± 1.1
Mg503H	19.41 ± 0.01	9.51 ± 0.8
50:50	17.66 ± 0.01	4.54 ± 0.1
Mg503H+MgCO ₃	9.98 ± 0.01	5.95 ± 0.4

Figure A. 7: Liraglutide loading in microspheres. Loading was performed using 10mg microspheres in 1 mL of 5.0 mg/mL liraglutide solution in HEPES buffer pH 7.4 at 37°C for 24 hours. Table at right includes loading values and initial burst (24-hour release) determined in HBS. Data represent mean ± SEM, n=3.

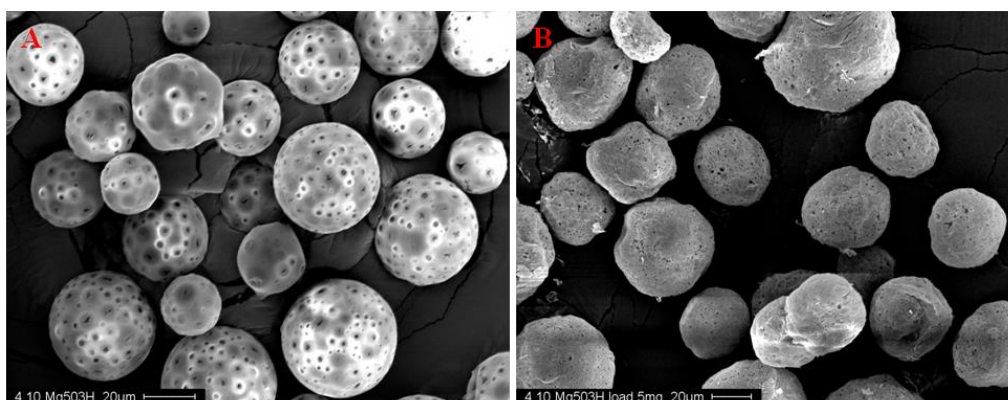


Figure A. 8: SEM images of Mg-503H microspheres before (A) and after (B) liraglutide loading for 24 hours at 37°C.

Based on the success of these preliminary microsphere formulations and the stability data reported in the patent literature previously discussed, loading conditions were optimized to maximize encapsulation efficiency while maintaining high loading and low initial burst during *in vitro* release. Loading solutions were made based on the solution formulation of Victoza®, containing 3.75mM Na₂HPO₄ at pH 8.1. The decrease in ionic strength of the loading solution and increased stability due to the slightly basic pH resulted in greater encapsulation efficiencies than were previously achieved by using loading solutions prepared in HEPES buffer at pH 7.4. The two most promising formulations from preliminary studies were chosen to move forward using the optimized loading conditions: Mg-503H and Mg-503H + MgCO₃. Using a loading concentration of 1.0 mg/mL liraglutide, encapsulation in the latter formulation was almost 100% (Figure A. 9).

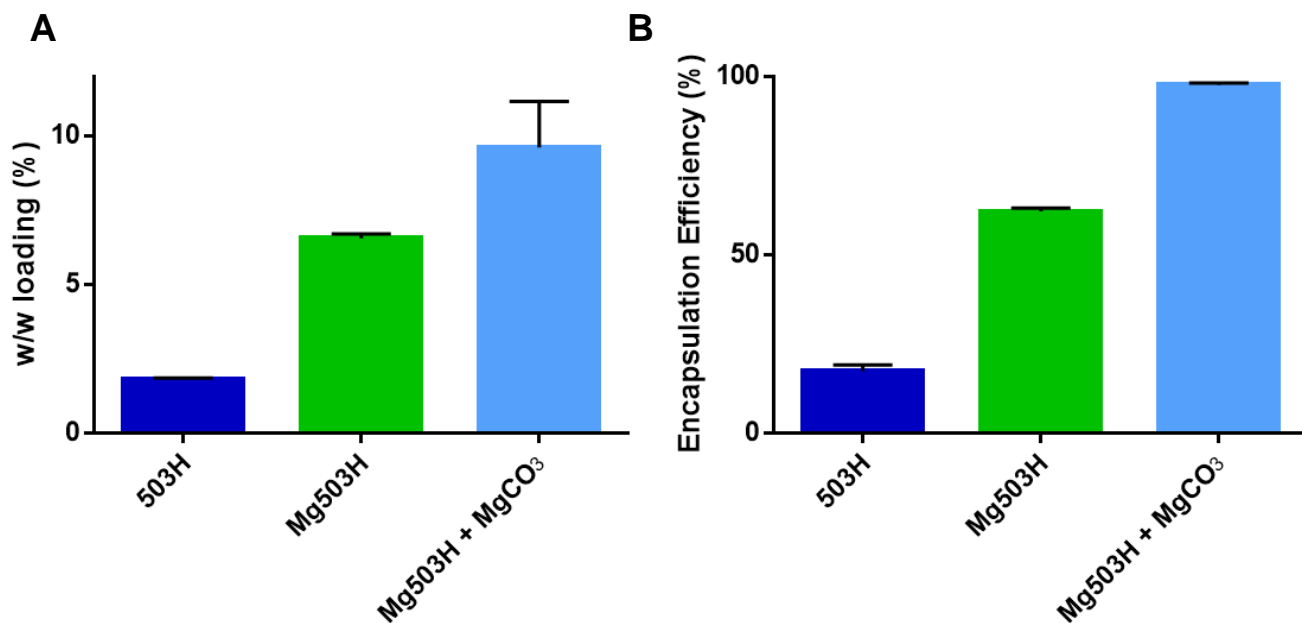


Figure A. 9: Liraglutide loading (A) and encapsulation efficiency (B) in PLGA 503H microspheres. Loading was performed using 10mg microspheres in 1 mL of 1.0 mg/mL liraglutide solution in 3.75mM Na₂HPO₄ pH 8.1 at 37°C for 24 hours. Data represent mean ± SEM, n=3.

In vitro release from these microspheres was slow and continuous following initial burst in HBS pH 7.4 (Figure A. 10A). During quantification of release, however, a shift in the chromatogram peak was noticed in the release samples as compared to the standards (Figure A. 11). This raised concerns over peptide stability in the release media, and so the concentration of liraglutide in HBS was measured at two concentrations relevant to release samples over time at 37°C. The peptide concentration decreased in all three HBS-based media, indicating that measuring release from media concentrations alone may not be reliable (Figure A. 12).

Release was also measured in PBST pH 7.4, a more commonly-used release medium of higher ionic strength. Initial burst in this media was high from all three microsphere formulations and negligible release was seen after just one week (Figure A. 10B). Interestingly, however, release samples taken in this media did not exhibit the same peak shift as was observed in the HBS media. Due to the conflicting *in vitro* release results, amino acid analysis was employed to confirm controlled release. This direct measurement of peptide remaining in microspheres suggested slow and continuous release over two weeks, though the release rates were different than reported by the *in vitro* release tests performed in HBS and PBST (Figure A. 10C). Given this data suggesting controlled release, Mg503H + MgCO₃ microspheres loaded with liraglutide were selected for *in vivo* studies.

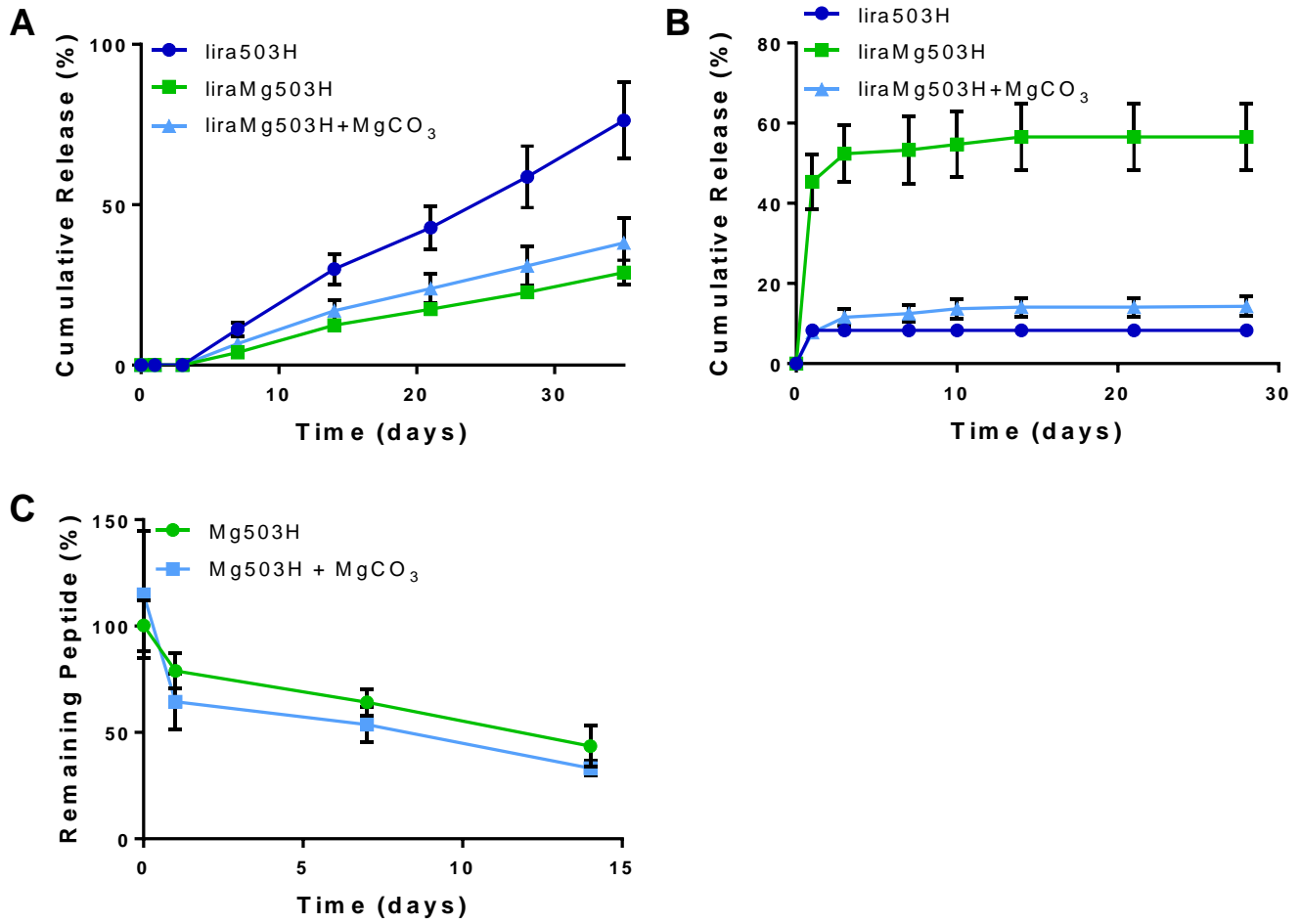


Figure A. 10: *in vitro* release of liraglutide from microspheres in HBS pH 7.4 (A and C), PBST pH 7.4 (B). Release was quantified by UPLC of release media (A and B) or amino acid analysis of microspheres (C). Data represent mean \pm SEM, $n=3$.

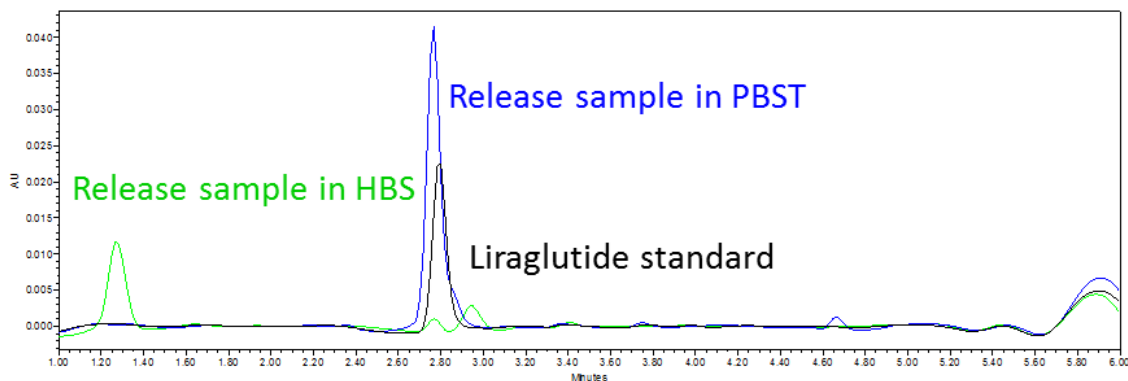


Figure A. 11: UPLC chromatograms of release from Mg503H + MgCO₃ microspheres in HBS and PBST; and a standard prepared in loading solution. Peak shift was observed in release samples in HBS (retention time 1.2 minutes vs. 2.8 minutes)

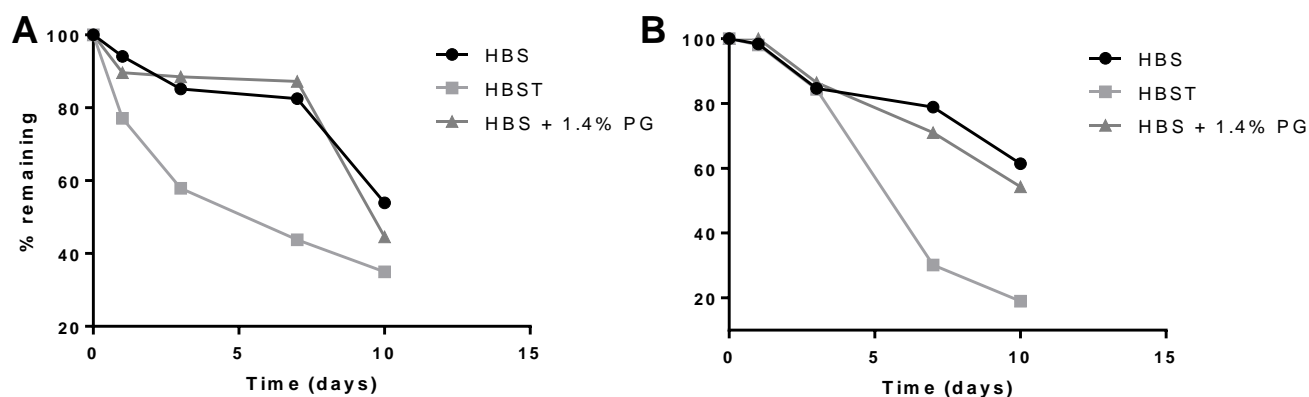


Figure A. 12: Liraglutide content remaining in solution during incubation at 37°C. Initial concentrations were 100 µg/mL (A) and 50 µg/mL (B).

Based on the in vitro release of liraglutide, the in vivo pharmacokinetics of liraglutide from microspheres were surprising. At both dose levels, high initial burst was observed in the first day followed by low concentrations in the plasma for two months (Figure A. 13). The sustained concentrations were approximately 3 ng/mL and 5 ng/mL for the low and high dose rats, respectively. Therapeutic concentrations fall within the range of 35-100 ng/mL [15-17]. With the initial burst concentrations being well above the therapeutic range and the long-term concentrations being far below, these microspheres in their current state would not be suitable

for controlled release treatment of T2D. The high initial burst suggests that the majority of the “loaded” peptide is likely precipitated on the surface of the microspheres, rather than being well encapsulated and homogeneously loaded in the PLGA. Therefore, more optimization is needed to promote further penetration of the peptide in the polymer phase for long-term controlled release.

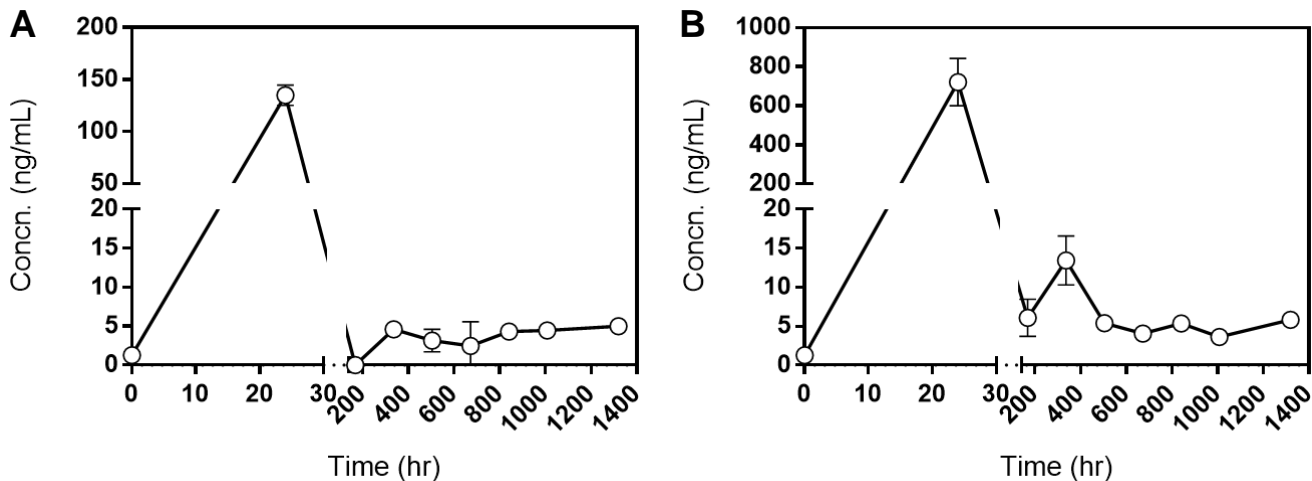


Figure A. 13: Liraglutide concentrations in plasma of SD rats following a single subcutaneous injection of liraglutide-loaded Mg503H + MgCO₃ microspheres at low (A) or high (B) dose.

A.5 Conclusions

Although the PLGA microspheres developed here for encapsulation and release of liraglutide did not exhibit the desired controlled release *in vivo*, the work discussed here shows the utility of using free-acid terminated PLGAs for loading peptides. We have also shown that salt treatment of these polymers leads to electrostatic interaction with anionic peptides and thus this simple remote loading strategy can be exploited for encapsulation of cationic and anionic peptides.

A.6 References

1. *IDF Diabetes Atlas, 6th ed.* 2014; Available from: <http://www.idf.org/diabetesatlas>.
2. Kahn, S.E., M.E. Cooper, and S. Del Prato, *Pathophysiology and treatment of type 2 diabetes: perspectives on the past, present, and future.* The Lancet. **383**(9922): p. 1068-1083.
3. King, S. *FirstWord Lists: Blockbuster diabetes drugs 2014 and 2020.* 2015 [cited 2015; Available from: <http://www.firstwordpharma.com/node/1282421#axzz3j65VNOBI>.
4. *Competitor Analysis: GLP-1 Receptor Agonists Development Pipeline Report 2014*, in *Competitor Analysis*, R.a. Markets, Editor. 2014: La Merie Publishing.
5. *Global Guideline for Type 2 Diabetes (2012).* International Diabetes Federation.
6. Gershell, L., *Type 2 diabetes market.* Nat Rev Drug Discov, 2005. **4**(5): p. 367-368.
7. Holst, J.J., *The Physiology of Glucagon-like Peptide 1.* Vol. 87. 2007. 1409-1439.
8. Hui, H., et al., *The short half-life of glucagon-like peptide-1 in plasma does not reflect its long-lasting beneficial effects.* Eur J Endocrinol, 2002. **146**(6): p. 863-9.
9. *Byetta® [package insert].* Amylin Pharmaceuticals, Inc., San Diego, CA; 2005.
10. Drucker, D.J., A. Dritselis, and P. Kirkpatrick, *Liraglutide.* Nat Rev Drug Discov, 2010. **9**(4): p. 267-268.
11. Agersø, H., et al., *The pharmacokinetics, pharmacodynamics, safety and tolerability of NN2211, a new long-acting GLP-1 derivative, in healthy men.* Diabetologia, 2002. **45**(2): p. 195-202.
12. Agersø, H. and P. Vicini, *Pharmacodynamics of NN2211, a novel long acting GLP-1 derivative.* European Journal of Pharmaceutical Sciences, 2003. **19**(2-3): p. 141-150.
13. Sophocleous, A.M., et al., *The nature of peptide interactions with acid end-group PLGAs and facile aqueous-based microencapsulation of therapeutic peptides.* Journal of Controlled Release, 2013. **172**(3): p. 662-670.
14. *Victoza® [package insert].* Novo Nordisk, Inc., Bagsværd, Denmark; 2010.
15. Bock, T., B. Pakkenberg, and K. Buschard, *The endocrine pancreas in non-diabetic rats after short-term and long-term treatment with the long-acting GLP-1 derivative NN2211.* APMIS, 2003. **111**(12): p. 1117-1124.
16. Larsen, P.J., et al., *Systemic Administration of the Long-Acting GLP-1 Derivative NN2211 Induces Lasting and Reversible Weight Loss in Both Normal and Obese Rats.* Diabetes, 2001. **50**(11): p. 2530-2539.
17. Rolin, B., et al., *The long-acting GLP-1 derivative NN2211 ameliorates glycemia and increases β -cell mass in diabetic mice.* American Journal of Physiology - Endocrinology And Metabolism, 2002. **283**(4): p. E745-E752.
18. Meier, J.J., *GLP-1 receptor agonists for individualized treatment of type 2 diabetes mellitus.* Nat Rev Endocrinol, 2012. **8**(12): p. 728-742.
19. Elbrond, B., et al., *Pharmacokinetics, pharmacodynamics, safety, and tolerability of a single-dose of NN2211, a long-acting glucagon-like peptide 1 derivative, in healthy male subjects.* Diabetes Care, 2002. **25**(8): p. 1398-404.
20. Ludvigsen, S., et al., *US Pat. No. 0173844 A1.* 2010.
21. Liu, Y. and S.P. Schwendeman, *Mapping Microclimate pH Distribution inside Protein-Encapsulated PLGA Microspheres Using Confocal Laser Scanning Microscopy.* Molecular Pharmaceutics, 2012. **9**(5): p. 1342-1350.

22. Kang, J. and S.P. Schwendeman, *Comparison of the effects of Mg(OH)₂ and sucrose on the stability of bovine serum albumin encapsulated in injectable poly(d,l-lactide-co-glycolide) implants*. *Biomaterials*, 2002. **23**(1): p. 239-245.
23. Zhu, G., S.R. Mallery, and S.P. Schwendeman, *Stabilization of proteins encapsulated in injectable poly (lactide- co-glycolide)*. *Nat Biotech*, 2000. **18**(1): p. 52-57.
24. Zhu, G. and S. Schwendeman, *Stabilization of Proteins Encapsulated in Cylindrical Poly(lactide-co-glycolide) Implants: Mechanism of Stabilization by Basic Additives*. *Pharmaceutical Research*, 2000. **17**(3): p. 351-357.

Appendix B: : Poly (lactic acid) and Poly (lactic-co-glycolic acid) Microspheres for Intraocular Controlled Release of the Glaucoma Drug Brimonidine

B.1 Abstract

Glaucoma is one of the leading causes of blindness in the United States and its treatment is currently plagued by poor patient adherence to common treatment options such as eye drops. The purpose of this work was to develop biodegradable microparticle formulations of two glaucoma drugs, timolol and brimonidine, using poly (lactic acid) (PLA) and poly (lactic-co-glycolic acid) (PLGA) for supraciliary injection and subsequent controlled release and reduction in intraocular pressure. Sustained delivery of these molecules may decrease the need for frequent drug administration and therefore improve patient compliance. An initial microsphere formulation prepared from PLA (free acid terminated, inherent viscosity 0.20 dl/g) encapsulated brimonidine with an efficiency (EE) of $38 \pm 1\%$ and loading of $2.3 \pm 0.1\%$ w/w. These microspheres exhibited an initial burst of $16.5 \pm 0.2\%$ of loaded brimonidine. In order to minimize the initial burst and improve encapsulation efficiency, three different formulation strategies were developed. Removal of low molecular weight acids from PLA prior to formulation, increased PLA concentration in oil phase, and formulation using a blend of PLA and PLGA 75:25 (ester terminated, inherent viscosity 1.13 dl/g) decreased the initial burst to $8.0 \pm 1.3\%$, $1.8 \pm 0.3\%$, and $1.2 \pm 0.1\%$, and increased EE to $85 \pm 0.4\%$, $67 \pm 6\%$, and $53 \pm 8\%$, respectively. *In vitro* release from all four brimonidine formulations was slow and continuous over 35 days.

B.2 Introduction

Primary open angle glaucoma is a leading cause of blindness, affecting nearly 2 million individuals in the United States with an annual cost of \$2.9 billion [1, 2]. Glaucoma is the most common form of optic neuropathy, where loss of retinal ganglion cell axons permanently disrupts transmission of visual information from the retina to the brain [1, 3, 4]. Patients with glaucoma experience a painless and gradual loss of vision starting from the periphery and eventually claiming central vision [3, 5]. Intraocular pressure (IOP) is the only modifiable risk factor [6, 7] and reducing IOP prevents the progression of glaucoma-related vision loss [5, 8].

IOP is mediated by the balance of aqueous humor production and aqueous humor removal [9]. Aqueous humor is a clear nutrient-rich fluid secreted by the ciliary body that provides nutrients to the avascular ocular tissues of the anterior segment and pressurizes the eye. Clearance of aqueous humor occurs through either the trabecular meshwork into the episcleral veins or the uveoscleral outflow pathway into the suprachoroidal space [9, 10]. Medical and surgical therapy for glaucoma seek to control IOP by reducing production of aqueous humor and/or increasing clearance of aqueous humor [5, 11]. Since these medications only prevent the progression of glaucoma, patients require chronic treatment for their lifetime [11]. Topical eye drops, such as timolol, latanoprost, and brimonidine, are first-line medical therapies for glaucoma patients. Brimonidine is a α_2 -adrenergic agonist that both decreases aqueous humor secretion by the ciliary body, and increases aqueous humor clearance [12]. Because topical eye drops have low bioavailability through the cornea (<5%), eye drops are needed multiple times per day to ensure sufficient drug dosing (e.g., brimonidine eye drops are dosed three times per day) [11, 13].

Patient adherence to topical eye drops is low, estimated to be only 41% to 76% [11, 14-18]. Due to the chronic nature of glaucoma and the rigorous administration schedule, it can be difficult for patients to administer their eye drops on a regular basis. The most common reasons for patients to miss a dose are being otherwise preoccupied, forgetting, cost, and motivational [15]. Since any loss of vision is permanent, increasing patient compliance will preserve functional vision and decrease progression to blindness [11].

Patient compliance can be increased through methods such as memory tools that remind patients of their required doses, and improved formulations that do not require refrigeration or require simpler, less frequent administration regimens [11]. Perhaps the most attractive method to improve patient compliance is through the use of controlled-release drug delivery systems that obviate the need for the patient to apply eye drops daily. Poly(lactic acid) (PLA), poly(glycolic acid) (PGA), and their copolymers (PLGA) are polymers which have been extensively studied for intraocular controlled drug release because of their safety and biodegradable nature [19].

In this study, we formulated brimonidine into controlled release microspheres using polylactic acid (PLA) for later sustained release in the supraciliary space of the eye adjacent to the drug's site of action at the ciliary body. Brimonidine was chosen because it is an FDA-approved IOP-lowering agent currently prescribed to glaucoma patients [12, 13, 20]. Strategies were used to increase the loading and encapsulation efficiency of the microspheres while maintaining controlled release characteristics. One microsphere formulation was chosen for *in vivo* efficacy studies in rabbits performed by our collaborators. In these studies, PLA microspheres encapsulating brimonidine were injected using a microneedle for targeted administration into the supraciliary space and IOP was monitored.

B.3 Materials

Brimonidine, poly-lactic acid (PLA) with an inherent viscosity (i.v.) of 0.20 dL/g (free acid terminated, RESOMER® 202H), and polyvinyl alcohol (PVA, 80% hydrolyzed, MW ~9,000-10,000) were purchased from Sigma Aldrich (MO, USA). PLGA (75:25, i.v. = 1.13 dL/g, ester terminated) was purchased from Lactel (AL, USA). All solvents used were HPLC grade and were purchased from Fisher Scientific and unless otherwise noted, all other chemicals were purchased from Sigma Aldrich.

B.4 Methods

B.4.1 Removal of LMW acids from PLA

In some formulations, to remove low molecular weight (LMW) acids, PLA (~5g) was dissolved in 10mL CH₂Cl₂ and added to a stirring ddH₂O bath maintained at 60°C. After evaporating CH₂Cl₂ for 3 hours, the aqueous phase containing water-soluble low molecular weight acids (LMW) was removed [21]. The resulting polymer was dried under vacuum and stored at -20°C until used.

B.4.2 Microsphere preparation

All microspheres were prepared by using oil-in-water (o/w) emulsion solvent evaporation methods. First, brimonidine and the selected polymer(s) (Table B. 1) were dissolved in 1 mL CH₂Cl₂. Two mL 5.0% PVA was added and vortexed at the highest setting for 60 s to create the o/w emulsion, which was then poured rapidly into a stirring bath of 0.5% PVA. After 3 h, the hardened microspheres were screened to 20-45 µm using stainless steel sieves (Newark Wire Cloth Company, NJ, USA), washed thoroughly with ddH₂O, and then lyophilized and stored at -20°C for future use.

Table B. 1: Brimonidine Microsphere Formulation Parameters

Polymer	Polymer Concentration (mg/mL CH ₂ Cl ₂)	Theoretical w/w Loading (L _T)	Formulation Name
PLA	800	6.00%	800PLA
PLA	1000	6.25%	800PLA-T
PLA hot-water treated	800	5.00%	1000PLA
50 : 50 Blend PLGA : PLA	500	10.00%	PLA/PLGA

B.4.3 Scanning Electron Microscopy

Prior to imaging, lyophilized microspheres were mounted by using double sided carbon tape and coated with a thin layer of gold under vacuum. Scanning electron microscopy (SEM) was performed on a Hitachi S3200N scanning electron microscope (Hitachi, Japan). Images were captured by EDAX® software.

B.4.4 Determination of Brimonidine Loading and Encapsulation Efficiency

Prepared microspheres (~5 mg) were dissolved in 1 mL acetonitrile. The resulting solution was filtered and analyzed for brimonidine content by ultraperformance liquid chromatography (UPLC), as described below. Drug loading and encapsulation efficiency were calculated using equations 1 and 2, respectively.

$$\% \text{ W/W loading } (L_A) = \left(\frac{\text{mass of brimonidine}}{\text{total mass of microspheres}} \right) \times 100 \% \quad \text{Eq. 1}$$

$$\text{encapsulation efficiency } (\%) = \left(\frac{\text{actual loading } (L_A)}{\text{theoretical loading } (L_T)} \right) \times 100 \% \quad \text{Eq. 2}$$

B.4.5 *In vitro* Release Kinetics of Brimonidine

Microspheres (~5 mg) were suspended in 1 mL phosphate buffered saline + 0.02% Tween 80 (PBST, pH 7.4) at 37°C under mild agitation. Release media was completely removed and replaced at 1, 3, 5, 7 days and weekly thereafter for 7 weeks. Release media was assayed for brimonidine content by UPLC.

B.4.6 *Brimonidine Quantification*

Brimonidine content in loading solutions and release media was determined using UPLC (Acquity UPLC, Waters, USA). The mobile phase was composed of 40 : 60 v/v (acetonitrile : ddH₂O) and the flow rate was set to 0.5 mL/minute. Samples and standards prepared in either acetonitrile or PBST were injected (8 µL) onto a C18 (Acquity BEH C18, 1.7µm, 2.1 x 100mm) column maintained at 30°C. Brimonidine was detected at 254 nm.

B.5 Results and Discussion

Table B. 2: Characterization of Brimonidine Microencapsulation (Data expressed as mean ± SE, n=3)

Formulation	Loading (w/w %)	Encapsulation Efficiency (%)	Initial Burst (%)
800 mg/mL untreated PLA (800PLA)	2.3 ± 0.1	38 ± 1	16.5 ± 0.2
800 mg/mL hot-water treated PLA (800PLA-T)	5.3 ± 1.3	85 ± 0.4	8.0 ± 1.3
1000 mg/mL untreated PLA (1000PLA)	3.3 ± 0.3	67 ± 6	1.8 ± 0.3
PLA / PLGA Blend (PLA/PLGA)	5.3 ± 0.7	53 ± 8	1.2 ± 0.1

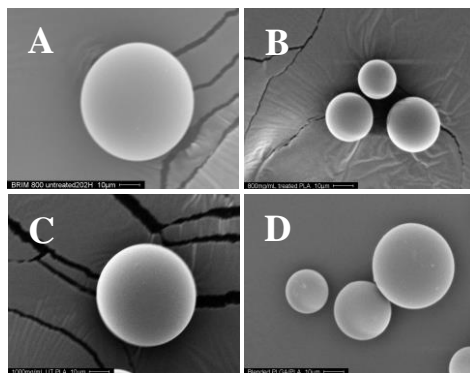


Figure B. 1: Representative SEM images of four microsphere formulations. A) 800PLA, B) 800PLA-T, C) 1000PLA, D) PLA/PLGA

Brimonidine was initially encapsulated in free-acid terminated PLA (800PLA) with low efficiency and moderate initial burst 24-h release of ~17% (Table B. 2). As brimonidine is highly water soluble, it is likely that the drug leaches into the aqueous phase during microsphere formulation [22]. This can result in poor loading and may also contribute to high burst due to any poorly encapsulated, surface-associated drug. Initial burst is often an undesired property of controlled release formulations as it may cause exposure to toxic drug levels *in vivo* and/or waste drug for later release. In order to improve loading efficiency and to decrease the initial burst from the microspheres, we employed three alternative formulation strategies for encapsulation of brimonidine.

As seen in Table B. 2, by using a higher concentration of PLA during preparation (1000PLA) and blending PLA with a high molecular weight, ester end capped PLGA (PLA/PLGA), both approaches increased brimonidine loading and decreased initial burst, likely due to a denser polymer matrix which can be more efficient in trapping the molecule during microsphere formulation [23]. Although these formulations were successful in improving loading and burst, the long-term release from these microspheres *in vitro* was slow incomplete through 7 weeks (Figure B. 2) and not desirable for our initial *in vivo* evaluation (see below).

The last formulation we developed, 800PLA-T, was prepared with the same free-acid terminated PLA 202H as was used in our initial formulation. Prior to microsphere manufacturing, we stirred the dissolved polymer in a hot water bath in order to remove low molecular weight, water-soluble acids; this strategy has been used successfully in the past to encapsulate the LHRH peptide leuprolide with high efficiency and resulting in low initial burst [21, 24]. During storage, lactic acid monomers and oligomers formed during polymerization may catalyze the degradation of the polymer, leading to a decline in PLA molecular weight and a buildup of additional acidic byproducts. Removal of these acidic monomers and oligomers can markedly improve the stability of the polymer during storage and can effectively increase the molecular weight of the bulk PLA [24]. As previously mentioned, higher molecular weight polymers create a denser matrix during microparticle manufacturing, leading to more efficient encapsulation. Microspheres formed using hot-water treated PLA to remove LMW greatly improved brimonidine loading to achieve $85 \pm 0.4\%$ efficiency. As shown in Table B. 2, these microspheres exhibited improved initial burst ($8.0\% \pm 1.3$) as compared to the initial 800PLA microspheres ($16.5\% \pm 0.2$).

Brimonidine release from all four formulations was slow and continuous for 6-8 weeks (Figure B. 2) but the most favorable release profile resulted from the 800PLA-T microspheres. These microspheres were selected for *in vivo* efficacy studies performed by our collaborators in the Prausnitz Lab at Georgia Tech. Briefly, 800PLA-T microsphere were injected using a microneedle for targeted administration in the supraciliary space. IOP of treated New Zealand White rabbits and was reduced by as much as 6 mm Hg for approximately 30 days.

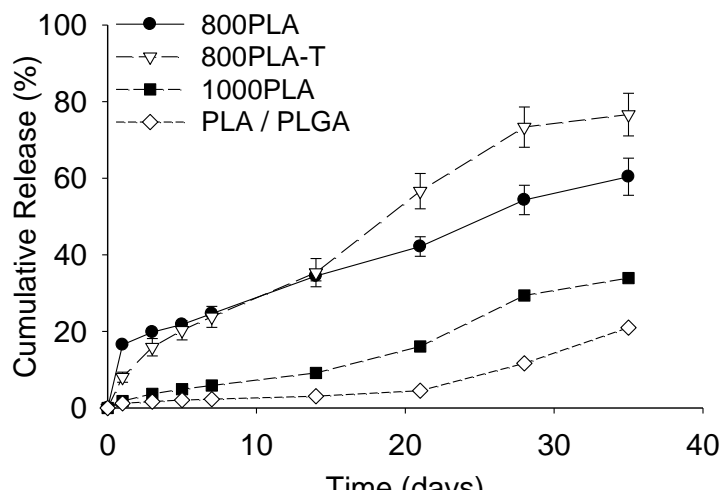


Figure B. 2 Brimonidine release from four polymer microsphere formulations *in vitro*, PBST pH 7.4. Data are expressed as mean \pm SE, $n=3$.

B.6 Conclusions

Four microsphere formulations of brimonidine were successfully prepared from the biodegradable polymers, PLA and PLGA. Removal of low-molecular weight acids from PLA prior to encapsulation resulted in improved loading, encapsulation efficiency, initial burst, and long-term controlled release *in vitro*. This microsphere formulation also exhibited controlled release and long-term efficacy *in vivo* (data not shown).

This work, including the in vivo studies, has been prepared as a manuscript and has been submitted for review to Journal of Controlled Release

B.7 References

1. Quigley, H.A. and A.T. Broman, *The number of people with glaucoma worldwide in 2010 and 2020*. Br J Ophthalmol, 2006. **90**(3): p. 262-7.
2. Quigley, H.A., et al., *The cost of glaucoma care provided to Medicare beneficiaries from 2002 to 2009*. Ophthalmology, 2013. **120**(11): p. 2249-57.
3. Giacony, J., S. Law, and J. Caprioli, *Primary Open-Angle Glaucoma*, in *Duane's Ophthalmology*, W. Tasman and E. Jaeger, Editors. 2009, Lippincott Williams & Wilkins: Philadelphia, Pa.
4. Weinreb, R.N. and P.T. Khaw, *Primary open-angle glaucoma*. Lancet, 2004. **363**(9422): p. 1711-20.
5. Gooch, N., et al., *Ocular Drug Delivery for Glaucoma Management*. Pharmaceutics, 2012. **4**(4): p. 197-211.
6. Gordon, M.O., et al., *The Ocular Hypertension Treatment Study - Baseline factors that predict the onset of primary open-angle glaucoma*. Archives of Ophthalmology, 2002. **120**(6): p. 714-720.
7. Sommer, A., et al., *Relationship between Intraocular-Pressure and Primary Open Angle Glaucoma among White and Black-Americans - the Baltimore Eye Survey*. Archives of Ophthalmology, 1991. **109**(8): p. 1090-1095.
8. Lavik, E., M.H. Kuehn, and Y.H. Kwon, *Novel drug delivery systems for glaucoma*. Eye (Lond), 2011. **25**(5): p. 578-86.
9. Ethier, C.R., M. Johnson, and J. Ruberti, *Ocular biomechanics and biotransport*. Annu Rev Biomed Eng, 2004. **6**: p. 249-73.
10. Alm, A. and S.F. Nilsson, *Uveoscleral outflow--a review*. Exp Eye Res, 2009. **88**(4): p. 760-8.
11. Ghate, D. and H.F. Edelhauser, *Barriers to glaucoma drug delivery*. J Glaucoma, 2008. **17**(2): p. 147-56.
12. Toris, C.B., et al., *Effects of brimonidine on aqueous humor dynamics in human eyes*. Arch Ophthalmol, 1995. **113**(12): p. 1514-7.
13. Konstas, A.G.P., et al., *Brimonidine 0.2% given two or three times daily versus timolol maleate 0.5% in primary open-angle glaucoma*. American Journal of Ophthalmology, 2001. **131**(6): p. 729-733.
14. Robin, A.L., et al., *Adherence in glaucoma: objective measurements of once-daily and adjunctive medication use*. Am J Ophthalmol, 2007. **144**(4): p. 533-40.
15. Tsai, J.C., et al., *Compliance barriers in glaucoma: a systematic classification*. J Glaucoma, 2003. **12**(5): p. 393-8.
16. Rotchford, A.P. and K.M. Murphy, *Compliance with timolol treatment in glaucoma*. Eye (Lond), 1998. **12** (Pt 2): p. 234-6.
17. Patel, S.C. and G.L. Spaeth, *Compliance in patients prescribed eyedrops for glaucoma*. Ophthalmic Surg, 1995. **26**(3): p. 233-6.
18. Gurwitz, J.H., et al., *Treatment for glaucoma: adherence by the elderly*. Am J Public Health, 1993. **83**(5): p. 711-6.
19. Kimura, H. and Y. Ogura, *Biodegradable Polymers for Ocular Drug Delivery*. Ophthalmologica, 2001. **215**(3): p. 143-155.

20. Jansen, J., et al., *Intraocular degradation behavior of crosslinked and linear poly(trimethylene carbonate) and poly(d,l-lactic acid)*. *Biomaterials*, 2011. **32**(22): p. 4994-5002.
21. Yamamoto, M., et al., *Polymer, production and use thereof*. 1989, Takeda Chemical Industries, Ltd.
22. Chang, J. and P. Hughes, *Oil-in-water method for making alpha-2 agonist polymeric drug delivery systems*. 2009, Allergan, Inc.
23. Huang, X. and C.S. Brazel, *On the importance and mechanisms of burst release in matrix-controlled drug delivery systems*. *Journal of Controlled Release*, 2001. **73**(2-3): p. 121-136.
24. Yamamoto, M., et al., *Polymer, production and use thereof*. 1993, Takeda Chemical Industries, Ltd.